WILEY-BLACKWELL

Cladistics (2021) 1–38

Cladistics

10.1111/cla.12460

Phylogenetic value of jaw elements of lacertid lizards (Squamata: Lacertoidea): a case study with Oligocene material from France

Lukardis Charlotte Marie Wencker*[a], Emanuel Tschopp[a,b,c], Andrea Villa[a,d], Marc Louis Augé[e] and Massimo Delfino[a,f]

[a]*Dipartimento di Scienze della Terra, Università degli Studi di Torino, Via Valperga Caluso, 35, Turin, 10125, Italy;* [b]*Centrum für Naturkunde, Universität Hamburg, Martin-Luther-King-Platz 3, Hamburg, 20146, Germany;* [c]*Division of Paleontology, American Museum of Natural History, Central Park West & 79th Street, New York, NY, 10024, USA;* [d]*SNSB-Bayerische Staatssammlung für Paläontologie und Geologie, Richard-Wagner-Straße 10, Munich, 80333, Germany;* [e]*CR2P, UMR 7207 CNRS, MNHN, Muséum National d'Histoire naturelle, 57 rue Cuvier, Paris, 75231, France;* [f]*Institut Català de Paleontologia Miquel Crusafont, Universitat Autònoma de Barcelona, Edifici ICTA-ICP, Carrer de les Columnes s/n, Campus de la UAB, Cerdanyola del Vallès, Barcelona, 08193, Spain*

Accepted 5 April 2021

Abstract

Several extinct species are known from the family Lacertidae, but due to poor preservation, many of them are based on single bones. Here, we compare phylogenetic signals of disarticulated premaxillae, maxillae and dentaries of lacertids from four French Oligocene localities (Coderet, La Colombière, Roqueprune 2, Mas de Got B). We identified five morphotypes among the premaxillae, six among the maxillae, and ten among the dentaries. These morphotypes were scored as individual taxa per locality into three separate character matrices with the same 246 characters, one matrix for each jaw element. Subsequently, the phylogenetic position of the morphotypes was tested using maximum parsimony. The consensus trees with the dentaries and the maxillae found a large polytomy including all taxa except the outgroup taxon *Gekko gecko*. The consensus tree with the premaxillae showed a considerably more resolved topology but found all morphotype taxa outside Lacertidae. In a second step, we compared the constitution of our three datasets and the morphotype taxa. Our results suggest that a combination of convergent characters and missing data led to the outgroup position of the premaxilla morphotype taxa. The poor resolution of the maxillae strict consensus is likely a consequence of their fragmentary preservation. For the dentaries, a high amount of missing data due to the high number of morphotype taxa most likely caused the poor tree resolution. Indeed, tests with fewer morphotypes found tree resolutions comparable to the premaxilla data. When linking the morphotypes, five possible lacertid "species" were found. Comparison with already known French Oligocene lacertid species points to a slightly higher species richness of Lacertidae at that time than known before. Reliable species classification based on phylogeny only seems possible when combining the jaw elements or in association with other cranial and postcranial material, putting some doubt on species identifications based on single bones.

Introduction

The family Lacertidae constitutes the taxonomically dominant reptile group in Europe (Arnold et al., 2007; Sillero et al., 2014; Speybroeck et al., 2016; Villa and Delfino, 2019a; Speybroeck et al., 2020). These small to medium-sized lizards are represented by >300 extant species from Eurasia and Africa (Arnold et al., 2007; Uetz et al., 2018). Lacertidae includes endemic "island giants" such as *Gallotia stehlini* and *Gallotia simonyi* from the Canary Islands (Arnold, 1973), but also the widely distributed species *Lacerta agilis*, which occurs from Western Europe all the way east to Mongolia (Arnold et al., 2007).

The place and time of origin of Lacertidae are still being debated. Their geographical origin was suggested to be located in Europe (Estes, 1983a; Fu, 1998). Also

*Corresponding author.
E-mail address: lukardischarlottemarie.wencker@unito.it

crown-group lacertids are thought to have originated in Europe, based on the fact that fossils considered to be close to or at the base of the crown group were found on this continent (Borsuk-Bialynicka et al., 1999; Čerňanský and Augé, 2013). Moreover, the lacertid sister clade Eolacertidae is also known from the Eocene of Europe (Čerňanský and Smith, 2018). In terms of timing, molecular clock analyses identified a middle Cretaceous age for the most recent common ancestor of Lacertidae and Amphisbaenia (98 Myr old; Wiens et al., 2006) but the calibration date used has since been questioned (Hipsley et al., 2009). The earliest putative crown-lacertid was *Plesiolacerta* from the middle Eocene of Lissieu (Mammal Palaeogene zone (MP) 14; Augé, 2005; Čerňanský and Augé, 2013). Additionally, a recent study found strong morphological similarities between modern Lacertidae and skeletal material from the early Eocene of Mutigny, France (MP 8–9; Čerňanský et al., 2020). These studies are further supported by molecular clock analyses yielding estimates for the split between Lacertinae and Gallotiinae during the late Palaeocene (58–56 Ma; Hipsley et al., 2009). Challenges regarding the interpretation of the time of origin of Lacertidae also derive from the difficulties in resolving higher-level phylogenetic relationships.

Molecular and morphological data have created contradictory relationships among major clades within Squamata (Losos et al., 2012). Morphological studies recovered Iguania as sister to all other squamates (Scleroglossa), and Lacertidae as sister to Scincoidea within Scincomorpha (Estes et al., 1988; Conrad, 2008; Gauthier et al., 2012). However, molecular-based phylogenies found Iguania nested more crown-ward within Squamata and Lacertidae as sister to Amphisbaenia (Townsend et al., 2004; Vidal and Hedges, 2005; Wiens et al., 2012; Pyron et al., 2013). Attempts with total-evidence analyses including fossils found tree topologies within Squamata that were congruent with relationships among higher-level clades recovered based on molecular data only, implying that differences between morphological and molecular phylogenies are the result of convergence, and confirming the close relationship of Lacertidae and Amphisbaenia (Wiens et al., 2010; Müller et al., 2011; Reeder et al., 2015). Only recently, two studies found for the first time morphological phylogenies that were in agreement with molecular and combined analyses, as they recovered Gekkota as the earliest squamate crown clade and Iguania further up in the tree: one study was performed with a subset of morphological characters (vertebrae) (Augé and Guével, 2018); the second study had a larger outgroup sampling compared to earlier morphological analyses (and the whole skeleton considered) and found Lacertidae as sister to Amphisbaenia (Simões et al., 2018). Additional challenges impacting studies of the origin of Lacertidae derive from the state of preservation of early extinct members of the group.

Taxonomic and systematic studies are greatly complicated because fossil squamates generally are found disarticulated (Rage, 2013). Disarticulation can result both from preservation and collection bias, and is especially widespread among Palaeogene lacertid lizards, so information about their early history is limited (Čerňanský and Augé, 2013). Among the few exceptions of articulated fossil lacertids worth mentioning are exceptional cases of preservations in amber, on slabs/blocks and in dry environments. An almost complete specimen preserved in Baltic amber has been referred to *Succinilacerta succinea* by Borsuk-Bialynicka et al. (1999). Thanks to a block containing an almost complete and previously unpublished skull with a few associated postcranial bones, the osteology and phylogenetic relationships of the Oligocene lacertid *Dracaenosaurus croizeti* is now known in detail (Čerňanský et al., 2017). *Janosikia ulmensis* has been revisited and redescribed on the basis of two partially preserved individuals represented by several cranial and some postcranial elements embedded in early Miocene slabs from Germany (Čerňanský et al., 2016). Two mummified and therefore articulated partial skeletons of giant lacertids, coming from the Quaternary filling of a basaltic cavity on the Canary Islands, have been originally described by Castillo et al. (1994), and were subsequently used to extract ancient mtDNA by Maca-Meyer et al. (2003). However, the majority of extinct lacertid species were erected based on single bones only, mostly tooth-bearing bones (maxillae and dentaries in particular) as well as parietals (for European post-Palaeogene taxa, see Villa and Delfino, 2019a, and references therein; for the osteology of European lizards, see Villa and Delfino, 2019b, and references therein). These are generally considered as being the most diagnostic elements and thus having the highest taxonomic value in the lacertid skull. However, such an approach to taxonomy can be problematic.

Species descriptions and identifications based on highly fragmentary material can lack true diagnostic features. An example is the species *Lacerta altenburgensis*. This species was described by Rauscher (1992) based on a single maxilla with an uniquely shaped zygomatic process. However, personal observation of the type maxilla by one of us (E. Tschopp in 2016) revealed that the proposed diagnostic shape of the dorsal edge of the zygomatic process is most likely the result of damage because the orbital margin of the zygomatic process seems to have sharp edges derived from breakage. The validity of other species is more difficult to test because they are based on subtle differences in shapes or ratios of completely preserved bones

or teeth, without a detailed assessment of variability of these traits in a fossil sample or among extant species. This issue obviously impacts any further analysis using species occurrences to reconstruct evolution and/or study biodiversity through time.

Species identifications are crucial to understand the systematics of a particular group, as well as its evolutionary history. Assessments of evolutionary patterns and rates within clades generally rely on the number of reported species or genera (Barrett and Upchurch, 2005; Pereira, 2015; Wiens, 2015; Tennant et al., 2016), which can then be tested for correlations with ecology, palaeoenvironmental or climatic changes in order to understand potential drivers of biodiversity. A great study system to analyze the impact of climatic changes on lacertid evolution is the Oligocene with its abruptly cold temperatures after the Palaeocene–Eocene Thermal Maximum (PETM) (Zachos et al., 2001, and references therein) and the warm period registered in the Eocene (Prothero, 1994) leading to the so called "Grande Coupure Eocène/Oligocène" (Stehlin, 1909). The response of the lacertids to these climatic and environmental changes is of high interest, especially considering the assumed close temporal association with the origin of crown-group lacertids. However, in order to understand how these climatic changes influenced taxonomic diversity, it is of crucial importance to assess the validity of the species that occurred during that period of time, as well as the methodology that was used to distinguish them at first place (see also Tschopp et al., in review). Here, we test the latter by comparing the phylogenetic signal of three tooth-bearing jaw elements of lacertid lizards that often were used to distinguish and erect new species from that period: premaxillae, maxillae and dentaries.

Institutional abbreviations

BSPG, Bayerische Staatssammlung für Paläontologie und Geologie, Munich, Germany; CIPA, Osteoteca, Laboratorio Arqueociencias, Lisbon, Portugal; COMGR, Collezione Osteologica Mauro Grano, Rome, Italy; FMNH, Field Museum of Natural History, Chicago, USA; GMZ, Grant Museum of Zoology and Comparative Anatomy, University College London, UK; HUJ-OST, Osteological Collections, Hebrew University of Jerusalem, Israel; ICP, Institut Català de Paleontologia Miquel Crusafont, Barcelona, Spain; IRSNB, Institut Royal des Sciences Naturelles de Belgique, Brussels, Belgium; MDHC, Massimo Delfino Herpetological Collection in the Museum of Geology and Paleontology of the Department of Earth Sciences of the University of Turin, Italy; MNCN, Museo Nacional de Ciencias Naturales, Madrid, Spain; MNHN, Muséum National d'Histoire Naturelle, Paris, France; MRAC, Musée Royal de l'Afrique Centrale, Tervuren, Belgium; NHMUK, Natural History Museum, London, UK; NHMW, Naturhistorisches Museum Wien, Austria; PIMUZ, Paläontologisches Institut und Museum der Universität Zürich, Switzerland; SRK, Sammlung Ralf Kosma, Staatliches Naturhistorisches Museum Braunschweig, Germany; UAM, Universitad Autónoma de Madrid, Spain; UCBL, Université Claude Bernard, Lyon, France; YPM, Yale Peabody Museum, New Haven, USA; ZZSiD, Institute of Systematics and Evolution of Animals, Polish Academy of Sciences, Krakow, Poland.

Materials and methods

Studied material

The studied material from four Oligocene localities in France (Coderet, La Colombière, Roqueprune 2, Mas de Got B; Fig. 1) was initially assigned to Lacertidae and is stored in the collections of the MNHN in Paris. All studied remains are associated with preliminary collection numbers which include a code indicating the collecting site (e.g. MdGB-1, MdGB-2, ... for remains from Mas de Got B). We studied a selected set of samples containing 156 disarticulated jaw elements from these localities. Although for La Colombière, Roqueprune 2 and Mas de Got B one single sample from each locality was selected, we had six samples from Coderet: Fouilles Viret, Coderet Couche 1 sup, Coderet Couche Verte sup 1-25, Coderet E1-0, Coderet H1-100 and Coderet H1-75. Each sample of Coderet corresponds to a different spot or stratigraphic layer within the locality. The latter three samples were taken during excavations in the 1960s (Hugueney, 1969). The labelling of those samples corresponds to the excavation grid, which was numbered A to J from East to West, and 0 to 2 from South to North. Samples were taken from different stratigraphic levels in those sectors, dividing them into increments of 0.25 m from the surface level downwards (e.g. Coderet E1-0 was taken from sector E1 at a depth of 0–0.25 m below surface; Hugueney, 1969; de Bonis et al., 1999). We have no information on the precise place and stratigraphic layer for the other samples. In order to keep the information gained from the sample sets separated, we did not create one large set for Coderet but instead retained the original subsamples.

Geological background

In the South of France, Roqueprune 2 is located in the Département Tarn-et-Garonne and Mas de Got B in the Département Lot; both are approximately 100 km N of Toulouse. They belong to the karstic phosphate deposits of Quercy (Phosphorites du Quercy; Vianey-Liaud, 1974; Vianey-Liaud and Wood, 1976) and originated from slow fissure fillings. In most cases, the deposits of Quercy did not retain the original order of sedimentation and younger layers are mixed with older ones (Vianey-Liaud and Marivaux, 2016). Therefore, the precise age of the fossils often is uncertain (de Bonis, 1974, 2011, and references therein). However, the sediments of Mas de Got B were correlated with the MP 22, and thus represent the oldest of the fossil localities studied herein; Roqueprune 2 was correlated with the slightly younger MP 23 (Schmidt-Kittler et al., 1987; Aguilar et al., 1997). Therefore, both localities represent Rupelian deposits.

Coderet is located at the northern part of the Allier basin in the Département Allier, 30 km SW of Moulins at Limagne

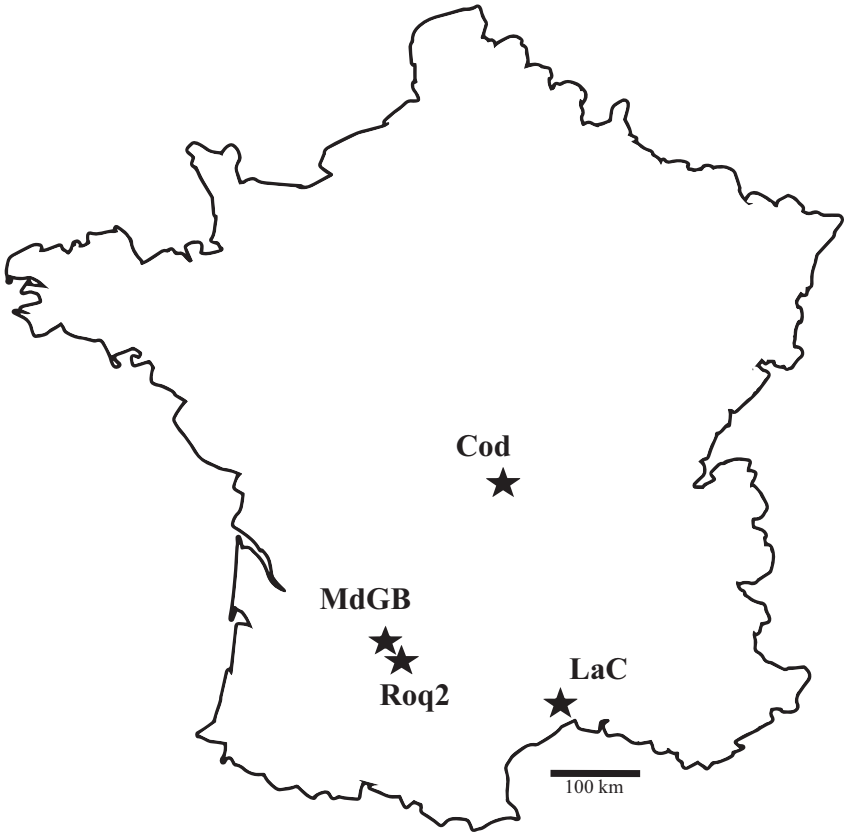

Fig. 1. Map of France indicating the geographical positions of the four Oligocene localities with black stars. Cod, Coderet; LaC, La Colombière; Roq2, Roqueprune 2; MdGB, Mas de Got B.

bourbonnaise. Limagne is a collapsed basin orientated in a N–S direction (Hugueney, 1969; de Bonis et al., 1999). It is backfilled with detrital and carbonate sediments (lacustrine and local forest resources). The quarry of Coderet is in contact with the western border fault of Limagne (Hugueney, 1969; de Bonis et al., 1999). It was correlated to MP 30 (Schmidt-Kittler et al., 1987; Aguilar et al., 1997) and is therefore of Chattian age.

La Colombière is located in the Département Hérault in the suburbs of the city of Montpellier. It is a depositional group of narrow fissure fillings (Thaler, 1966). It belongs to the Coderet zone and is, therefore, of Chattian age as well (MP 30; Thaler, 1966; Schmidt-Kittler et al., 1987).

Character matrix construction

The three lacertid jaw elements on which we focused (premaxilla, maxilla, dentary) were classified into individual morphotypes based on morphological differences such as, for example, the complexity of their tooth crowns, which were based on the character matrix explained below. These morphotypes were divided into single morphotype operational taxonomic units (mOTUs) based on their respective localities. We minimized the amount of missing data and kept the geographical and stratigraphic information separated by creating those bone-specific mOTUs. This procedure of treating disarticulated elements for phylogenetic analysis is, to our knowledge, performed here for the first time in squamates. To label the mOTUs, we used the names for the morphotypes, which contain the letter P for premaxilla, M for maxilla and D for dentary plus a successive cipher, and combined it with an abbreviation of the locality (FV: Fouilles Viret; CC1sup: Coderet Couche 1 sup; CCVsup: Coderet Couche Verte sup 1-25; CE1-0: Coderet E1-0; CH1-100: Coderet H1-100; CH1-75: Coderet H1-75; LaC: La Colombière; Roq2: Roqueprune 2; MdGB: Mas de Got B). For instance, the mOTU identified as premaxilla morphotype P1 from the sample of Fouilles Viret was given the name P1 FV.

We then created three phylogenetic matrices with the same 246 osteological characters (180 cranial and 66 postcranial ones), each of which included the morphotypes of a single jaw element. In this way, we avoided potential problems for the algorithm resulting from lacking anatomical overlap among the elements under study (Tschopp et al., 2018a). The matrices were created with MESQUITE (v.3.51, build 898; Maddison and Maddison, 2018). They are based on the matrix of Tschopp et al. (2018b), which was, in turn, an updated version of the matrix used by Villa et al. (2017). Twenty-four characters were added based on literature (including one that was used by Villa et al., 2017, but excluded in Tschopp et al., 2018b) and on personal observations (see Appendix 1 and references therein). We excluded one character from the original matrix of Tschopp et al. (2018b) (Character 217: Inscriptional ribs: absent (0); present (1)) because it had the same character state for all scored taxa and was, therefore, uninformative in our specific case. Moreover, we added seven outgroup and 11 ingroup operational taxonomic units (OTUs). The matrix consists mostly of extant species, with the addition of extinct lacertid species known from the Oligocene: *Ligerosaurus pouiti* (Augé, 1993), *Mediolacerta roceki* Augé, 2005, *Plesiolacerta lydekkeri* Hoffstetter, 1942, *Pseudeumeces cadurcensis* (Filhol, 1877), *Dracaenosaurus croitezi* Gervais, 1848–1852, and "*Lacerta*" *filholi* Augé, 1988. We created two separate locality-level OTUs for *Dracaenosaurus croizeti*, one representing the

material found in Cournon (approximately 10 km E of Clermont-Ferrand; MP 28; Schmidt-Kittler et al., 1987; Čerňanský et al., 2017), and the other including material from Coderet. The same strategy was applied for "*Lacerta*" *filholi*, with one OTU representing the material found in Pech-du-Fraysse (including the holotype; approximately 30 km SE from Aurillac; Quercy Phosphorites; MP 28; Schmidt-Kittler et al., 1987), and the other combining the information from material from Coderet (see the Supplementary material for a complete list of taxa and characters).

The outgroup now comprises *Gekko gecko* (Linnaeus, 1758) as a representative of the most basal squamatan clade Gekkota (molecular, total-evidence and morphological analyses agree on Gekkota being one of the most basal groups within Squamata; Gauthier et al., 2012; Reeder et al., 2015; Zheng and Wiens, 2015; Simões et al., 2018). Where specimens were available for first-hand scoring, the more derived outgroups were represented by more than one species, following the recommendations by Brusatte (2010) and Tschopp and Upchurch (2019). Squamatan clades represented in this updated matrix are the Scincoidea, Anguimorpha, Teiidae and Amphisbaenia. Scincoidea is represented by *Chalcides ocellatus* (Forskal, 1775), *Broadleysaurus major* (Duméril, 1851) and *Ablepharus kitaibelii* (Bibron and Bory de Saint-Vincent, 1833). The position of Scincoidea is unclear, with molecular data indicating a position near the base of the squamate tree as the sister taxon to Lacertoidea + Toxicofera (Pyron et al., 2013; Reeder et al., 2015; Zheng and Wiens, 2015), and morphological data recovering the group close to Lacertoidea, with which it forms the clade Scincomorpha (Estes et al., 1988; Conrad, 2008; Gauthier et al., 2012). Anguimorpha is represented herein by *Varanus exanthematicus* (Bosc, 1792), *Anguis veronensis* Pollini, 1818, and *Pseudopus apodus* (Pallas, 1775). The relative position of this clade is unclear too, being recovered in the opposite positions compared to Scincoidea. Molecular and morphological data find Anguimorpha within a clade that includes also Iguania and Serpentes (among other groups), and which forms the sister taxon to Lacertoidea (Reeder et al., 2015; Zheng and Wiens, 2015; Simões et al., 2018). Within Lacertoidea, Teiidae are represented by *Salvator merianae* Duméril and Bibron, 1839. Amphisbaenia is represented by *Blanus rufus* (Hemprich, 1820) and *Blanus strauchi* (Bedriaga, 1884) and is thought to be the sister taxon of Lacertidae based on molecular data (Zheng and Wiens, 2016). The ingroup Lacertidae is scored at species-level herein, mostly based on observations of ten or fewer specimens per species by one or more of the authors. In order to accurately represent intraspecific polymorphisms, we used majority scoring for polymorphic characters, following Wiens (1995). Where an equal number of specimens showed different character states, we scored the species as polymorphic. Hence, variation of character states that occurred only in a minority of the specimens belonging to one species was not factored in, this should be born in mind during data interpretation.

Phylogenetic analysis

For the species-level phylogenetic analysis with a maximum parsimony approach, we used the software TNT (v.1.5; Goloboff and Catalano, 2016). Extended implied weighting with a *k*-value of 5, 12 and 20, and the default setting for assumed homoplasy for missing entries was applied to reduce the influence of highly variable characters and missing data (Goloboff, 2014; Goloboff et al., 2018; see also recommendations in Tschopp and Upchurch, 2019). The tree search was performed using the New Technology search, enabling all algorithms with their default settings, and stabilizing the consensus tree five times with a factor of 75. The resulting best-fitting trees were used as a starting point for a second iteration of tree bisection and reconnection (traditional heuristic search) to ensure a better tree space coverage. Twenty-seven multistate characters were treated as ordered, as they were either quantitative characters or formed a morphocline (Brazeau, 2011).

Preliminary analyses recovered vast polytomies in the strict consensus trees, most likely due to the highly incomplete state of many of the fossil OTUs to be tested herein. Therefore, the analyses were run with 13 constraints to ensure the generally accepted basic structure of the trees (as obtained from molecular data; Zheng and Wiens, 2016). The constraints defined Scincoidea (*Chalcides*, *Broadleysaurus*, *Ablepharus*), Lacertoidea (Amphisbaenia, Lacertidae, Teiidae), Anguimorpha (*Varanus*, *Anguis*, *Pseudopus*), Amphisbaenia (*Blanus*), Lacertidae (Gallotiinae and Lacertinae), Gallotiinae (*Gallotia* and *Psammodromus*), Lacertinae (Eremiadini and Lacertini), Eremiadini (*Acanthodactylus*, *Eremias*, *Mesalina*, *Ophisops*), Lacertini (*Algyroides*, *Anatololacerta*, *Archaeolacerta*, *Iberolacerta*, *Lacerta*, *Phoenicolacerta*, *Podarcis*, *Takydromus*, *Timon*, *Zootoca*), and the genera *Podarcis*, *Algyroides*, *Iberolacerta* and *Lacerta*. We excluded the French mOTUs, and the extinct species *Dracaenosaurus croizeti, Ligerosaurus pouiti*, *Mediolacerta roceki, Pseudeumeces cadurcensis*, *Plesiolacerta lydekkeri* and "*Lacerta*" *filholi* from all constraints, as no molecular data for those taxa are available. Therefore, they are considered to be "wild card taxa" and could be recovered at any position in the tree by the analysis. It should be noted that the constrained clades might only be recovered partly or not at all in the resulting strict consensus tree as a consequence of conflicting tree topologies in some cases.

Jaw element comparison

Character testing. In order to be able to compare the phylogenetic values of the three different jaw elements (premaxilla, maxilla, dentary) we had to ensure the comparability of the three datasets. To do so, we used both a quantitative and a qualitative approach for character comparison. First, we compared the number of characters existing in the matrix for each jaw element individually; characters scored for two or more elements at once were counted multiple times (e.g. characters that code for maxillary and dentary teeth).

In a second step, the characters describing the three jaw elements were classified into "quantitative" and "qualitative" characters, with a further subdivision of the quantitative characters into "meristic" and "morphometric", and of qualitative characters into "countable/measurable" and "shape-describing" characters (Table 1; classifications of the individual characters can be found in the Supplementary material). The distribution of the different character types then was expressed as a percentage of the total number of characters for each jaw element.

Morphotype testing. Based on the number of characters describing the premaxilla, maxilla and dentary obtained from the first part of the character testing, we took into account the preservation state or "specimen" completeness of the individual mOTUs. We calculated the actual percentages of scorable characters among the previously regarded characters describing the individual jaw elements.

The three jaw elements were represented by different numbers of morphotypes for each sample, changing the number of total OTUs, and thus effectively the taxon sampling among the three matrices. In order to avoid a potentially confounding impact on the analysis based on the number of OTUs, we ran the phylogenetic analysis ten times per jaw element under the same conditions as stated above, with subsampled datasets reduced to five randomly picked mOTUs for each analysis and ensuring that each mOTU was picked at least once.

In addition, we tested the stability of the mOTUs with respect to their tree position. We followed the procedure for rogue taxa

Table 1
List of character types and subtypes used for the quantitative approach of jaw element comparison with their definitions and examples.

Character type	Character subtype	Definition	Example
Quantitative	Meristic	character states are countable	Maxilla, number of labial foramina: 6 or less (0); >6 (1)
	Morphometric	character states are measurable	Premaxilla, tooth-bearing portion, curvature, anterior-posterior length to transverse width: <0.2 (wide) (0); 0.2–0.4 (intermediate) (1); >0.4 (narrow) (2)
Qualitative	Countable/measurable	character states are neomorphic (absent/present; Sereno, 2007) or have a "countable" state	Premaxilla, ascending nasal process, posterior end of medial ridge, shape in lateral view: bifid, with dorsal and ventral spurs (0); single (1)
	Shape-describing	character states are transformational (Sereno, 2007): they describe shapes that are not "measurable"/ "countable"	Dentary, subdental ridge, shape: straight (0); concave (1)

identification used in Pei et al. (2020) with minor modifications to their TNT script (improvecombin.run). In a first step, unstable (rogue) taxa were identified heuristically (prune nelsen). We allowed a maximum of $n + 1$ taxa to be pruned at the same time (n = number of mOTUs per jaw element). In a second step, the heuristically identified unstable taxa were checked by testing the tree resolution when adding or removing the unstable taxa in different combinations (prune-up-and-down). Here, combinations of up to $n + 1$ taxa could be reinserted in the tree and the pruning was evaluated with a factor F of 0.9. Factor F defines the penalty for the removal of a taxon, it varies between 0 and 1; the higher the number the more costly the removal. Given that our mOTUs were very fragmentary, we decided to select a higher factor F to identify the taxa whose removal increased the tree resolution the most. We identified unstable taxa for all analyses of the complete datasets (k = 5, 12 and 20). As last, we included only the stable mOTUs of each jaw element dataset. The analyses were run under the same parameters as before.

As a last test, we merged the locality-level mOTUs belonging to the same morphotype into a single cross-regional mOTU by following the majority rule. In this way, the amount of missing data could be reduced in some cases. Consequently, we created, in congruence with the number of observed morphotypes, five cross-regional mOTUs for the premaxilla, six for the maxilla and ten for the dentary dataset. The following morphotypes were present only in a single locality and therefore were kept as they were: P4 CE1-0, M2 CC1sup, M5 CE1-0, M6 CE1-0, D5 CE1-0, D6 CE1-0 and D10 Roq2. We reran the analyses in two steps: first, using only one cross-regional mOTU at a time, and then using all cross-regional mOTUs per jaw-element-dataset. The analyzing parameters were the same as before.

Results

Morphotype descriptions

Among the jaw elements in our sample, the dentaries were the most abundant representing 68%, with maxillae and premaxillae comprising 23% and 9% of the sample, respectively. In general, the sample from Coderet contained the highest number of jaw elements with 91% of the studied jaw elements coming from this locality. The distribution for Coderet was 66% dentaries, 25% maxillae and 9% premaxillae. For the localities La Colombière and Mas de Got B, neither premaxillae nor maxillae were present. The sample from Roqueprune 2 included 10% premaxillae and 90% dentaries.

Premaxillae. Five different lacertid morphotypes for the premaxilla were identified among the sample of Roqueprune 2 and five subsamples of Coderet (Table 2). The preservation of the studied elements generally comprises the tooth-bearing portion with partially preserved teeth, and the anterior part of the ascending nasal process, whereas the posterior end of the nasal process plus the articulation with the nasal are never preserved.

Morphotype P1 (Fig. 2a) is characterized by seven tooth positions, of which the median tooth is enlarged. The preserved teeth are monocuspid and somewhat globose with narrow longitudinal striae. In one specimen, we observed some indication of bicuspidity in one of the posterior-most teeth (within the sample from Fouilles Viret). The facets for articulation with the maxillae are large. The palatine processes bordering the depression on the horizontal plate are preserved in about half of the specimens. A small pit can be present at the transition of the tooth-bearing portion to the ascending nasal process. The ascending nasal process has a circular cross-section at its base. The ethmoidal foramina at the base of the ascending nasal process are not situated within fossae. The medial ridge on the ventral side of the preserved part of the ascending nasal process is not visible and it therefore probably does not reach far anteriorly.

Morphotype P2 (Fig. 2b) is rather slender, with seven tooth positions accommodating pencil-shaped teeth, which all seem to be of the same size. The tooth crowns are monocuspid with relatively less dense, narrowly spaced striae, compared to morphotype P1. Large maxillary facets are present, and the ethmoidal foramina are situated within fossae, which are posteriorly bordered by a ridge. Palatine processes were never preserved, so their real absence or presence cannot be

Table 2
Occurrences of morphotypes and their abundance given in absolute numbers. P1–P5, premaxillary morphotypes; M1–M6, maxillary morphotypes; D1–D10, dentary morphotypes; Cod, Coderet; FV, Fouilles Viret; CC1sup, Coderet Couche 1 sup; CCVsup, Coderet Couche Verte sup 1–25; CE1–0, Coderet E1–0; CH1–100, Coderet H1–100; CH1–75, Coderet H1–75; LaC, La Colombière; Roq2, Roqueprune 2; MdGB, Mas de Got B.

Locality	P1	P2	P3	P4	P5	M1	M2	M3	M4	M5	M6	D1	D2	D3	D4	D5	D6	D7	D8	D9	D10
Cod																					
FV	1	-	-	-	1	4	-	-	-	-	-	2	5	-	-	-	-	-	-	-	-
CC1sup	2	1	-	-	-	4	3	4	1	-	-	21	10	6	-	-	-	-	-	-	-
CCVsup	1	-	-	-	-	5	-	-	1	-	-	-	4	-	1	-	-	6	3	-	-
CE1-0	2	2	1	1	-	7	-	-	2	1	1	5	6	-	3	2	3	5	-	-	-
CH1-100	-	-	-	-	-	1	-	1	1	-	-	-	3	2	-	-	-	-	1	-	-
CH1-75	-	-	-	-	1	-	-	-	-	-	-	-	2	2	1	-	-	-	-	-	-
LaC	-	-	-	-	-	-	-	-	-	-	-	-	-	-	-	-	-	-	-	2	-
Roq2	-	-	1	-	-	-	-	-	-	-	-	-	-	-	-	-	-	-	1	7	1
MdGB	-	-	-	-	-	-	-	-	-	-	-	-	-	-	2	-	-	-	-	-	-

confirmed. The horizontal plate seems to have no depression. The ascending nasal process is very slender, dorsoventrally higher than wide, and the medial ridge on its ventral side does not reach far anteriorly.

Morphotype P3 (Fig. 2c) has an overall shape which is similar to morphotype P2. It has seven tooth positions with monocuspid, rounded and narrowly striated teeth. The maxillary facets on the tooth-bearing portion are smaller than in morphotype P2 but still large. The ethmoidal foramina are situated within fossae, which are not completely closed and delimited posteriorly by a ridge. A pit at the base of the ascending nasal process can be present. Palatine processes might be absent or broken off, and the horizontal plate has no depression. The preserved part of the ascending nasal process has parallel lateral margins and the medial ridge on its ventral side does not seem to reach far anteriorly, as it is not visible on the preserved part of the ascending nasal process.

Morphotype P4 (Fig. 2d) differs from the other morphotypes in having nine teeth. The teeth are slender, rather fang-like and curved posteriorly. Their tooth crowns show no sign of striation. The tooth-bearing portion is relatively wide and straight with steep and small maxillary facets. The ethmoidal foramina are located lateral to the ascending nasal process, penetrating the horizontal lamina. The ascending nasal process is wider than dorsoventrally high and seems to be straight throughout its entire length with the medial ridge probably being restricted to the posterior part.

Morphotype P5 (Fig. 2e) has seven tooth positions with monocuspid, globose-like teeth which bear narrowly spaced, longitudinal striae. The maxillary facets are deep and large. The horizontal plate is depressed and continues into two palatine processes. At the base of the ascending nasal process, two pairs of ethmoidal foramina are present; they are not situated within fossae. The ascending nasal process has parallel margins and is wider than dorsoventrally high. The medial ridge is not reaching far anteriorly on its ventral side.

Maxillae. The preservation of the maxillae was rather fragmentary. Less than 50% of a single element was preserved on average, mostly representing isolated anterior, central and posterior parts. Anterior parts were generally preserved without the facial process and with broken anteromedial/-lateral premaxillary processes. In total, six morphotypes among the maxillae were identified in five subsamples of Coderet (Table 2).

Morphotype M1 (Fig. 3a) has a maximum of 12 tooth positions preserved in a single element, the total number of teeth in one element is probably between 16 and 20. Most teeth seem to be tricuspid with smooth tooth crowns. In the anterior half, large and robust teeth are present, followed by abruptly smaller teeth in the central part, which are relatively consistent in size. The tooth size increases gradually posteriorly, where the most robust teeth are located. The tooth row is straight in ventral view. For the articulation of the palatine, a slight medial extension is present. The anterolateral premaxillary process has a concave ventral edge. The facial process has a uniform external surface with a well-developed dermal ornamentation. The anterior margin of the facial process is perpendicular to the dental crest for some distance and a small subtriangular process projects anteriorly from the anterodorsal corner of the facial process. On the medial side, the anterior margin is connected with the carina maxillaris by a small ridge. There is no step visible at the orbital margin of the zygomatic process.

Morphotype M2 (Fig. 3b) was never preserved with a facial process. An indication of dermal ornamentation is present. The maximum number of observed teeth in a single element is 12, whereas the total number is probably approximately 16–20 teeth. The

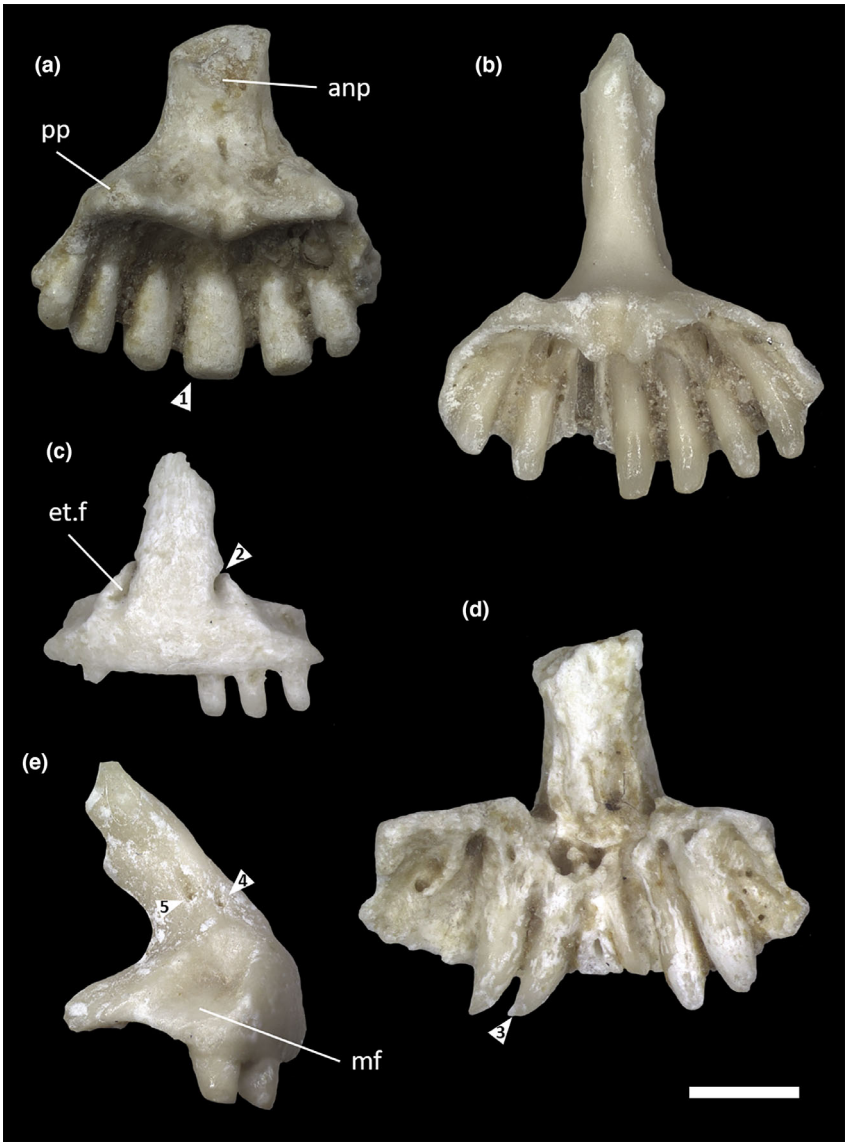

Fig. 2. Overview of premaxilla morphotypes. (a) Morphotype P1, premaxilla from Coderet Couche 1 sup (CC1sup-1) in posterior view. (b) Morphotype P2, premaxilla from Coderet Couche 1 sup (CC1sup-3) in posterior view. (c) Morphotype P3, premaxilla from Coderet E1-0 (CE1-0-5) in anterior view. (d) Morphotype P4, premaxilla from Coderet E1-0 (CE1-0-6) in posterior view. (e) Morphotype P5, premaxilla from Fouilles Viret (FV-2) in right lateral view. The arrowheads mark important diagnostic structures: 1, enlarged median tooth; 2, ethmoidal foramen within fossa which is not completely closed and bordered posteriorly by a ridge; 3, fang-like, pointed tooth; 4, ethmoidal foramen without fossa; 5, second ethmoidal foramen without fossa. anp, ascending nasal process; et.f, ethmoidal foramen; mf, maxillary facet; pp, palatine process. Scale bar 1 mm. Individual and more detailed figures of the morphotypes can be found in the Supplementary material.

majority of the tooth crowns seem to be tricuspid with widely spaced striae, but bicuspid teeth do occur in the anterior part. The four posterior-most teeth are significantly smaller and less robust than the succeeding ones in the posterior half. Teeth in the central part decrease gradually in size and robustness. The tooth row is straight in ventral view, and the supradental shelf extends slightly for the articulation with the palatine. The orbital margin of the zygomatic process seems to be smooth.

Morphotype M3 (Fig. 3c) was always preserved without the premaxillary processes, but the nasal recess and central-posterior parts were present. The facial process is incomplete in all elements. Its anterior margin is clearly perpendicular to the dental crest and connected with the carina maxillaris on the medial side by a small ridge. The lateral surface is uniform without a distinct groove, but with well-developed dermal ornamentation. The zygomatic process seems to be slightly undulating, but without a distinct step. The

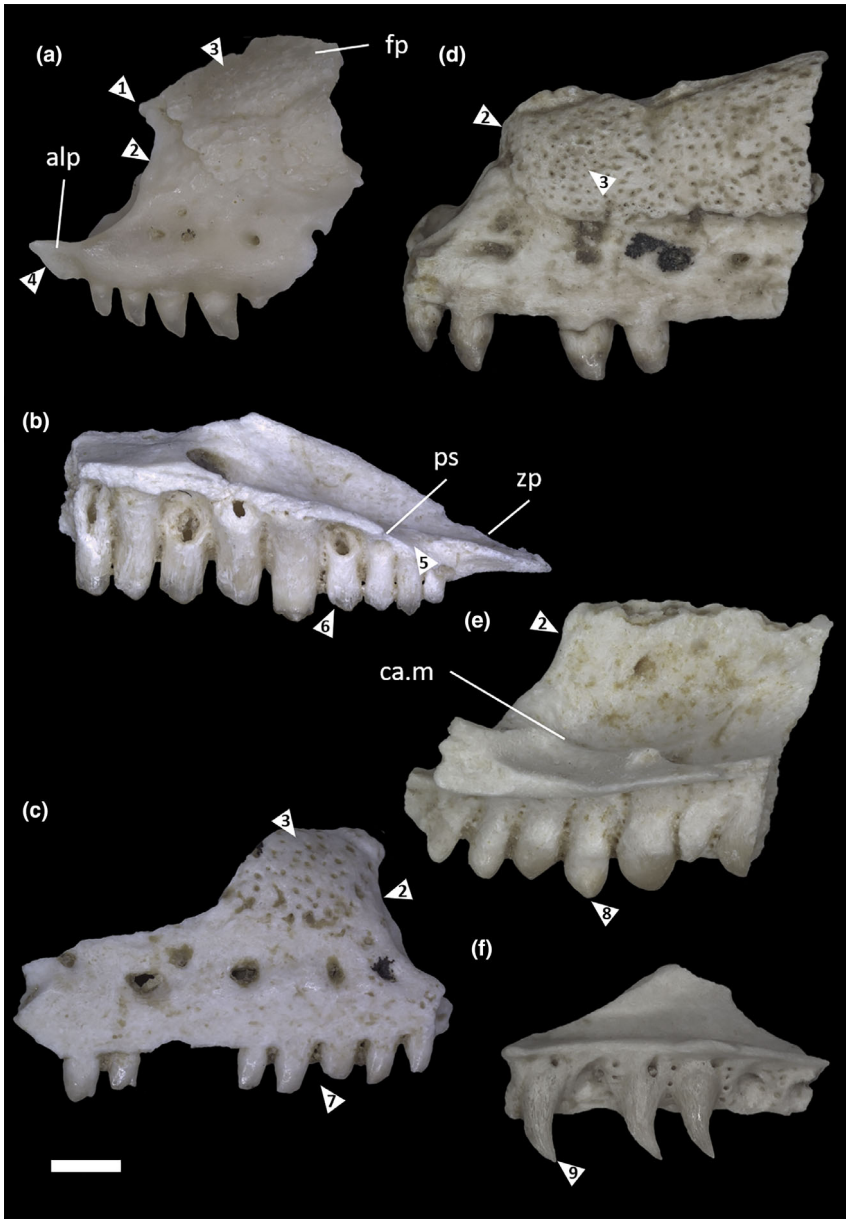

Fig. 3. Overview of maxilla morphotypes. (a) Morphotype M1, left maxilla from Coderet E1-0 (CE1-0-7) in lateral view. (b) Morphotype M2, right maxilla from Coderet Couche 1 sup (CC1sup-8) in medial view. (c) Morphotype M3, right maxilla from Coderet Couche 1 sup (CC1sup-11) in lateral view. (d) Morphotype M4, left maxilla from Coderet Couche 1 sup (CC1sup-15) in lateral view. (e) Morphotype M5, right maxilla from Coderet E1-0 (CE1-0-16) in medial view. (f) Morphotype M6, right maxilla from Coderet E1-0 (CE1-0-17) in medial view. The arrowheads mark important diagnostic structures: 1, subtriangular process; 2, facial process which is perpendicular to dental crest; 3, dermal ornamentation; 4, concave ventral edge of anterolateral premaxillary process; 5, slight medial extension for articulation with palatine; 6, abruptly smaller and less robust posterior-most teeth; 7, larger tooth in anterior-half; 8, globose-like, monocuspid tooth; 9, fang-like, pointed tooth. alp, anterolateral process; ca.m, carina maxillaris; fp, facial process; ps, palatine shelf; zp, zygomatic process. Scale bar 1 mm. Individual and more detailed figures of the morphotypes can be found in the Supplementary material.

development of tooth size and robustness throughout the tooth row is similar to morphotype M1, but the tri- and bicuspid teeth have widely spaced striae instead of being smooth. The preserved teeth in the anterior half are more robust than the posteriorly succeeding teeth, whereas the posterior-most teeth seem to be the most robust.

Morphotype M4 (Fig. 3d) is more robust and larger than morphotypes M1, M2 and M3, as well as M6. Only the anterior part is preserved. The lateral surface has no groove that would separate the ventral and dorsal portions, but a well-developed dermal ornamentation is present. The anterior margin of the partly preserved facial process is perpendicular to the dental

crest for some distance. On the medial side, the anterior margin is connected with the carina maxillaris by a small ridge. The anterolateral premaxillary process has a concave ventral edge in lateral view. The anteromedial premaxillary process bears a dorsomedially projecting spur close to the anterior end. The three to four anterior-most teeth are smaller and less robust than the (approximately) two succeeding ones, which are then followed by again less robust teeth; the increase in size seems to be gradual. The teeth are slightly fang-like with tooth apices pointing posteriorly. The tooth crowns are mostly mono- or bicuspid with widely spaced striae; there is some indication of tricuspidity present in the more posterior teeth.

Morphotype M5 (Fig. 3e) is relatively robust with a uniform external surface and no dermal ornamentation. The anterior margin of the facial process is perpendicular to the dental crest and does not bear a subtriangular process. On the medial side, the anterior margin is connected to the carina maxillaris by a small ridge. The preserved onset of the anterolateral premaxillary process shows a concave ventral edge. The teeth are similar to the ones of the premaxilla morphotype P1 in being monocuspid and globose-like with narrowly spaced striae on the tooth crowns. In general, the tooth size seems to increase distinctly posteriorly.

Morphotype M6 (Fig. 3f) has a rather slender shape with a uniform external surface and no dermal ornamentation. The teeth are monocuspid and fang-like with strongly backwards curved apices. The crown surfaces have no striation.

Dentaries. The dentaries always lack the angular process, and for most of the elements, either only the posterior or only the anterior part is preserved. However, one almost complete mandible and some almost complete dentaries were among the samples. In total, ten morphotypes could be identified among the studied bones from all four localities (Table 2).

Morphotype D1 (Fig. 4a) is slender, but continuously broadens dorsoventrally towards its distal end. The maximum number of teeth observed in a complete tooth row is 23. Most of the teeth seem to be bicuspid and no striation is visible. However, tricuspid teeth are present in the posterior half. The change in tooth size is gradual with the most robust teeth being located in the posterior part. The subdental ridge is concave; its thickness increases anteriorly. A distinct splenial facet is present, which indicates a splenial extending for approximately ¾ of the tooth row. The anterior-most teeth are strongly tilted anteriorly. The Meckelian canal is triangular and reaches the symphysis, which seems to have a distinct articular facet. The coronoid facet is distinct.

Morphotype D2 (Fig. 4b,c) is very similar to morphotype D1. Its shape also is rather slender, but continuously broadening distally. The majority of the preserved teeth are bicuspid, a few tricuspid teeth occur in the posterior half. At the tip of the dentary, the teeth are procumbent. The tooth crowns have widely spaced striae. The Meckelian canal reaches the symphysis. The articulation facet of the symphysis seems to be distinct. The subdental ridge is concave and thickens anteriorly. Two elements are preserved with parts of the splenial (among the sample of Fouilles Viret, Coderet E1-0), which has a bifid anterior end. The extent of the splenial seems to be approximately ¾ of the tooth row with a distinct splenial facet. The coronoid facet is distinct.

Morphotype D3 (Fig. 4d,e) is more robust than the other dentary morphotypes. The concave subdental ridge is very thick, with the greatest thickness anteriorly, and a well-developed splenial facet. Teeth at the tip of the dentary are tilted anteriorly. The most robust teeth in the posterior part of the dentary show clear tricuspidity, whereas bicuspid teeth are present in the anterior part. The tooth crowns have widely spaced longitudinal striae. The coronoid facet is distinct. The Meckelian canal is triangular and open until the symphysis, which seems to have a distinct articulation facet.

Morphotype D4 (Fig. 4f,g) is similar to the morphotypes D1 and D2. The element is continuously broadening with the most robust teeth in the posterior part. The tooth size gradually decreases anteriorly. Tricuspid teeth are present in the posterior part, whereas the teeth become bicuspid anteriorly and might be monocuspid close to the symphysis. The anterior-most teeth are strongly anteriorly tilted. The tooth crowns have narrowly spaced striae. The subdental ridge is concave and its thickness is increasing anteriorly. The splenial facet is distinct and the posterior end of the splenial is

Fig. 4. Overview of dentary morphotypes D1–D5. (a) Morphotype D1, right dentary from Coderet Couche 1 sup (CC1sup-16) in medial view. (b, c) Morphotype D2, right dentary from Coderet Couche Verte sup 1-25 (CCVsup-8) in medial view (b), tooth of a left dentary from Coderet Couche 1 sup (CC1sup-46) in medial view (c). (d, e) Morphotype D3, right dentary from Coderet Coche 1 sup (CC1sup-47) in medial view (d), teeth of a left dentary from Coderet H1-100 (CH1-100-7) in medial view (e). (f, g) Morphotype D4, right dentary from Coderet E1-0 (CE1-0-29) in medial view (f), tooth of a left dentary from Coderet E1-0 (CE1-0-31) in medial view (g). (h, i, j) Morphotype D5, right dentary from Coderet E1-0 (CE1-0-32) in medial (h) and ventral (i) view, tooth of a left dentary from Coderet E1-0 (CE1-0-33) in medial view (j). The arrowheads mark important diagnostic structures: 1, tricuspid tooth crown; 2, distinct articular facet on symphysis; 3, distinct splenial facet; 4, widely spaced striae; 5, narrowly spaced striae; 6, bicuspid tooth crown; 7, Meckelian canal that opened up at the tip. mk.c, Meckelian canal; spl.ft, splenial facet; sy, symphysis. Scale bars 1 mm. Individual and more detailed figures of the morphotypes can be found in the Supplementary material.

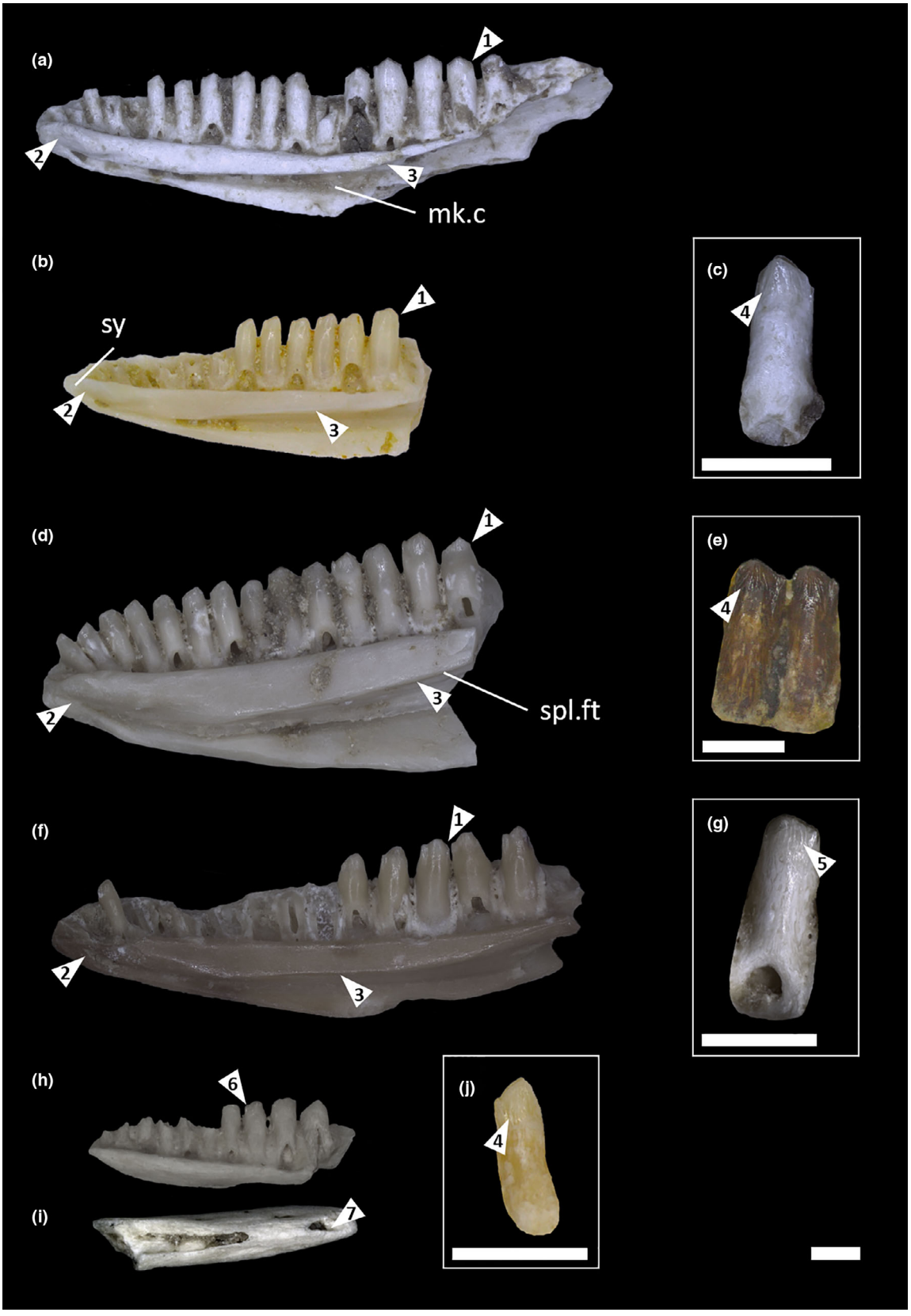
(a)
1
2
3
mk.c
(b)
sy
1
2
3
(c)
4
(d)
1
2
3
spl.ft
(e)
4
(f)
1
2
3
(g)
5
(h)
6
(i)
7
(j)
4

single and pointed. The articulation facet of the symphysis and the coronoid facet are distinct. The angular process is exceeding the apex of the coronoid.

Morphotype D5 (Fig. 4h–j) has, on the contrary to all other morphotypes, a Meckelian canal which is closed in the anterior part for approximately ¼ of the dental shelf, and that opens again at the very tip. It is situated rather ventrally. The articulation of the symphysis is fairly indistinct, and the teeth do not seem to be tilted anteriorly. The tooth crowns have widely spaced striae and are at least bicuspid. The tooth size increases posteriorly. The subdental ridge is rather straight. The dentary seems to be rather sickle-shaped. No distinct splenial articulation facet is visible. However, only the anterior part of this morphotype is preserved.

Morphotype D6 (Fig. 5a) is very slender and fragile. It appears to be sickle-shaped with a slightly concave subdental ridge and a weakly developed splenial facet. The preserved teeth are bicuspid with smooth tooth crowns.

Morphotype D7 (Fig. 5b–d) is slender, but its shape is continuously broadening posteriorly. The subdental ridge is similar to morphotype D6, and less strongly concave than in morphotypes D1, D2, D3 and D4. The splenial facet is distinct, but the splenial seems to extend less far anteriorly than in the other morphotypes (approximately ⅔ of tooth row). Therefore, the triangular Meckelian canal appears to be narrower than in the aforementioned morphotypes. The open portion of the canal reaches the symphysis, which has a distinct facet. The teeth at the tip are procumbent. In the posterior part, teeth with very distinct tricuspidity are present with widely spaced striae. The striation is less distinct in the specimens found in Coderet Couche Verte sup 1–25. The tooth size gradually decreases anteriorly. The coronoid facet is distinct.

Morphotype D8 (Fig. 5e,f) is similar to the morphotype D3. The subtriangular element has a concave subdental ridge that thickens anteriorly. The splenial facet is distinct; it probably extended for approximately ¾ of the tooth row. The most robust teeth are present in the posterior part, but the two or three posterior-most teeth are significantly less robust than their neighbouring teeth. Tooth size gradually decreases anteriorly. The tooth crowns have narrowly spaced striae and show tricuspidity in the posterior half, whereas bicuspid teeth are present in the anterior half. The coronoid facet is distinct, whereas the symphysis is relatively indistinct. The teeth at the tip do not seem to be tilted anteriorly.

Morphotype D9 (Fig. 5g) is similar to morphotype D7. It is relatively slender, with a concave subdental ridge. The teeth have bicuspid tooth crowns, and no indication of tricuspid teeth is visible. The tooth crowns appear to be smooth. The coronoid facet is very distinct. The splenial probably extended for approximately ⅔ of the tooth row, based on the distinct facets. The Meckelian canal is open until it reaches the seemingly indistinct symphysis. The most robust teeth are present in the posterior part of the dentary, but the two posterior-most teeth seem to be a bit less robust than their anterior neighbours. The teeth in the tip are procumbent.

Morphotype D10 (Fig. 5h,i) is preserved only as a single anterior tip. The teeth are upright, bulky and globose, with monocuspid tooth crowns bearing narrowly spaced striae. The anterior-most tooth also is the most robust one and the tooth size seems to decrease abruptly posteriorly. The Meckelian canal seems to be triangular (but is not preserved entirely), and reaches the symphysis, which has a distinct articulation facet. The teeth overtop the dental crest by approximately ⅔, whereas in all other observed dentaries the teeth overtop the dental crest by less than half of their height.

Phylogenetic analysis

Premaxillae. The analysis of the complete premaxilla dataset produced by far the best strict consensus tree resolution among the three jaw elements. However, all mOTUs were recovered outside Lacertidae (Fig. 6). A polytomy was present at the base of the tree. It was composed of four OTUs (P1 CCVsup, *Ablepharus kitaibelii*, *Chalcides ocellatus* and *Varanus exanthematicus*) and four branches: (1) a partly recovered Anguimorpha clade with ((P4 CE1-0, *Anguis veronensis*), *Pseudopus apodus*); (2) a smaller polytomy with ((*Broadleysaurus major*, P3 Roq2), (P2 CC1sup, P2 CE1-0), P3 CE1-0)); (3) a second smaller polytomy with ((*Dracaenosaurus croizeti* (Cod),

Fig. 5. Overview of dentary morphotypes D6–D10. (a) Morphotype D6, right dentary from Coderet E1-0 (CE1-0-34) in medial view. (b, c, d) Morphotype D7, left dentary from Coderet E1-0 (CE1-0-37) in medial view (b), left dentary from Coderet E1-0 (CE1-0-38) in medial view (c), tooth of a left dentary from Coderet Couche Verte sup 1-25 (CCVsup-14) in medial view (d). (e, f) Morphotype D8, right dentary from Coderet H1-100 (CH1-100-9) in medial view (e), tooth of a left dentary from Coderet Couche Verte sup 1-25 (CCVsup-19) in medial view (f). (g) Morphotype D9, left dentary from La Colombière (LaC-1) in medial view. (h, i) Morphotype D10, right dentary from Roqueprune 2 (Roq2-10) in medial view (h), tooth of the right dentary from Roqueprune 2 (Roq2-10) in lateral view (i). The arrowheads mark important diagnostic structures: 1, weakly developed splenial facet; 2, very distinct tricuspid tooth crown; 3, distinct splenial facet; 4, distinct articular facet on symphysis; 5, widely spaced striae; 6, smaller and less robust posterior-most teeth; 7, narrowly spaced striae; 8, large and globose-like monocuspid tooth. Scale bars 1 mm. Individual and more detailed figures of the morphotypes can be found in the Supplementary material.

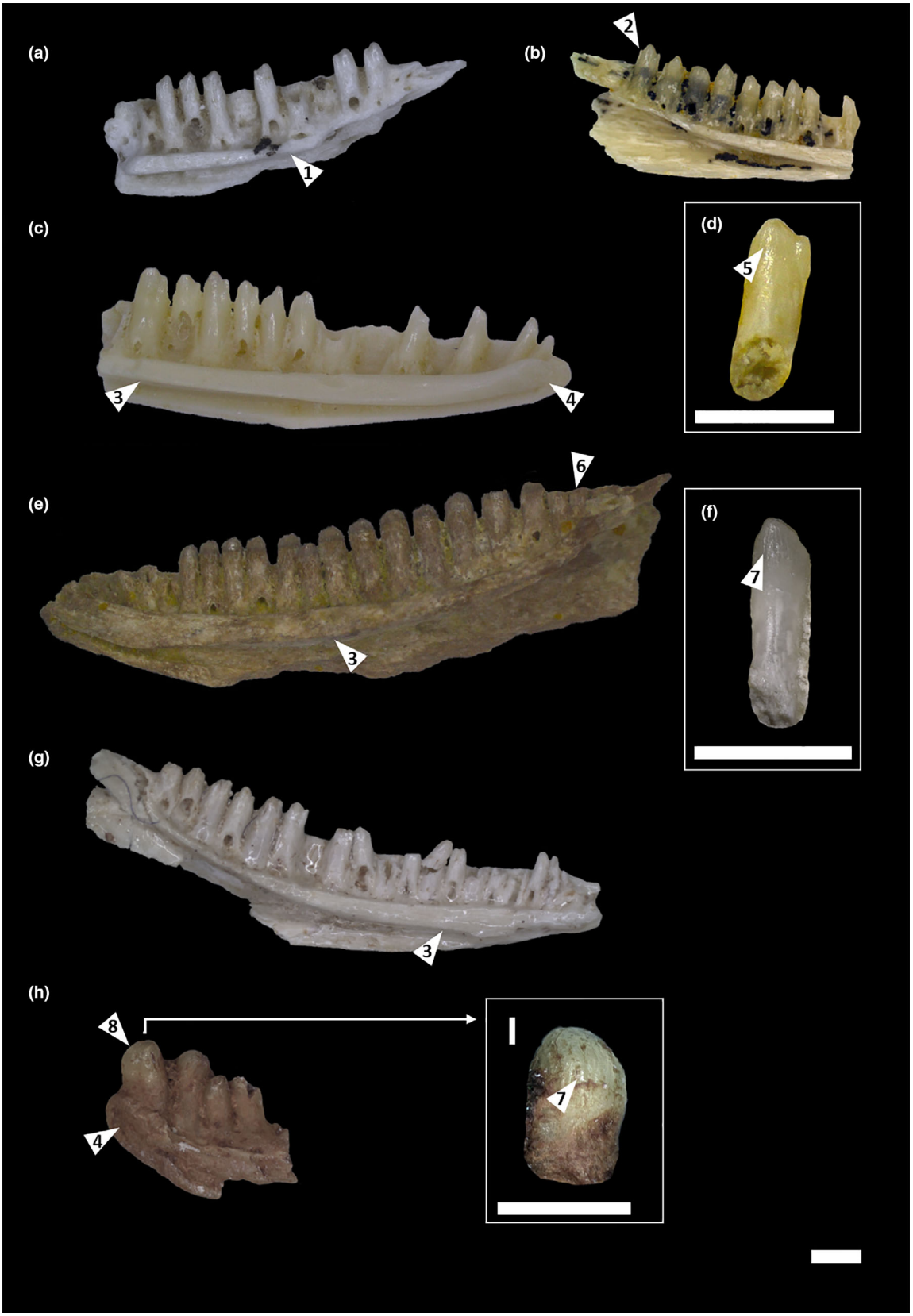
(a)
1
(b)
2
(c)
3
4
(d)
5
(e)
6
3
(f)
7
(g)
3
(h)
8
4
7

Dracaenosaurus croizeti (Cou), P1 FV, P1 CC1sup, P1 CE1-0), (P5 FV, P5 CH1-75)); and (4) an entirely resolved clade of Lacertoidea.

When applying a $k = 5$, higher taxonomic relationships were almost completely resolved, showing the general topology of (Gekkota, (Anguimorpha, (Scincoidea, Lacertoidea))). The mOTUs P3 Roq2 and P4 CE1-0 were recovered within the same clades as stated before. The other mOTUs were recovered as part of Lacertoidea with P1 CCVsup at the base forming a polytomy with two other branches: (1) a smaller polytomy (*Dracaenosaurus croizeti* (Cod), *Dracaenosaurus croizeti* (Cou), P1 FV, P1 CC1sup, P1 CE1-0, P5 FV, P5 CH1-75, (*Blanus rufus*, *Blanus strauchi*)); and (2) (P2 CC1sup, P2 CE1-0, P3 CE1-0, (*Salvator merianae* + Lacertidae).

Maxillae. The strict consensus trees with the maxilla mOTUs recovered a large polytomy, which consisted of all OTUs but the outgroup taxon *Gekko gecko* (Fig. 7). No further resolved subclades including any of the mOTUs were recovered, but two clades involving mOTUs within the large polytomy were found only for the analysis with $k = 5$: (1) a polytomy with (M3 CC1sup, M3 CH1-100, M4 CC1sup, M4 CE1-0, M4 CH1-100, *"Lacerta" filholi* (PdF)); and (2) a clade with (M2 CC1sup, *Ligerosaurus pouiti*).

Dentaries. Similar to the recovered trees based on the maxilla mOTUs, the strict consensus trees with the dentary mOTUs included a large polytomy consisting of all OTUs but the outgroup taxon (Fig. 8). Four resolved clades (three for $k = 5$) comprising mOTUs were found within the polytomy: (1) (*Iberolacerta cyreni* (Müller and Hellmich, 1937), D5 CE1-0), *Iberolacerta monticola* (Boulenger, 1905)); (2) (*Algyroides nigropunctatus* (Duméril and Bibron, 1839), D6 CE1-0), *Algyroides fitzingeri* (Wiegmann, 1834)); (3) (*Blanus strauchi*, *Blanus rufus*), D10 Roq2); and (4) (D9 LaC, *Podarcis tiliguerta* (Gmelin, 1789)) (only for $k = 12$ and 20).

Fossil wild card taxa. The positions of the eight extinct taxa were not consistent throughout. Resolved positions for *Mediolacerta roceki* and *Pseudeumeces cadurcensis* were observed only for the analysis with the premaxillae. They were recovered at the base of Lacertidae with *Pseudeumeces cadurcensis* being more basal. Also, *Ligerosaurus pouiti* was only recovered at a resolved position when analyzing the premaxilla dataset. It was found within the clade of *Iberolacerta* ($k = 12$ and 20) or within Gallotiinae ($k = 5$). For *Plesiolacerta lydekkeri* only the analyses with premaxillae and maxillae resulted in a resolved position within *Timon*, as sister to *Timon lepidus* (Daudin, 1802) ($k = 12$ and 20) or as sister to *Timon pater* (Lataste, 1880) ($k = 5$). The two *Dracaenosaurus croizeti* OTUs (from Cournon and Coderet) were always sister to each other, and for analyses with dentaries and maxillae they were recovered within Anguimorpha. In the case of the premaxilla dataset, the two taxa were found outside of Lacertoidea without further resolution ($k = 12$ and 20) or in close relationship to Amphisbaenia ($k = 5$). The two OTUs of "*Lacerta*" *filholi* (from Pech-du-Fraysse and Coderet) were found, for the analysis with premaxillae, nested within Gallotiinae. For the analysis with dentaries, only the taxon from Coderet was found sister to *Gallotia caesaris* (Lehrs, 1914).

Jaw element comparison

Character testing. Our character matrix contains 32 characters coding for premaxillae, 28 characters for maxillae and 24 characters for dentaries from the total number of 180 cranial characters. The classification of the characters describing the premaxilla, maxilla and dentary into quantitative, qualitative and their subtypes, showed that the majority of the characters are qualitative (84% of the premaxillary characters, 89% of the maxillary characters and 92% of the dentary characters; Table 3). When comparing the distribution of characters among the subtypes "countable/measurable", and "shape-describing", a smaller number of characters is attributed to the subtype "shape-describing" (31% in the premaxillae, 32% in the maxillae and 41% in the dentaries). The character distribution among the subtypes of quantitative characters shows that maxillary and dentary characters are exclusively meristic in the used dataset, whereas for the premaxillae 60% of the quantitative characters are attributed to morphometric characters.

Morphotype testing. The state of completeness was calculated based on the number of applicable

Fig. 6. Strict consensus tree of analysis of the complete premaxilla dataset using a value of $k = 20$ based on six most parsimonious trees (MPTs). Length of strict consensus: 1547 steps; CI of strict consensus: 0.180; RI of strict consensus: 0.441. Length of MPTs: 1499 steps; CI of MPTs: 0.186; RI of MPTs: 0.462. Arrowheads indicate the premaxilla mOTUs; daggers show the fossil OTUs; locks mark clades with fulfilled constraining. Black branches, non-crown-lacertids; blue branches, Gallotiinae; green branches, Lacertinae. FV, Fouilles Viret; CC1sup, Coderet Couche 1 sup; CE1-0, Coderet E1-0; CH1-75, Coderet H1-75; CCVsup, Coderet Couche Verte sup 1-25; Roq2, Roqueprune 2; PdF, Pech-du-Fraysse; Cod, Coderet; Cou, Cournon. Strict consensus trees of $k = 5$ and 12 can be found in the Supplementary material.

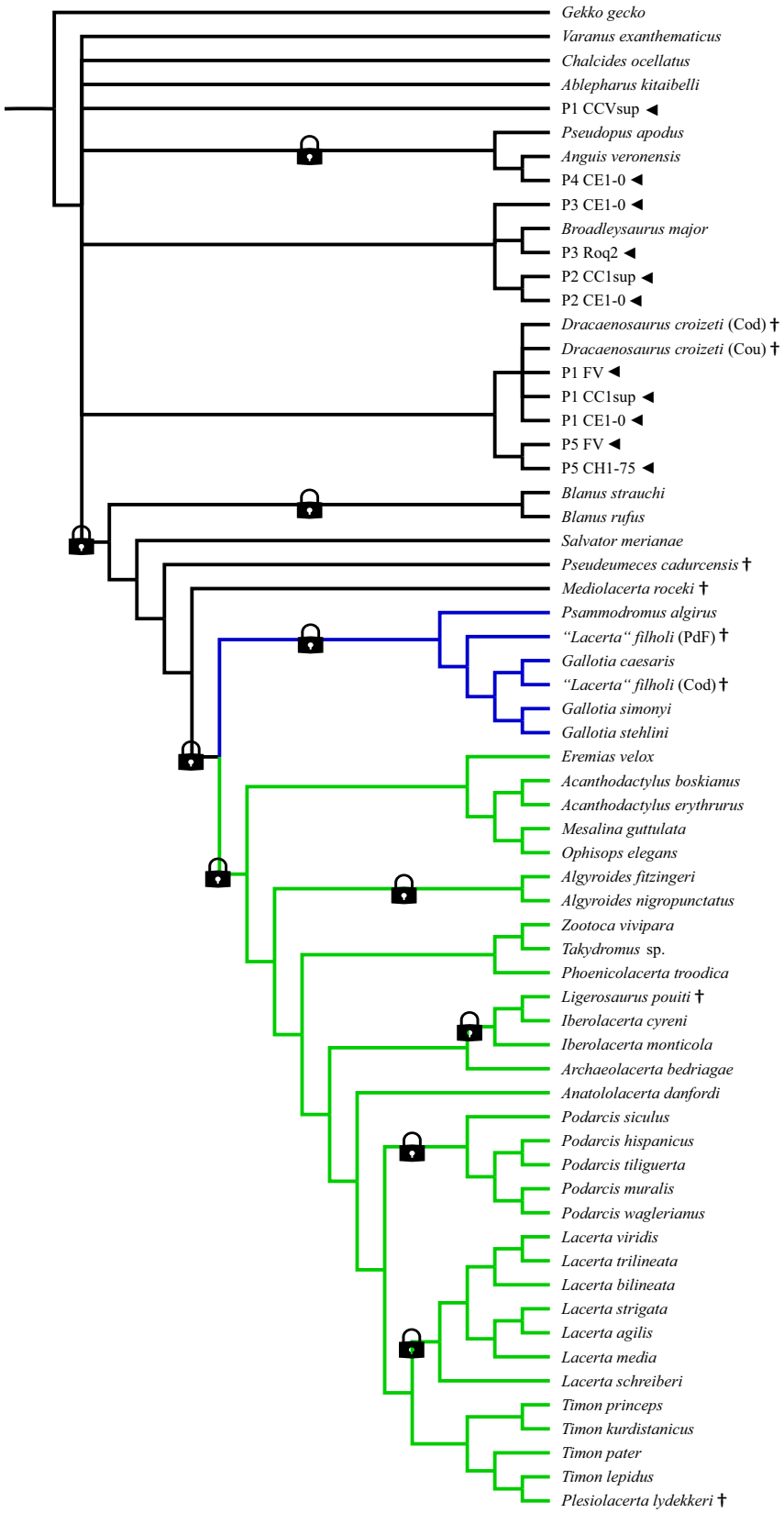
Gekko gecko
Varanus exanthematicus
Chalcides ocellatus
Ablepharus kitaibelli
P1 CCVsup ◄
Pseudopus apodus
Anguis veronensis
P4 CE1-0 ◄
P3 CE1-0 ◄
Broadleysaurus major
P3 Roq2 ◄
P2 CC1sup ◄
P2 CE1-0 ◄
Dracaenosaurus croizeti (Cod) †
Dracaenosaurus croizeti (Cou) †
P1 FV ◄
P1 CC1sup ◄
P1 CE1-0 ◄
P5 FV ◄
P5 CH1-75 ◄
Blanus strauchi
Blanus rufus
Salvator merianae
Pseudeumeces cadurcensis †
Mediolacerta roceki †
Psammodromus algirus
"Lacerta" filholi (PdF) †
Gallotia caesaris
"Lacerta" filholi (Cod) †
Gallotia simonyi
Gallotia stehlini
Eremias velox
Acanthodactylus boskianus
Acanthodactylus erythrurus
Mesalina guttulata
Ophisops elegans
Algyroides fitzingeri
Algyroides nigropunctatus
Zootoca vivipara
Takydromus sp.
Phoenicolacerta troodica
Ligerosaurus pouiti †
Iberolacerta cyreni
Iberolacerta monticola
Archaeolacerta bedriagae
Anatololacerta danfordi
Podarcis siculus
Podarcis hispanicus
Podarcis tiliguerta
Podarcis muralis
Podarcis waglerianus
Lacerta viridis
Lacerta trilineata
Lacerta bilineata
Lacerta strigata
Lacerta agilis
Lacerta media
Lacerta schreiberi
Timon princeps
Timon kurdistanicus
Timon pater
Timon lepidus
Plesiolacerta lydekkeri †

characters describing the premaxilla, maxilla and dentary. However, for some dentary morphotypes we were also able to score characters describing the splenial and/or coronoid, given that they were found articulated. Nonetheless, only characters describing the dentary were included in the calculation here. Therefore, the preservation state of the premaxillae, maxillae and dentaries allowed us to score the respective mOTUs for an average of 68% (range 59%–75%), 39% (25%–61%) and 64% (38%–79%) of the available characters, respectively (for state of completeness of the individual mOTUs and their individual positions during analyses, see Appendix 2).

The analysis of the reduced datasets with the premaxillae generally recovered the same tree topologies as seen for the complete dataset. In 80% of the cases, the higher systematic topologies were resolved (as seen in complete premaxilla analysis under $k = 5$). The mOTUs of P1, P4 and P5 were all recovered within Anguimorpha with mOTU P4 always being sister to *Anguis veronensis*. Under $k = 5$, the P5 mOTUs and P1 CE1-0 fluctuated between Anguimorpha and a basal position within Lacertoidea with the P5 mOTUs being in a clade with Amphisbaenia. mOTUs P1 FV and P1 CC1sup were always found in a clade with Amphisbaenia when applying $k = 5$. The mOTUs P2 and P3 were recovered within the clade of Scincoidea, with P3 Roq2 being consistently found as the sister taxon to *Broadleysaurus major*. But P2 mOTUs and P3 CE1-0 were also found as sister to or in polytomy with *Salvator merianae* + Lacertidae ($k = 5$).

The analyses with the reduced maxilla datasets still resulted in strict consensus trees with large polytomies. However, 30% of the trees had the clade of Anguimorpha resolved, and in another 30%, the large polytomy was restricted to Lacertidae. Within the polytomies, some smaller clades were found. mOTUs M5 CE1-0 and M6 CE1-0 were never found in a resolved position. The M1 mOTUs were mostly recovered within Lacertidae, with M1 CCVsup ($k = 5$) and M1 CH1-100 found within *Podarcis*. Among the M1 mOTUs only M1 FV ($k = 12$ and 20) and M1 CC1sup were positioned in the clade of Gallotiinae. mOTU M2 CC1sup was always recovered as Gallotiinae. The mOTU M3 CC1sup was found within Gallotiinae ($k = 5$), and M3 CH1-100 was either recovered as sister to "*Lacerta*" *filholi* (from Pech-du-Fraysse) within the unresolved Lacertoidea clade ($k = 5$ and 12) or as well within Gallotiinae ($k = 20$). The M4 mOTUs were found unresolved within Lacertidae, and M4 CC1sup also was recovered as Gallotiinae ($k = 5$). Only M4 CCVsup was found in no further resolved position within Lacertoidea.

When analyzing the reduced dentary datasets, remarkably better resolved strict consensus trees were obtained than for the complete dataset. The resolution of the reduced dentary datasets was comparable to the one of the premaxilla datasets, and the same general tree topology was observed. However, larger polytomies were still present in about half of the cases. The three mOTUs D5 CE1-0, D6 CE1-0 and D10 Roq2 were recovered at the same positions as when analyzing the complete dataset. The D1 mOTUs fluctuated between the clade of Gallotiinae and *Lacerta*, with only D1 FV being consistently found within *Lacerta*. Among the D2 mOTUs, D2 FV and D2 CCVsup were always recovered within *Lacerta*. mOTU D2 CE1-0 switched between a position within Gallotiinae (all *k*-values), *Podarcis* ($k = 5$), or as sister to *Timon* + *Lacerta* ($k = 12$ and 20), D2 CH1-100 was found unresolved within Lacertidae ($k = 5$ and 12) and Gallotiinae ($k = 20$), and D2 CH1-75 was in an undetermined position within Lacertoidea. For mOTUs D3, only D3 CC1sup was found further resolved than Lacertoidea as part of Gallotiinae ($k = 20$) or *Lacerta* (all *k*-values). All D4 mOTUs were recovered as Lacertoidea, with D4 CE1-0 being found within Gallotiinae (all *k*-values), *Podarcis* ($k = 5$), or as sister to *Timon* + *Lacerta* ($k = 12$ and 20), and D4 MdGB being found as part of *Podarcis* ($k = 5$) or as sister to *Timon* + *Lacerta* ($k = 20$). The mOTU D4 CCVsup switched between a position within Lacertoidea or Scincoidea. mOTU D7 CE1-0 was consistently found within *Lacerta*, whereas D7 CCVsup was found in an unresolved position within Lacertoidea. Among the D8 mOTUs, only D8 CH1-100 was found further resolved in a clade with Gallotiinae, the others were found only as Lacertoidea (D8 CCVsup) or in no resolved position at all (D8 Roq2). The D9 mOTUs were found either within *Podarcis* or as sister to *Timon* + *Lacerta*, and in a few cases (under $k = 20$) within Gallotiinae.

The stability tests identified in total three of 11 premaxillae, eight of 14 maxillae and seven of 26 dentary mOTUs as unstable (Appendix 2). After excluding the unstable mOTUs and rerunning the analyses, the tree resolution improved significantly compared to the

Fig. 7. Strict consensus tree of analysis of the complete maxilla dataset using a value of $k = 20$ based on more than 100 000 MPTs (overflow). Length of strict consensus: 2269 steps; CI of strict consensus: 0.123; RI of strict consensus: 0.112. Length of MPTs: 1499 steps; CI of MPTs: 0.186; RI of MPTs: 0.455. Arrowheads indicate the maxilla mOTUs; daggers show the fossil OTUs; black locks mark clades with fulfilled constraining, the two grey connected locks represent a single constraint which split up into two clades during analysis. Black branches, non-crown-lacertids; blue branches, Gallotiinae; green branches, Lacertinae. FV, Fouilles Viret; CC1sup, Coderet Couche 1 sup; CE1-0, Coderet E1-0; CH1-100, Coderet H1-100; CCVsup, Coderet Couche Verte sup 1-25; PdF, Pech-du-Fraysse; Cod, Coderet; Cou, Cournon. Strict consensus trees of $k = 5$ and 12 can be found in the Supplementary material.

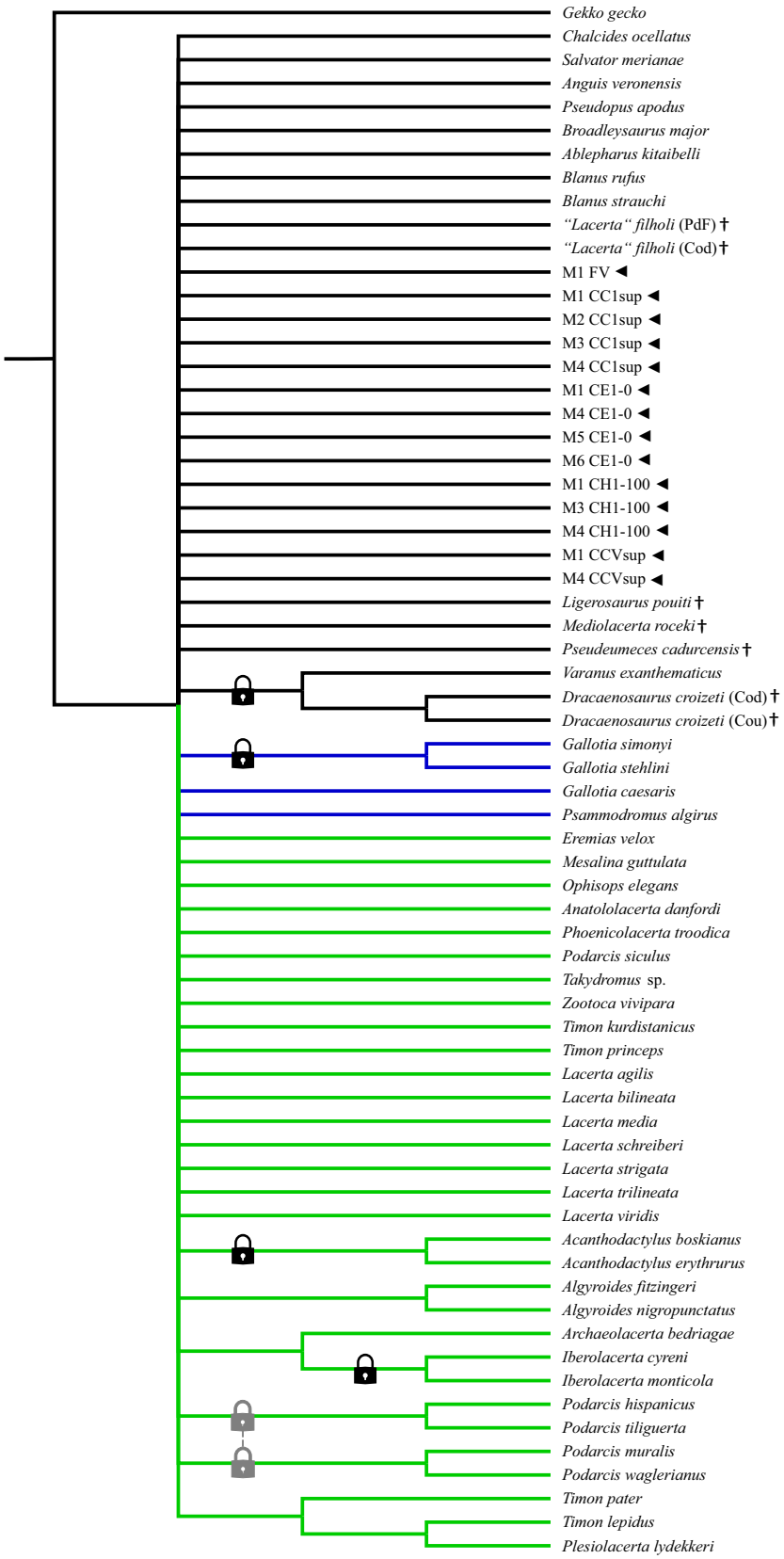
Gekko gecko
Chalcides ocellatus
Salvator merianae
Anguis veronensis
Pseudopus apodus
Broadleysaurus major
Ablepharus kitaibelli
Blanus rufus
Blanus strauchi
"Lacerta" filholi (PdF) †
"Lacerta" filholi (Cod) †
M1 FV ◄
M1 CC1sup ◄
M2 CC1sup ◄
M3 CC1sup ◄
M4 CC1sup ◄
M1 CE1-0 ◄
M4 CE1-0 ◄
M5 CE1-0 ◄
M6 CE1-0 ◄
M1 CH1-100 ◄
M3 CH1-100 ◄
M4 CH1-100 ◄
M1 CCVsup ◄
M4 CCVsup ◄
Ligerosaurus pouiti †
Mediolacerta roceki †
Pseudeumeces cadurcensis †
Varanus exanthematicus
Dracaenosaurus croizeti (Cod) †
Dracaenosaurus croizeti (Cou) †
Gallotia simonyi
Gallotia stehlini
Gallotia caesaris
Psammodromus algirus
Eremias velox
Mesalina guttulata
Ophisops elegans
Anatololacerta danfordi
Phoenicolacerta troodica
Podarcis siculus
Takydromus sp.
Zootoca vivipara
Timon kurdistanicus
Timon princeps
Lacerta agilis
Lacerta bilineata
Lacerta media
Lacerta schreiberi
Lacerta strigata
Lacerta trilineata
Lacerta viridis
Acanthodactylus boskianus
Acanthodactylus erythrurus
Algyroides fitzingeri
Algyroides nigropunctatus
Archaeolacerta bedriagae
Iberolacerta cyreni
Iberolacerta monticola
Podarcis hispanicus
Podarcis tiliguerta
Podarcis muralis
Podarcis waglerianus
Timon pater
Timon lepidus
Plesiolacerta lydekkeri

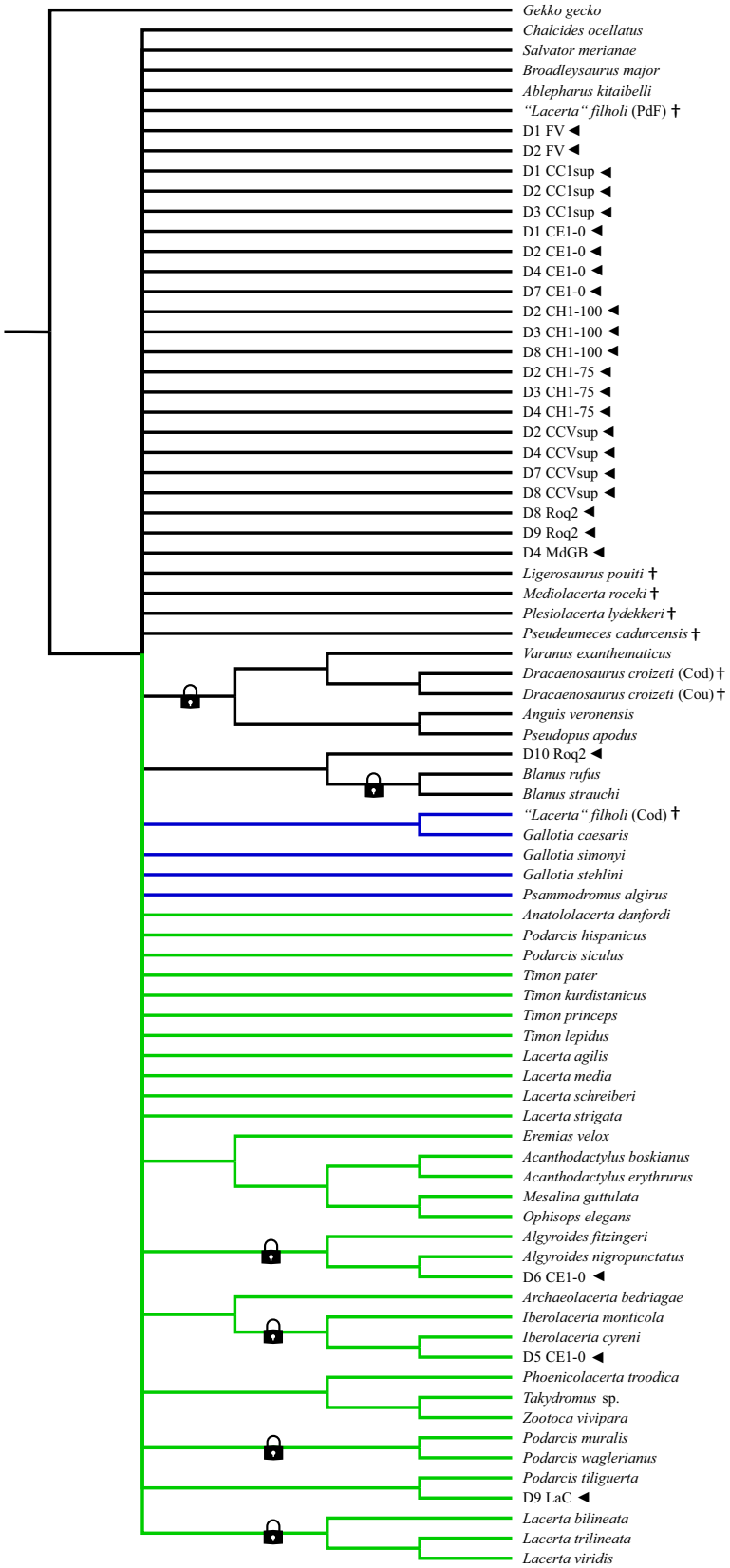
Gekko gecko
Chalcides ocellatus
Salvator merianae
Broadleysaurus major
Ablepharus kitaibelli
"Lacerta" filholi (PdF) †
D1 FV ◄
D2 FV ◄
D1 CC1sup ◄
D2 CC1sup ◄
D3 CC1sup ◄
D1 CE1-0 ◄
D2 CE1-0 ◄
D4 CE1-0 ◄
D7 CE1-0 ◄
D2 CH1-100 ◄
D3 CH1-100 ◄
D8 CH1-100 ◄
D2 CH1-75 ◄
D3 CH1-75 ◄
D4 CH1-75 ◄
D2 CCVsup ◄
D4 CCVsup ◄
D7 CCVsup ◄
D8 CCVsup ◄
D8 Roq2 ◄
D9 Roq2 ◄
D4 MdGB ◄
Ligerosaurus pouiti †
Mediolacerta roceki †
Plesiolacerta lydekkeri †
Pseudeumeces cadurcensis †
Varanus exanthematicus
Dracaenosaurus croizeti (Cod) †
Dracaenosaurus croizeti (Cou) †
Anguis veronensis
Pseudopus apodus
D10 Roq2 ◄
Blanus rufus
Blanus strauchi
"Lacerta" filholi (Cod) †
Gallotia caesaris
Gallotia simonyi
Gallotia stehlini
Psammodromus algirus
Anatololacerta danfordi
Podarcis hispanicus
Podarcis siculus
Timon pater
Timon kurdistanicus
Timon princeps
Timon lepidus
Lacerta agilis
Lacerta media
Lacerta schreiberi
Lacerta strigata
Eremias velox
Acanthodactylus boskianus
Acanthodactylus erythrurus
Mesalina guttulata
Ophisops elegans
Algyroides fitzingeri
Algyroides nigropunctatus
D6 CE1-0 ◄
Archaeolacerta bedriagae
Iberolacerta monticola
Iberolacerta cyreni
D5 CE1-0 ◄
Phoenicolacerta troodica
Takydromus sp.
Zootoca vivipara
Podarcis muralis
Podarcis waglerianus
Podarcis tiliguerta
D9 LaC ◄
Lacerta bilineata
Lacerta trilineata
Lacerta viridis

Fig. 8. Strict consensus tree of analysis of the complete dentary dataset using a value of $k = 20$ based on more than 100 000 MPTs (overflow). Length of strict consensus: 2074 steps; CI of strict consensus: 0.135; RI of strict consensus: 0.215. Length of MPTs: 1505 steps; CI of MPTs: 0.185; RI of MPTs: 0.464. Arrowheads indicate the dentary mOTUs; daggers show the fossil OTUs; locks mark clades with fulfilled constraining. Black branches, non-crown-lacertids; blue branches, Gallotiinae; green branches, Lacertinae. FV, Fouilles Viret; CC1sup, Coderet Couche 1 sup; CE1-0, Coderet E1-0; CH1-100, Coderet H1-100; CH1-75, Coderet H1-75; CCVsup, Coderet Couche Verte sup 1-25; LaC, La Colombière; Roq2, Roqueprune 2; MdGB, Mas de Got B; PdF, Pech-du-Fraysse; Cod, Coderet; Cou, Cournon. Strict consensus trees of $k = 5$ and 12 can be found in the Supplementary material.

analyses with the complete datasets, and all three datasets resulted in trees with a similar general tree topology. The remaining stable premaxillary mOTUs generally were recovered in the same positions as in the analyses of the reduced datasets with their respective *k*-value. For the maxilla dataset, the new analyses recovered all stable mOTUs within crown-Lacertidae, except for mOTU M5 CE1-0, which formed a grade with *Salvator merianae* being more basal to it, and the lacertids *Pseudeumeces cadurcensis*, *Ligerosaurus pouiti* and *Mediolacerta roceki* as successively more derived branches. Under $k = 5$, all stable maxilla mOTUs were either recovered within Gallotiinae or forming a sister clade to it. With $k = 12$ and 20, the maxilla mOTUs were found in a polytomy within Lacertidae and only M1 CC1sup was found as Gallotiinae. The analyses with the stable dentary mOTUs found the mOTU D10 Roq2, D5 CE1-0 and D6 CE1-0 in the same positions as in the previous analyses. All remaining stable dentary mOTUs were recovered within *Podarcis*, except that D8 CH1-100 was found within Gallotiinae ($k = 5$ and 12) or as sister to *Ligerosaurus pouiti*, together forming the sister clade to *Timon*. For a tabular summary of the mOTU positions for the complete, reduced and only-stable-mOTUs analyses, see Appendix 2.

The analysis with the cross-regional mOTUs of the premaxillae found, when including only one at a time, the cross-regional mOTUs P1, P2 and P5 within Anguimorpha as sister taxon to the two *Dracaenosaurus croizeti* OTUs. Only when applying $k = 5$, the cross-regional mOTU P1 was found as sister to the two *Blanus* taxa. mOTU P4 (no cross-regional OTU; P4 occurs in a single sample only) was recovered as sister to *Anguis veronensis* within Anguimorpha. The cross-regional mOTU P3 was found as sister to *Broadleysaurus major* within Scincoidea. For the analysis including all premaxilla cross-regional mOTUs at the same time (including also P4), the strict consensus tree found all mOTUs recovered in the same positions as before, except for P2, which was now found within Scincoidea, in a polytomy with cross-regional mOTU P3 and *Broadleysaurus major* (Fig. 9; for the trees of the cross-regional mOTUs analyzed individually, see Supplementary material). For the analysis of the cross-regional mOTUs under $k = 5$, the clade of Scincoidea collapsed into the following polytomy: (P2, P3, *Ablepharus kitaibelii*, *Broadleysaurus major*, *Chalcides ocellatus*, (P1, (*Blanus strauchi*, *Blanus rufus*)), (*Salvator merianae*, Lacertidae)).

When analyzing the single maxilla cross-regional mOTUs, the cross-regional mOTU M1 was found in a clade with *Zootoca vivipara*, *Takydromus* sp. and *Phoenicolacerta troodica*, as the sister taxon to *Zootoca vivipara*. The mOTU M2 (no cross-regional OTU; M2 occurs in a single sample only) was found as sister to *Ligerosaurus pouiti*, within a clade composed of the two *Iberolacerta* species and *Archaeolacerta bedriagae*. Under $k = 5$, it was found in polytomy with *Ligerosaurus pouiti* as part of Gallotiinae. The cross-regional mOTUs M3 and M4 were both found as sisters to the clade *Timon* + *Lacerta*. The analysis including only morphotype M5 (no cross-regional OTU; M5 was found in a single sample only) recovered it in a grade with *Salvator merianae* as more basal, and the lacertids *Pseudeumeces cadurcensis*, *Ligerosaurus pouiti* and *Mediolacerta roceki* in successively more derived positions. The strict consensus tree of the analysis with mOTU M6 (no cross-regional OTU; M6 is represented in a single sample only) was poorly resolved with a large polytomy excluding only the outgroup taxon *Gekko gecko* but including mOTU M6. When including all cross-regional maxilla mOTUs simultaneously (including M2, M5 and M6), the tree topology showed the same large polytomy as found by the analysis restricted to the mOTU M6 (Fig. 10; for the trees of the cross-regional mOTU analyzed individually, see Supplementary material). The cross-regional mOTUs M1 and M3 were found in a smaller polytomy within the large polytomy, including the *"Lacerta" filholi* OTU from Pech-du-Fraysse. The cross-regional mOTU M4 was found at the same position as when analyzed alone. The other cross-regional mOTUs were not found in a resolved position in the strict consensus tree. For the analysis under $k = 5$, the clade of Gallotiinae was resolved in the larger polytomy and included the cross-regional mOTUs M1, M2, M3 and M4.

The separate analyses for the dentary cross-regional mOTUs found D1 and D7 within Gallotiinae, as sister taxa to a clade including the three taxa of *Gallotia* and the two "*Lacerta*" *filholi* OTUs. The analysis with the cross-regional mOTU D2 recovered it within *Lacerta*, as sister to the clade *Lacerta media* + *L. schreiberi*. The cross-regional mOTU D3 was recovered within *Lacerta* as well, but in a polytomy with *L. media* and *L. schreiberi*. The analysis including the cross-regional

Table 3
Distribution of character types coding for premaxillae, maxillae, and dentaries. The distribution is given in absolute numbers and relative percentages in brackets (rounded to the nearest integer). morph: morphometric; c/m: countable/measurable; shape: shape describing.

	Quantitative			Qualitative		
	Total	Meristic	Morpho	Total	c/m	Shape
Premaxilla	5 (16%)	2 (6%)	3 (9%)	27 (84%)	17 (53%)	10 (31%)
Maxilla	3 (11%)	3 (11%)	0 (0%)	25 (89%)	17 (61%)	8 (28%)
Dentary	2 (8%)	2 (8%)	0 (0%)	22 (92%)	13 (54%)	9 (38%)

mOTU D4 found it within Gallotiinae, as sister to the clade *Gallotia stehlini* + *G. simonyi*. mOTU D5 (no cross-regional OTU; D5 occurs only in a single sample) was found as part of *Iberolacerta*, forming the sister taxon to *I. monticola*. As before, mOTU D6 (no cross-regional OTU; D6 is known from a single sample only) was found within *Algyroides*, forming the sister taxon to *A. nigropunctatus*. The cross-regional mOTU D8 and *Ligerosaurus pouiti* were found as sister clade to *Timon*. Under $k = 5$, D8 was still close to *Ligerosaurus pouiti* but those two were positioned within Gallotiinae. The cross-regional mOTU D9 was recovered as sister to *Timon* + *Lacerta*, or in a polytomy with *Podarcis* and *Timon* + *Lacerta* ($k = 5$). As already observed in the trees of the previous analysis, mOTU D10 (no cross-regional OTU; D10 is represented in a single sample only) was positioned as sister to the clade *Blanus strauchi* + *B. rufus* (Amphisbaenia). When including all cross-regional dentary mOTUs at the same time (including D5, D6 and D10), D5, D6, D8 and D10 were recovered at the same positions as before (Fig. 11; for the trees of the cross-regional mOTU analyzed individually, see Supplementary material). By contrast, the other cross-regional mOTUs (D1, D2, D3, D4, D7, D9) were recovered in different positions, namely within *Podarcis*, where D9 was sister to *P. tiliguerta*. Under $k = 5$, the cross-regional mOTU D8 was found within Gallotiinae.

During morphotype testing, the eight other extinct taxa, which were treated as wild card taxa, were found mostly in the same positions as recovered by analyses with the complete datasets. *Mediolacerta roceki* and *Pseudeumeces cadurcensis* were always found close to each other. They were positioned at the base of Lacertidae with *Pseudeumeces cadurcensis* being more basal (all datasets: all k-values), within Gallotiinae (premaxilla and dentary datasets: $k = 20$) or as sister to *Timon* + *Lacerta* (dentary datasets: $k = 20$). *Ligerosaurus pouiti* was found at the base of Lacertidae, between *Pseudeumeces cadurcensis* and *Mediolacerta roceki* (maxilla dataset: all k-values; dentary dataset: $k = 20$), as part of Gallotiinae (premaxilla datasets: $k = 5$ and 20; maxilla datasets: $k = 5$; dentary dataset: all k-values), within *Iberolacerta* (premaxilla dataset: $k = 12$ and 20; maxilla datasets: $k = 12$ and 20; dentary datasets: $k = 12$) or as sister to *Timon* + *Lacerta* (dentary datasets: $k = 20$). *Plesiolacerta lydekkeri* was found within *Timon*, as sister to *Timon lepidus* (all datasets: $k = 12$ and 20) or to *Timon pater* (premaxilla and maxillae datasets: $k = 5$; dentary datasets: all k-values). The two *Dracaenosaurus croizeti* OTUs (Cournon and Coderet) were almost exclusively found in a sister relationship to each other within Anguimorpha (all datasets: all k-values); in some cases, the two taxa were found in close relationship to Amphisbaenia (premaxilla datasets: $k = 5$). The two OTUs of "*Lacerta*" *filholi* (Pech-du-Fraysse and Coderet) were consistently found within Gallotiinae.

Discussion

The recovered trees for premaxillae, maxillae and dentaries from our analyses with the complete datasets displayed different degrees of resolution, implying that the phylogenetic signal of tooth-bearing elements is incongruent within Lacertidae. This means that premaxillae, maxillae and dentaries alone are not equally suited for species identification based on phylogenetic analysis, and that taxa represented by single bones only often cannot be placed in a well-resolved position in a phylogenetic tree. Likewise, different bones from the same species, when found disarticulated, can be recovered in different positions along the tree. Here,

Fig. 9. Strict consensus tree of the premaxillary cross-regional analysis using a value of $k = 20$ based on two MPTs. Length of strict consensus and MPTs: 1494 steps; CI of strict consensus and MPTs: 0.187; RI of strict consensus and MPTs: 0.456. Length of MPTs: arrowheads indicate the premaxilla (cross-regional) mOTUs; daggers show the fossil OTUs; locks mark clades with fulfilled constraining. Grey dashed-line arrow indicates the position of the cross-regional mOTU when analyzing it individually ($k = 20$). Black branches, non-crown-lacertids; blue branches, Gallotiinae; green branches, Lacertinae. CE1-0, Coderet E1-0; PdF, Pech-du-Fraysse; Cod, Coderet; Cou, Cournon. Strict consensus trees of $k = 5$ and 12 can be found in the Supplementary material.

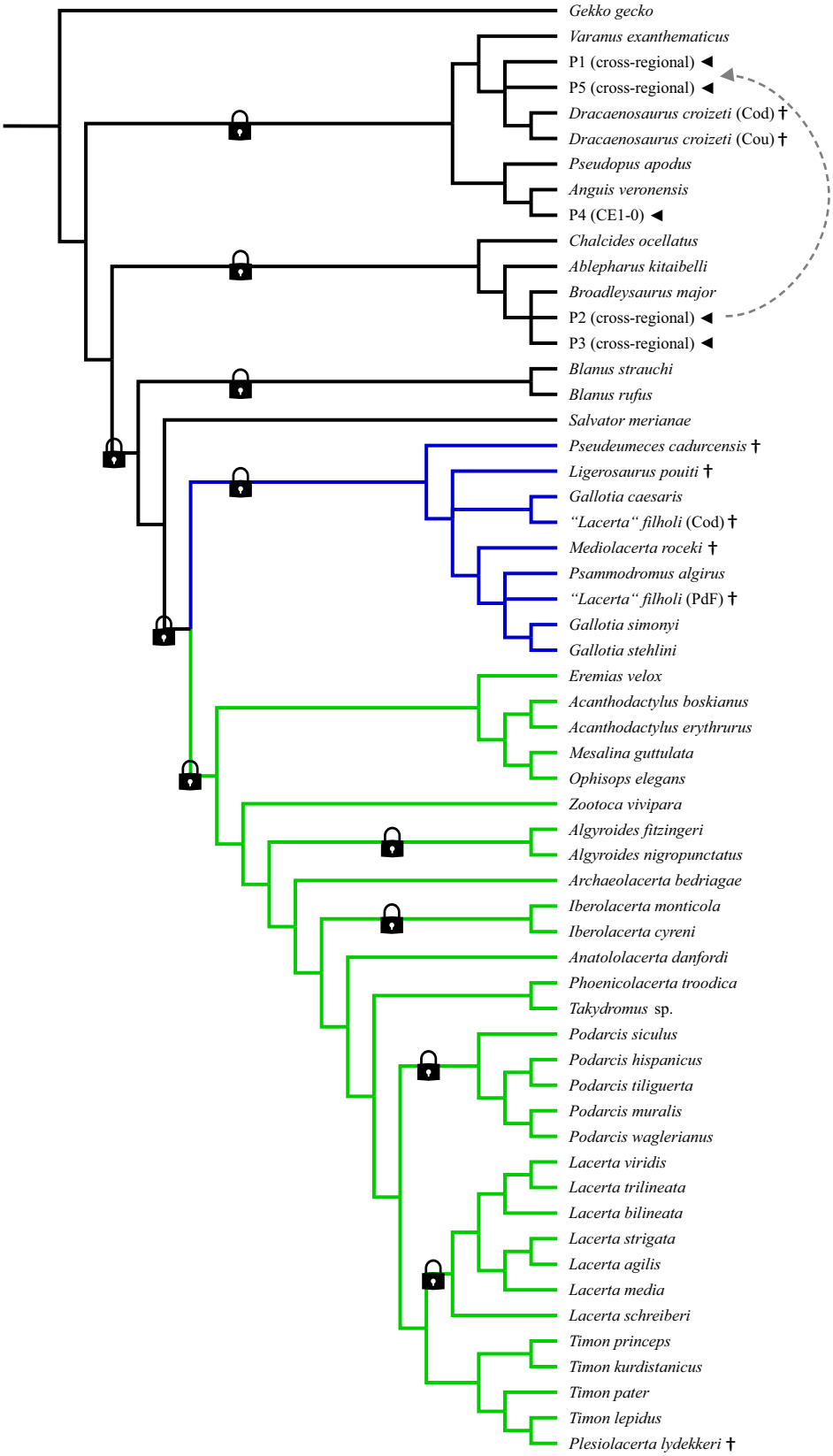
Gekko gecko
Varanus exanthematicus
P1 (cross-regional) ◄
P5 (cross-regional) ◄
Dracaenosaurus croizeti (Cod) †
Dracaenosaurus croizeti (Cou) †
Pseudopus apodus
Anguis veronensis
P4 (CE1-0) ◄
Chalcides ocellatus
Ablepharus kitaibelli
Broadleysaurus major
P2 (cross-regional) ◄
P3 (cross-regional) ◄
Blanus strauchi
Blanus rufus
Salvator merianae
Pseudeumeces cadurcensis †
Ligerosaurus pouiti †
Gallotia caesaris
"Lacerta" filholi (Cod) †
Mediolacerta roceki †
Psammodromus algirus
"Lacerta" filholi (PdF) †
Gallotia simonyi
Gallotia stehlini
Eremias velox
Acanthodactylus boskianus
Acanthodactylus erythrurus
Mesalina guttulata
Ophisops elegans
Zootoca vivipara
Algyroides fitzingeri
Algyroides nigropunctatus
Archaeolacerta bedriagae
Iberolacerta monticola
Iberolacerta cyreni
Anatololacerta danfordi
Phoenicolacerta troodica
Takydromus sp.
Podarcis siculus
Podarcis hispanicus
Podarcis tiliguerta
Podarcis muralis
Podarcis waglerianus
Lacerta viridis
Lacerta trilineata
Lacerta bilineata
Lacerta strigata
Lacerta agilis
Lacerta media
Lacerta schreiberi
Timon princeps
Timon kurdistanicus
Timon pater
Timon lepidus
Plesiolacerta lydekkeri †

we explore the possible reasons for this issue, and what this could mean for the systematics of extinct lacertids from the Oligocene of France.

Dataset comparison

The quantitative comparison of the characters showed no significant overrepresentation of any of the three elements compared to the other two. Concerning the qualitative character comparison, our dataset displayed only relatively few differences in character type distribution among premaxillary, maxillary and dentary characters. On the one hand, it has been argued that a high amount of "shape-describing" characters makes the analysis more error-prone, because state definitions in this kind of character often are vague and could thus be interpreted differently by different researchers. Consequently, qualitative, shape-describing characters often were regarded as less objective than "countable/measurable" qualitative characters (Catalano et al., 2010). However, qualitative characters in general have been interpreted to be less objective than quantitative characters by some phylogeneticists (e.g., Poe and Wiens, 2000). On the other hand, quantitative characters with discrete character states, as are being used in our dataset, can be problematic because the definition of their state boundaries may be subjective (Archie, 1985; Rae, 1998). Indeed, if a range of values is discretized into two distinct character states, taxa with significantly different values can be grouped together, whereas taxa displaying similar values, but on the two sides of the state boundary, will be scored differently (Farris, 1990). Therefore, several authors have suggested the use of continuous (Rae, 1998; Goloboff et al., 2006) or even morphometric characters (Catalano et al., 2010), which can both now also be scored and implemented directly in TNT (Goloboff et al., 2006; Goloboff and Catalano, 2016). However, discretizing continuous characters is a very straightforward approach, and the scoring of the OTUs into discrete states is easily reproducible. Discretizing continuous character states, as was done in our dataset, can also partially address the problem of outliers in the dataset, which can result from abiotic causes such as taphonomic deformation (Tschopp and Upchurch, 2019) that almost always affects fossils (Arbour and Currie, 2012; Tschopp et al., 2013). Nevertheless, among continuous characters, only the morphometric characters are affected by taphonomic deformation, given that meristic characters cannot logically be altered in this way. Although differences in the relative amount of different character types in our dataset are low (Table 3), they indicate that quantitative characters were slightly less error-prone and more reliable than qualitative characters in terms of recovering resolved phylogenetic trees. It seems unlikely, though, that these were the only factors impacting tree resolution and/or causing the sometimes conflicting positions of the morphotypes.

Morphological variability differs between tooth-bearing elements, the impact of which was tested with the analyses with a reduced mOTU sampling. When simply comparing the number of observed morphotypes, the premaxillae and maxillae had a similar number of morphotypes, whereas the dentaries represent the most variable jaw element (see also Table 2). The dentary also was the most frequent element in our sample at 68% of the material, whereas the maxillae and premaxillae constituted 23% and 9%, respectively. This distribution of the three jaw elements is comparable to other localities with squamate remains (e.g. Monte Tuttavista, Sardinia, Italy: 65% dentaries, 32% maxillae, 3% premaxillae; Tschopp et al., 2018b; Maramena, northern Greece: 73% dentaries, 25% maxillae, 2% premaxillae (considering only the squamate remains); Georgalis et al., 2019), indicating that the dentaries have a higher preservation probability compared to the relatively thin, and thus more fragile maxillae and premaxillae (and assuming that they are equally recognizable during picking and sorting activities). It also should be kept in mind that dentaries and maxillae are paired bones, whereas lacertid premaxillae are single bones making dentaries and maxillae twice as likely to be preserved. Hence, the observed higher variability might be due to preservation bias.

Missing scores in the mOTUs appear to have had a more profound impact on tree topology than character number and definition, because the possibility of determination and positioning of the taxa within the phylogenetic tree decreases with an increasing number of missing entries (Wiens, 2003). The resultant instability of the incomplete OTU leads to a recovery of a high number of conflicting most parsimonious trees (MPTs), and consequently to a poorly resolved strict consensus tree (Gauthier, 1986; Huelsenbeck, 1991; Wilkinson and Benton, 1995; Pol and Escapa, 2009).

Fig. 10. Strict consensus tree of the maxillary cross-regional analysis using a value of $k = 20$ based on 20 MPTs. Length of strict consensus: 1739 steps; CI of strict consensus: 0.160; RI of strict consensus. Length of MPTs: 1498 steps; CI of MPTs: 0.186; RI of MPTs: 0.452. Arrowheads indicate the maxilla (cross-regional) mOTUs; daggers show the fossil OTUs; locks mark clades with fulfilled constraining. Grey dashed-line arrows indicate the position of the (cross-regional) mOTUs when analyzing them individually ($k = 20$). Grey asterisk marks the mOTU which was found at a resolved position when analyzed individually, but still as non-lacertid. Black branches, non-crown-lacertids; blue branches, Gallotiinae; green branches, Lacertinae. CC1sup, Coderet Couche 1 sup; CE1-0, Coderet E1-0; PdF, Pech-du-Fraysse; Cod, Coderet; Cou, Cournon. Strict consensus trees of $k = 5$ and 12 can be found in the Supplementary material.

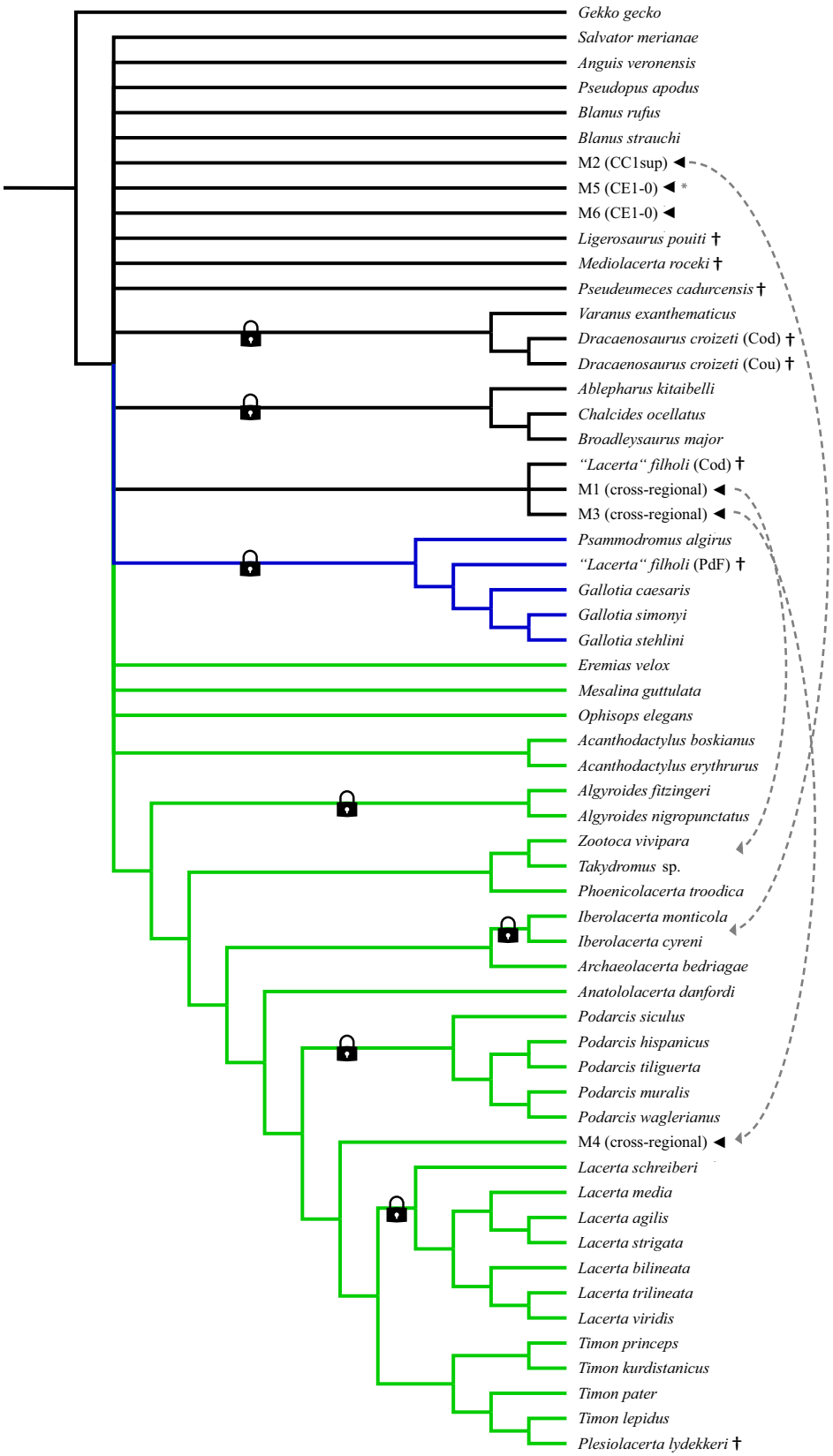
Gekko gecko
Salvator merianae
Anguis veronensis
Pseudopus apodus
Blanus rufus
Blanus strauchi
M2 (CC1sup) ◀
M5 (CE1-0) ◀ *
M6 (CE1-0) ◀
Ligerosaurus pouiti †
Mediolacerta roceki †
Pseudeumeces cadurcensis †
Varanus exanthematicus
Dracaenosaurus croizeti (Cod) †
Dracaenosaurus croizeti (Cou) †
Ablepharus kitaibelli
Chalcides ocellatus
Broadleysaurus major
"Lacerta" filholi (Cod) †
M1 (cross-regional) ◀
M3 (cross-regional) ◀
Psammodromus algirus
"Lacerta" filholi (PdF) †
Gallotia caesaris
Gallotia simonyi
Gallotia stehlini
Eremias velox
Mesalina guttulata
Ophisops elegans
Acanthodactylus boskianus
Acanthodactylus erythrurus
Algyroides fitzingeri
Algyroides nigropunctatus
Zootoca vivipara
Takydromus sp.
Phoenicolacerta troodica
Iberolacerta monticola
Iberolacerta cyreni
Archaeolacerta bedriagae
Anatololacerta danfordi
Podarcis siculus
Podarcis hispanicus
Podarcis tiliguerta
Podarcis muralis
Podarcis waglerianus
M4 (cross-regional) ◀
Lacerta schreiberi
Lacerta media
Lacerta agilis
Lacerta strigata
Lacerta bilineata
Lacerta trilineata
Lacerta viridis
Timon princeps
Timon kurdistanicus
Timon pater
Timon lepidus
Plesiolacerta lydekkeri †

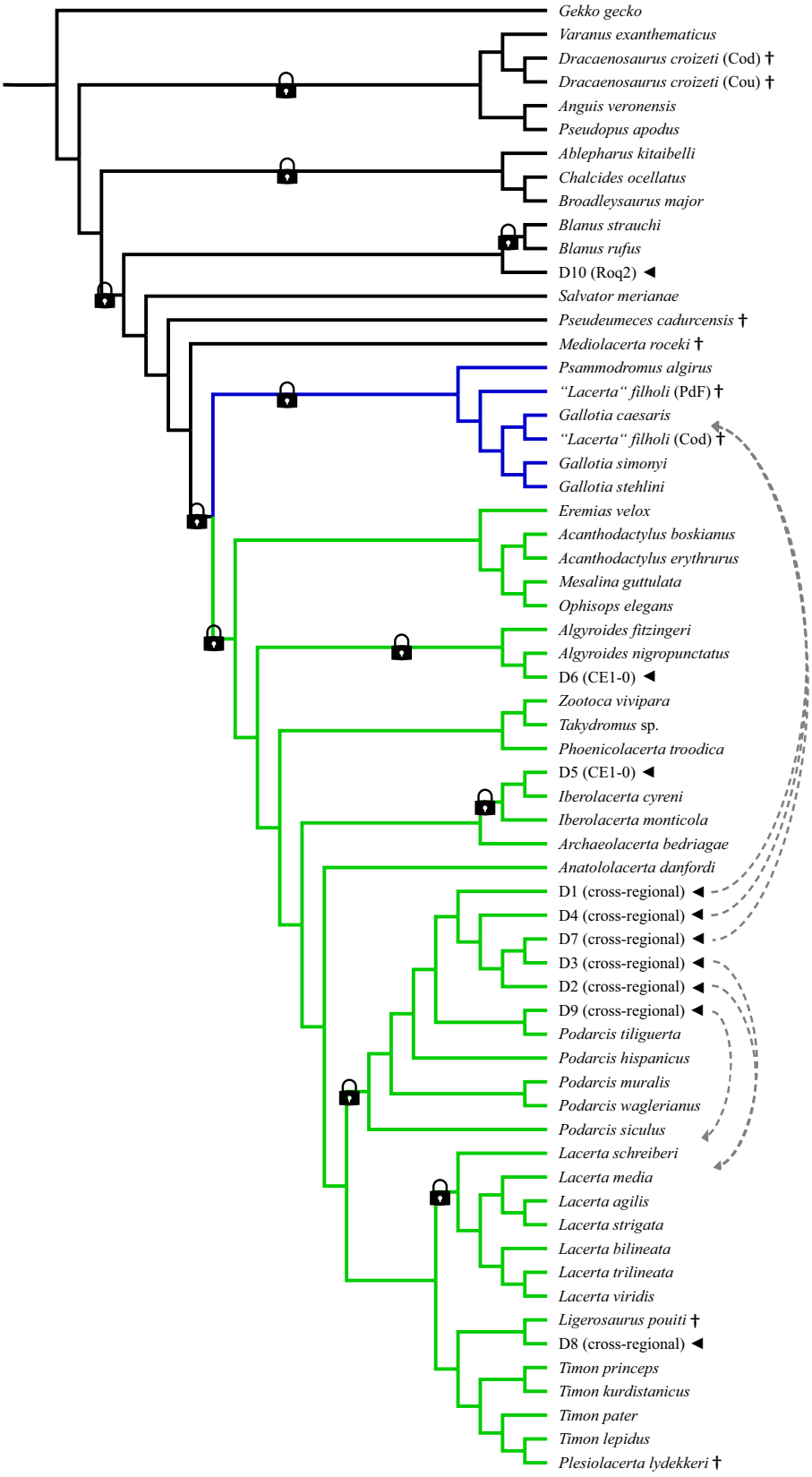
Gekko gecko
Varanus exanthematicus
Dracaenosaurus croizeti (Cod) †
Dracaenosaurus croizeti (Cou) †
Anguis veronensis
Pseudopus apodus
Ablepharus kitaibelli
Chalcides ocellatus
Broadleysaurus major
Blanus strauchi
Blanus rufus
D10 (Roq2) ◄
Salvator merianae
Pseudeumeces cadurcensis †
Mediolacerta roceki †
Psammodromus algirus
"Lacerta" filholi (PdF) †
Gallotia caesaris
"Lacerta" filholi (Cod) †
Gallotia simonyi
Gallotia stehlini
Eremias velox
Acanthodactylus boskianus
Acanthodactylus erythrurus
Mesalina guttulata
Ophisops elegans
Algyroides fitzingeri
Algyroides nigropunctatus
D6 (CE1-0) ◄
Zootoca vivipara
Takydromus sp.
Phoenicolacerta troodica
D5 (CE1-0) ◄
Iberolacerta cyreni
Iberolacerta monticola
Archaeolacerta bedriagae
Anatololacerta danfordi
D1 (cross-regional) ◄
D4 (cross-regional) ◄
D7 (cross-regional) ◄
D3 (cross-regional) ◄
D2 (cross-regional) ◄
D9 (cross-regional) ◄
Podarcis tiliguerta
Podarcis hispanicus
Podarcis muralis
Podarcis waglerianus
Podarcis siculus
Lacerta schreiberi
Lacerta media
Lacerta agilis
Lacerta strigata
Lacerta bilineata
Lacerta trilineata
Lacerta viridis
Ligerosaurus pouiti †
D8 (cross-regional) ◄
Timon princeps
Timon kurdistanicus
Timon pater
Timon lepidus
Plesiolacerta lydekkeri †

Fig. 11. Single MPT of the dentary cross-regional analysis using a value of $k = 20$. Length: 1504 steps; CI: 0.186; RI: 0.456. Arrowheads indicate the dentary (cross-regional) mOTUs; daggers show the fossil OTUs; locks mark clades with fulfilled constraining. Grey dashed-line arrows indicate the position of the cross-regional mOTUs when analyzing them individually ($k = 20$). Black branches, non-crown-lacertids; blue branches, Gallotiinae; green branches, Lacertinae. CC1sup, Coderet Couche 1 sup; CE1-0, Coderet E1-0; PdF, Pech-du-Fraysse; Cod, Coderet; Cou, Cournon. Strict consensus trees of $k = 5$ and 12 can be found in the Supplementary material.

The state of completeness of the various morphotypes (quantified by the relative number of characters that were scorable for the individual morphotypes of the tooth-bearing elements) showed remarkable differences. Whereas the premaxilla and the dentary mOTUs displayed comparable average percentages, the portion of scorable characters for the maxilla morphotypes was significantly lower (most complete maxilla mOTU: 61%; most incomplete premaxilla mOTU: 59%). This degree of "specimen" incompleteness in the case of the maxilla probably is the main reason for the poorly resolved strict consensus trees. Such an interpretation is also supported by the resolution of the strict consensus trees of analyses with the reduced datasets. The resolution of the strict consensus trees with the dentaries was slightly lower than the one of the premaxillae, probably owing to the somewhat lower "specimen" completeness. However, when a larger polytomy occurred, the dentary mOTUs were mostly recovered in the resolved part of the strict consensus trees. By contrast, the reduced datasets with the maxillae still recovered larger polytomies with the majority of mOTUs involved. The stability tests revealed a strong correlation of stability and completeness of the mOTUs. Generally, the higher the completeness of an mOTU, the more stable its position among the MPTs, regardless of the weighting strength. However, some mOTUs with low completeness values were nonetheless identified as stable, implying the importatance of not only the number of scored characters, but also the character itself (e.g. an apomorphic feature for a specific group in the dataset).

By creating the cross-regional mOTUs, the amount of missing data was reduced without deleting taxa, as mOTUs of the same morphotype but with different states of preservation were merged. Moreover, a possible ecomorphological signal (i.e. directed noise) was weakened as data from different localities were combined and, thereby, the real phylogenetic signal was enhanced. The analyses did not result in completely different positions, but especially in the case of the maxillae, the morphotypes were recovered at much more resolved positions.

The different morphotype testing methods also can be seen as a less laborious approach to test alternative tree hypotheses. Of course, it is less powerful than using completely different datasets as done by Scarpetta (2020). But, by testing the different k-values and combinations of taxa, the general value of a taxon's position in the phylogenetic tree can readily be appraised. If needed, more rigorous methods could be used in a subsequent iteration.

Possible phylogenetic position of mOTUs

The phylogenetic positions found for the various mOTUs varied considerably in the different analyses, rendering taxonomic interpretations difficult for some morphotypes. Concerning the influence of the weighting strength applied to the maximum parsimony analyses, we generally observed poorer tree resolutions with $k = 5$, whereas $k = 12$ and 20 created better resolved tree topologies. Even though the latter two weighting strengths showed quite similar results, $k = 20$ generated the best tree resolution. The somewhat better performance of the milder downweighting against homoplastic characters, represented by the higher k-values (12 and 20), agrees with results from analyses with simulated data (Goloboff et al., 2018).

Premaxilla mOTUs. Even though all premaxilla mOTUs were recovered outside of Lacertidae, the outgroup position of the mOTUs belonging to morphotypes P1 (Fig. 2a), P2 (Fig. 2b), P3 (Fig. 2c) and P5 (Fig. 2e), is highly questionable and likely inaccurate. Several morphological features that generally are regarded to be diagnostic for Lacertidae are present in these morphotypes, supporting an assignment of these premaxillae to the ingroup. The observed number of teeth ranging from six to nine fits the range found in extant and extinct lacertids (Barahona Quintana, 1996; Barahona and Barbadillo, 1998; Evans, 2008; Khosravani et al., 2011; Čerňanský and Augé, 2013; Čerňanský et al., 2016; Čerňanský and Syromyatnikova, 2019; Villa and Delfino, 2019b). Moreover, the tooth arrangement and composition are lacertid-like with closely spaced teeth and rounded tooth apices (Villa and Delfino, 2019b). However, the prominent enlarged median tooth observed in P1 previously was regarded as an unambiguous synapomorphy for the clade composed of Amphisbaenia + Dibamidae (Gauthier et al., 2012), and probably impacts our analyses as well. Other features found in the premaxillae morphotypes also may be unusual in lacertids generally, but can be observed in some taxa. The slender ascending nasal process and the teeth of morphotype P2 are similar to the extant species *Lacerta strigata* Eichwald, 1831 (e.g. Čerňanský and Syromyatnikova, 2019, therein fig. 12), and the extinct species *Lacerta poncenatensis*

Müller, 1996, from the Miocene of Poncenat, France (e.g. Müller, 1996, therein fig. 5). The unclosed fossae around the ethmoidal foramina present in P3 (Fig. 2c), is a feature that also occurs in *Lacerta bilineata* Daudin, 1802 (MNCN-16505) and *Podarcis muralis* (MDHC 311). A second pair of ethmoidal foramina was present in P5. We observed this state also in the OTUs in our dataset: *Anguis veronensis* (MDHC 102; Anguimorpha), *Blanus strauchi* (MDHC 287; Amphisbaenia), *Gallotia simonyi* (NHMW 849), *Acanthodactylus erythrurus* (UAM.R. Ac-VII) and *Iberolacerta monticola* (UAM.R. Lm77; all three are lacertids). It also is known as a rare feature in *Podarcis muralis* (Laurentini, 1786) (Barahona Quintana, 1996; Villa and Delfino, 2019b). It seems that convergently acquired features pull the mOTUs of the aforementioned morphotypes out of the ingroup and overrule the real phylogenetic signal. Hence, they are likely representing lacertid remains.

Only the position of mOTU P4 (Fig. 2d), which was always recovered as sister to the anguimorph *Anguis veronensis*, seems to be plausible, and it was suggested to indeed represent an anguid (Rage, 2016, pers. comm.). It resembles the extinct anguid species *Pseudopus laurillardi* (Lartet, 1851) in terms of the dorsal shape of the tooth-bearing portion that is almost rectangular and quite robust, looking like the crossbar of the letter "T" (e.g. Klembara et al., 2010, therein fig. 3).

Maxilla mOTUs. All maxilla mOTUs generally were recovered within Lacertidae, except for morphotypes M5 and M6. The morphotypes M1 (Fig. 3a) and M3 (Fig. 3c) could represent the same species owing to their similar appearance; they differ only in the presence or absence of striae on their tooth crowns. Additionally, morphotypes M4 (Fig. 3d) and M3 also show similarities and differ (mostly) in their size. Also, phylogenetic analyses (individual cross-regional analyses) recovered them in the same position, as sister to *Timon* + *Lacerta*. It is possible that these two either represent different species or that the size difference originates from sexual dimorphism or ontogeny, because variation in the size of the skull between adult males and adult females or juveniles is common among lacertids (e.g. Klemmer, 1957; Darevsky, 1967), and it is usually male-biased (Vincent and Herrel, 2007, and references therein). The smaller morphotype M3 might represent the adult female or juvenile, and the larger morphotype M4 the adult male version of a single species. A classification of the three morphotypes to Lacertidae (maybe Lacertini) seems plausible, based on the tooth arrangement especially in the anterior part, with the small anterior teeth having slightly posteriorly pointing tooth apices. Adding to this, the texture of the dermal ornamentation is also similar to the one seen in *Lacerta* (e.g. Čerňanský and Syromyatnikova, 2019, therein fig. 13).

Morphotype M2 (Fig. 3b) with the abrupt change from smaller posterior-most teeth to preceding larger teeth in the posterior half which also had been observed in specimens belonging to the large-sized lacertid genus *Timon* and the extinct species *"Lacerta" siculimelitensis* Böhme and Zammit-Maempel, 1982 (Böhme and Zammit-Maempel, 1982; Mateo Miras, 1988; Tschopp et al., 2018b), can also be an identified as an indeterminate lacertid but the poor preservation renders a more precise classification difficult.

Morphotype M5 (Fig. 3e) has globose teeth with deep striae, which are similar to the teeth preserved in premaxillary morphotype P1; thus, the two may belong to a single species. Also, the two morphotypes overlap geographically (see Table 2). The phylogenetic position of morphotype M5 was never further resolved than basal most Lacertidae (or Lacertoidea), which makes a more specific classification speculative.

Morphotype M6 (Fig. 3f) is unlikely to represent a lacertid because of its fang-like, slender teeth. These characteristics appear to be shared with varanids (e.g., Georgalis et al., 2017, therein fig. 1; Villa et al., 2018; Villa and Delfino, 2019a, therein fig. 11). Our analysis did not recover M6 at any resolved position. Hence, based on our observations, the morphotype likely does not represent a lacertid, but rather an anguimorph. Given that mOTU P4 is also thought to be an anguimorph, and they both come from the same locality and sample (Coderet E1-0), those could represent the same (non-lacertid) species. Alternatively, they could be palaeovaranids, which also share a similar tooth morphology, but their tooth crowns have longitudinal striae (Georgalis, 2017). Their presence is not reported from Coderet, but they are well-known from the Quercy phosphorites (Georgalis, 2017, and references therein).

Dentary mOTUs. Except for morphotype D10, all dentary morphotypes were generally recovered as lacertids. The dentary morphotypes D1 (Fig. 4a), D2 (Fig. 4b,c) and D4 (Fig. 4f,g) are highly similar in their overall shape, with the only differences being the presence or absence of either widely or narrowly spaced striae. Their phylogenetic position was mainly within Gallotiinae or at different positions within Lacertini. Considering that the three morphotypes are rather slender, an identification of the three morphotypes as Lacertini rather than Gallotiinae might be reasonable but remains speculative.

The morphotypes D3 (Fig. 4d,e) and D8 (Fig. 5e,f) are similar in being rather robust. The two are distinguished by the distinctly smaller teeth of D8 in the posterior-most part of the jaw, with the most robust teeth preceding those. This morphology also was

observed in the maxillary morphotype M2, which also was relatively robust. The peculiar tooth morphology resembles certain specimens of *Timon* and the extinct species "*Lacerta*" *siculimelitensis* (Böhme and Zammit-Maempel, 1982; Mateo Miras, 1988; Tschopp et al., 2018b). Based on the aforementioned observations, the two morphotypes may or may not represent the same species, but their identification as lacertid is very likely.

The very slender morphotype D6 (Fig. 5a) from Coderet E1-0 always was recovered as part of the *Algyroides*-clade. However, its high incompleteness raises doubts on such a specific identification. In any case, a referral to Lacertidae and, given the slender morphology and its biogeography, to Lacertini seems to be plausible.

The morphotype D7 (Fig. 5b–d) has a very distinctly developed tricuspidity of the tooth crowns which is an attribute that was formerly used as a diagnostic feature for the extinct species *Miolacerta tenuis* (Roček, 1984). However, strong tricuspidity also has been observed in the lacertid genera *Takydromus* and *Gallotia*, in the gerrhosaurid *Tracheloptychus madagascariensis* (Barahona et al., 2000; Kosma, 2004), and in specimens of *"Lacerta" filholi* (e.g. Augé and Smith, 2009, therein fig. 2). Moreover, the overall appearance is *"Lacerta" filholi*-like with the rather slender subtriangular shape, the distinct coronoid facet and the posteriorly reduced subdental shelf (e.g. Augé and Smith, 2009). Hence, morphotype D7 might belong to "*Lacerta*" *filholi*, but currently available data only seem to allow for a classification as Lacertidae indet.

Morphotype D9 (Fig. 5g) also has strong similarities with "*Lacerta*" *filholi* in terms of shape, but tricuspid teeth as seen in "*Lacerta*" *filholi* (Augé, 2005) are absent. Morphotype D9 represents in all probability a lacertid and probably a member of the tribe Lacertini, as it has a fairly slender appearance.

Morphotype D10 (Fig. 5h,i) differs in its morphology from the other dentaries, because of the globose, very robust teeth that are distinctly different in size from each other and have narrowly spaced striae. This was also observed in morphotypes P1 and M5. A similar tooth morphology has been reported for the extinct lacertids *Pseudeumeces cadurcensis* (e.g. Augé and Hervet, 2009, therein fig. 2) and *Dracaenosaurus croizeti* (e.g. Müller, 2006; Čerňanský et al., 2017, therein fig. 9). It should be noted that there is no geographical or stratigraphic overlap of P1 and M5 with D10 (see Table 2). All phylogenetic analyses found the mOTU D10 forming a clade within Amphisbaenia. However, only the very tip of the dentary was preserved, which makes an identification barely possible, but a referral to lacertids might be plausible, also in consideration that *Dracaenosaurus croizeti* was as well recovered outside Lacertidae (see discussion below).

Morphotype D5 (Fig. 4h–j) was present only in the sample from Coderet E1-0. It was always recovered within the clade of *Iberolacerta*. However, a Meckelian canal which is closed in the anterior quarter and opening up at the tip was never detected by any of us in *Iberolacerta* (or lacertids in general). Instead, such a morphology is reported in skinks, for instance in *Trachylepis aurata* and *Chalcides ocellatus* (e.g. Caputo, 2004; Villa and Delfino, 2019b, therein fig. 43). Based on these data, the position of the morphotype remains uncertain. Because in lacertids, the Meckelian canal is known to be completely open (e.g. Estes et al., 1988), an identification of morphotype D5 as lacertid is highly unlikely. It might represent a skink or even some other, unidentified taxon.

Possible phylogenetic positions of the eight fossil wild card taxa

Regardless of the weighting strength and number of taxa (including mOTUs) in the dataset, *Plesiolacerta lydekkeri* was always recovered within the genus *Timon*, either as sister to *Timon lepidus* or *Timon pater*. Previous studies (e.g. Čerňanský and Augé, 2013; Čerňanský and Syromyatnikova, 2019) have already noticed shared features between *Plesiolacerta* and *Timon*. However, several issues render a close relationship of *Plesiolacerta lydekkeri* and *Timon lepidus* or *Timon pater* questionable. Molecular analysis of the six extant species of *Timon* have shown that they form a monophyletic group (Pyron et al., 2013). The genus can be subdivided into two subclades that are geographically separated into an eastern and a western clade. *Timon kurdistanicus* (Suchow, 1936) and *Timon princeps* (Blanford, 1874) form the eastern clade with a distribution across Turkey, northern parts of Iraq and Iranian areas (Zagros mountains) (Eiselt, 1968; Anderson, 1999; Ilgaz and Kumlutaş, 2008; Ahmadzadeh et al., 2012). The western clade is composed of two subclades: one is formed by *Timon pater* and *Timon tangitanus* (Boulenger, 1889), both from northwestern Africa (Paulo et al., 2008; Perera and Harris, 2010), whereas the second is formed by *Timon lepidus* and *Timon nevadensis* (Buchholz, 1963), which are distributed across southwestern Europe (Miraldo et al., 2012). Divergence time of the sister genera *Lacerta* and *Timon* has been estimated to 18.6 Ma (95% highest posterior density (HPD) interval: 17.5–20.6 Ma) and the split between the western and eastern clade of *Timon* to 7.4 Ma (HPD interval: 5.9−9.0 Ma; Ahmadzadeh et al., 2016). *Plesiolacerta lydekkeri* is known from the middle Eocene (Lutetian; MP 14) until the early Oligocene (Rupelian; MP 21) (Augé, 2005;

Čerňanský and Augé, 2013 and references therein), which pre-dates these estimated divergence times considerably. Therefore, although a close relationship of *Plesiolacerta* and *Timon* seems plausible, the position of *Plesiolacerta lydekkeri* within *Timon*, as recovered by our analyses, is here regarded questionable.

Estes (1983b) proposed a close relationship between the amblyodont lacertid species *Pseudeumeces cadurcensis* and *Dracaenosaurus croizeti*, suggesting they may form a morphological series. Based on similarities in tooth shape, a lacertid lineage from *"Lacerta" filholi* via *Mediolacerta roceki* and *Pseudeumeces cadurcensis* to *Dracaenosaurus croizeti* was hypothesized (Hoffstetter, 1944; Rage, 1987; Augé, 2005). To our knowledge, phylogenetic analyses have been carried out only with *Pseudeumeces cadurcensis* and *Dracaenosaurus croizeti* so far. Their position was consistently found within Gallotiinae (Čerňanský et al., 2016, 2017; Tschopp et al., 2018b; Garcia-Porta et al., 2019). In our analyses, only the two "*Lacerta*" *filholi* OTUs were found consistently within Gallotiinae. *Pseudeumeces cadurcensis* and *Mediolacerta roceki* were almost always found at the base of Lacertidae, with few analyses recovering them within Gallotiinae or Lacertini. In an even stronger contrast to earlier analyses, the two *Dracaenosaurus croizeti* OTUs were either part of Anguimorpha or forming a clade with Amphisbaenia (for some premaxillae analyses). Hence, our analyses did not recover the hypothesised lacertid amblyodont lineage, suggesting that amblyodonty evolved several times independently. Nevertheless, the position of *Dracaenosaurus croizeti* outside Lacertidae remains questionable, given that other analyses found it consistently within Gallotiinae (Čerňanský et al., 2017; Garcia-Porta et al., 2019).

The Miocene taxon *Ligerosaurus pouiti* was first described as part of the genus *Pseudeumeces* (Augé, 1993) and later assigned to its own genus despite superficial similarities in the dentition (Augé et al., 2003). Our analyses found it mostly within Gallotiinae or the genus *Iberolacerta*. In very few cases, *Ligerosaurus pouiti* also was recovered as sister to *Timon* + *Lacerta* and at the base of Lacertidae, with *Pseudeumeces cadurcensis* being more basal. The very inconsistently recovered closer relationship to *Pseudeumeces cadurcensis* seems to confirm the referral of *Ligerosaurus pouiti* to a different genus. The controversial or rather unstable positions of these wild card taxa in our analyses were likely also caused by the other added extinct mOTUs, which potentially render their recovered positions less reliable.

Regarding the completeness of the wild card taxa, *Mediolacerta roceki* and *Ligerosaurus pouiti* were the most incomplete taxa (9% and 6%, respectively), whereas *Plesiolacerta lydekkeri* was the most complete one (39%). This highlights again how specimen incompleteness and tree resolution are correlated.

Species diversity of the morphotypes

Given the observed morphological similarities and the phylogenetic positions of the fossil material in the several analyses, there is support for probably three lacertid and one anguimorphan species among the premaxillae, about four lacertid and one anguimorphan species among the maxillae, and about five lacertid and one non-lacertid species among the dentaries.

The disparity between the premaxilla morphotypes is quite distinct, but the number of different morphotypes was rather low. By contrast, the number of dentary morphotypes was relatively high, but the differences between those were less distinct. In the case of the maxilla, the number of morphotypes and the distinctness was in between those of the two other jaw elements. The variation in size observed in the dentary and maxilla morphotypes probably results from either sexual dimorphism (Klemmer, 1957; Darevsky, 1967; Vincent and Herrel, 2007, and references therein; Ljubisavljević et al., 2010; Borczyk et al., 2014) or ontogeny (Roček, 1980).

Considering possible connections between the jaw elements resulting from their morphological similarities, at least five different lacertid species (Fig. 12) and two non-lacertid species are present in our sample. The first lacertid species ("species 1") probably comprises the premaxilla morphotypes P1 and P5, the maxilla morphotype M5, and the dentary morphotype D10, as they share the same morphology of globose teeth with dense, narrowly spaced striae. A similar tooth morphology occurs in the species *Pseudeumeces cadurcensis* and *Dracaenosaurus croizeti* (Augé, 2005); the two could thus be plausible candidates for a species referral of morphotypes P1, P5, M5 and D10. The second lacertid species ("species 2") is likely represented by the maxilla morphotype M2 and the dentary morphotype D8. They have the same distribution of robust teeth with the most robust teeth being located in the posterior half followed by significantly less robust and smaller teeth in the posterior-most part of the jaw element (maxilla, dentary) which is also known in the extant genus *Timon* and the Pleistocene species *"Lacerta" siculimelitensis* (Böhme and Zammit-Maempel, 1982; Mateo Miras, 1988; Tschopp et al., 2018b). However, M2 has narrowly spaced striae, whereas D8 has widely spaced striae on their tooth crowns. Given that similarities of the two mentioned species with *Plesiolacerta lydekkeri* were reported already (e.g. Čerňanský and Augé, 2013; Čerňanský and Syromyatnikova, 2019), "species 2" might be closely related with it or even belong to *Plesiolacerta*

lydekkeri. As a third lacertid species ("species 3"), the two dentary morphotypes D1 and D9 may be conspecific with the maxilla morphotype M1, given that they all have smooth tooth crowns and a similar overall robustness. The fourth lacertid species ("species 4") may be represented by the maxilla morphotypes M3 and M4, which possibly show ontogenetic variation or sexual dimorphism, with the less robust M3 potentially showing the adult female or juvenile constitution. Those two maxilla morphotypes might be linked to the dentary morphotypes D2 and D3, which also might show a sexual dimorphism or variation in size due to ontogeny, with the slenderer morphotype D2 possibly representing the adult female or juvenile state. It is possible that the dentary morphotypes D4 and D7 also are referable to this species, because the differences among the four dentary morphotypes are quite small. However, all morphotypes assigned to this species have widely spaced striae on their tooth crowns, except for D4, which has narrowly spaced striae. Therefore, the informative character on the constitution of striae on tooth crowns (when present) seems to be questionable, as also seen in the previously mentioned "species 2". Apart from these minor differences, the morphotypes resemble "*Lacerta*" *filholi*, a species which is known already from Coderet, La Colombière, Mas de Got B and Roqueprune 2 (Augé, 2005). The fifth species ("species 5") is represented by dentary morphotype D6, which was the most fragile element in the sample; no comparable maxilla or premaxilla was observed for this species. It resembles *Algyroides* in its delicateness. The two premaxilla morphotypes P2 and P3 probably represent two separate species, but those are likely linked to some of the already defined five lacertid species. Both have tooth crowns with narrowly spaced striae, but as seen above, the condition of the striae might not be taxonomically significant at the species level.

One of the non-lacertid species probably consists of the premaxilla morphotype P4 and the maxilla morphotype M6, and are most plausible referred to an anguimorphan species. The second non-lacertid species is represented by the dentary morphotype D5, which may be a skink or some other "scincomorphan" lizard. However, it should be kept in mind that the dataset that we used was created specifically for lacertids, and therefore, it has a rather low taxon sampling for the outgroups. Because of this, the phylogenetic position of possible non-lacertid taxa is not very reliable.

During the Oligocene in France, five lacertid species are certainly known to have occurred: *Plesiolacerta lydekkeri*, "*Lacerta*" *filholi*, *Mediolacerta roceki*, *Pseudeumeces cadurcensis* and *Dracaenosaurus croizeti* (Augé, 2005; Augé and Hervet, 2009). In the four localities from where our samples are (Coderet, La Colombière, Roqueprune 2, Mas de Got B), *"Lacerta" filholi* is known to have been present in all of them, *Mediolacerta roceki* is reported from Roqueprune 2 and Coderet, *Dracaenosaurus croizeti* occurred only in Coderet, and no remains of *Plesiolacerta lydekkeri* and *Pseudeumeces cadurcensis* have been found in any of the four localities, although *Pseudeumeces cadurcensis* overlaps in age with Coderet and La Colombière (Augé, 2005). The last occurrence of *Plesiolacerta lydekkeri* was in the early Oligocene in the MP 21 (Augé, 2005), hence, there is no chronological overlap with our four French localities, as the oldest one is correlated to MP 22 (Mas de Got B). With respect to time, an increase in species variability is observable from the Rupelian to the Chattian. When reconciling our previously identified five lacertid "species" with the five already known ones, "species 5" seems to be unique. It is present in the sample from Coderet (Fig. 12), but it does not resemble any of the five known species due to its delicateness. However, ontogeny or sexual dimorphism might also play a role here. "Species 1" was found in the samples from Coderet and Roqueprune 2 (Fig. 12) and resembles or is related to the amblyodont species *Pseudeumeces cadurcensis* and *Dracaenosaurus croizeti*. The stratigraphic range of *Pseudeumeces cadurcensis* and *Dracaenosaurs croizeti* fits the age of Coderet (MP 30), but remains from this locality are reported only for *Dracaensaurus croizeti* (Augé, 2005). However, Roqueprune 2, which was correlated to MP 23, pre-dates the first occurrences of the two amblyodont species (*P. cadurcensis*: MP 25; *D. croizeti*: MP 28; Augé and Hervet, 2009). "Species 2" occurs in the samples from Coderet and Roqueprune 2 (Fig. 12). It might resemble or be related to *Plesiolacerta lydekkeri*, which last occurred in MP 21 (Augé, 2005); this pre-dates Coderet (MP 30) and Roqueprune 2 (MP23). "Species 4" was found in the samples from Coderet and Mas de Got B (Fig. 12), and probably represents *"Lacerta" filholi*, which has been reported from these localities before. "Species 3" was found in Coderet, La Colombière and Roqueprune 2 (Fig. 12). It could represent any of the five known species from the Oligocene of France except for the two amblyodont species (*Pseudeumeces cadurcensis* and *Dracaenosaurus croizeti*). Therefore, the species variability of lacertid lizards in the Oligocene of France seems to be somewhat greater than recognised previously with possibly six different species: *Plesiolacerta lydekkeri,* "*Lacerta*" *filholi*, *Mediolacerta roceki, Pseudeumeces cadurcensis, Dracaenosaurus croizeti* and "species 5". Possibly, the stratigraphic range of *Plesiolacerta lydekkeri* extends further into the Oligocene, whereas the first occurrence of *Pseudeumeces cadurcensis* or *Dracaenosaurus croizeti* might date further back than previously thought.

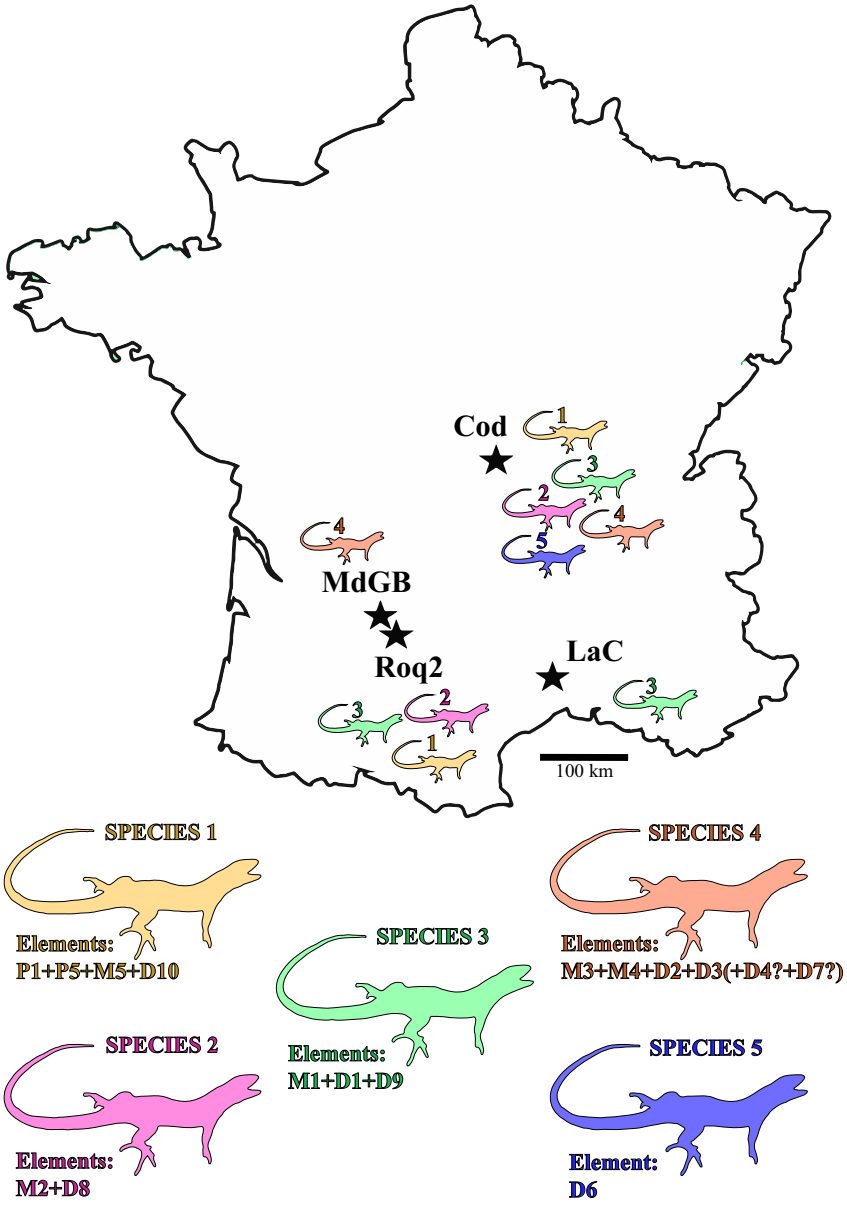

Fig. 12. Distribution pattern and constitution of the possible five lacertid species among the four French localities indicated by black stars. Although the morphotypes P2 and P3 were classified as lacertids, they are not included here, because a referral to one of the five "species" is too speculative. Cod, Coderet; LaC, La Colombière; Roq2, Roqueprune 2; MdGB, Mas de Got B.

Conclusions

Assessing the phylogenetic value of lacertid premaxillae, maxillae and dentaries is only possible to a limited extent. The phylogenetic trees resulting from three individual datasets of jaw elements show remarkable differences in terms of resolution of the strict consensus trees and number of MPTs. Also, analyses of the same dataset but with different weighting strengths and methods often led to conflicting positions of the single-bone morphotypes.

However, based on observations of the morphotypes, possibly five lacertid "species" could be identified in our samples from the four French localities. Reconciliation with the already known lacertid species in France during the Oligocene suggests a larger species diversity than thought previously, with six species in total, indicating a more rapid radiation of Lacertidae following the abrupt shift to colder temperatures after the Paleocene–Eocene Thermal Maximum (PETM) and the warm period during the Eocene. However, various iterations of phylogenetic analyses

with modified datasets failed to recover clear and consistent phylogenetic positions for most morphotypes, demonstrating the weakness of their phylogenetic signal. Also, a highly resolved tree does not necessarily imply that there was a reliable phylogenetic signal in the dataset. Therefore, it is important to be aware of the constitution of the data being used and to test the robustness of the taxa's positions. A precise classification at species-level of the individual jaw elements was not possible based on the phylogenetic analysis. Hence, species descriptions and classification based on single tooth-bearing elements should be treated with caution. Although real autapomorphic features may be present in some of these elements, these seem to be difficult to interpret as such, and if identified correctly, they do not seem to provide enough information to consistently reveal their true phylogenetic position, and so phylogenetic trees should undergo a conscientious "test of robustness".

Acknowledgements

We thank †Jean-Claude Rage, Salvador Bailon and Virginie Bouetel from the MNHN for kindly providing the key material for this study. Moreover, we thank the numerous people who helped during collection visits. Especially we thank Sónia Gabriel and Simon Davis (CIPA), Marta Calvo and Alberto Sanchez (MNCN), Jeff Streicher and Patrick Campbell (NHMUK), Heinz Grillitsch, Georg Gassner and Silke Schweiger (NHMW), Christian Klug and Winand Brinkmann (PIMUZ), Hannah Cornish and Tannis Davidson (GMZ), and Ralf Kosma (SRK). Additional specimens could be studied thanks to loans from HUJ-OST, MRAC, UAM and ZZSiD. We would like to specifically thank Rebecca Biton, Georgios Georgalis and Mauro Grano, who personally brought specimens from these collections to Turin for us to study, and Annelise Folie, Francisco Ortega and Zbigniew Szyndlar for approving and organizing loans. We furthermore thank the Willi Hennig Society and the Mesquite Project Team for providing their software TNT and MESQUITE, respectively, for free online. Furthermore, we thank Monique Vianey-Liaud who gave extremely useful information on the geological background. Thanks to Paul Upchurch and Rafael Omar Regalado Fernandez for discussions on phylogenetic analyses and to Emmanuel David who helped with the translation of French literature (University College London, UK). We further thank the editor-in-chief Rudolf Meier and associate editor Michael Pittman who gave incredibly helpful support and suggestions for improvement. Many thanks also to Andrej Čerňanský and two anonymous reviewers for their highly useful comments and corrections on our manuscript.

Financial support was provided for L.C.M.W. by a PhD fellowship from the Università degli Studi di Torino. Part of the dataset was assembled under the lead of E.T. when he was holding a Postdoctoral Fellowship funded by the European Union's Seventh Framework programme for research and innovation under the Marie Sklodowska-Curie grant agreement No. 609402 – 2020 researchers: Train to Move (T2M). A.V. is funded by a Humboldt Research Fellowship provided by the Alexander von Humboldt Foundation. M.D. acknowledges support from Fondi di Ateneo dell'Università di Torino (2017–2019), Generalitat de Catalunya (CERCA Programme, consolidated research group 2017 SGR 116 GRC) and Agencia Estatal de Investigación of Spain (CGL2016-76431-P, AEI/FEDER, EU). Further data collection was done during Synthesys grants to visit the MNHN (Paris, France) and NHMW (Vienna, Austria) financed by the European Community Research Infrastructure Action under the FP7 'Capacities' Programme (FR-TAF-5007 and 5839, to A.V. and E.T. respectively; AT-TAF-4591 and 5725, to A.V. and E.T., respectively) and during two Erasmus+ Traineeships (University College London, UK; NHMW, AT) to L.C.M.W. This is the publication number 354 of the Museo di Geologia e Paleontologia collections at the Università degli Studi di Torino.

Conflict of interest

None declared.

References

Aguilar, J.-P., Agustì, J., Alexeeva, N., Antoine, P.-O., Antunes, M.T., Legendre, S. and Wolsan, M., 1997. Synthèses et tablaux de corrélations [Overview and table of correlations]. In: Aguilar, J.-P., Legendre, S. & Michaux, J. (Eds.), Actes du Congrès BiochroM. Mém. Trav. Ecole Prat. Hautes Etudes, Inst. Montpellier, Vol. 21, pp. 769–805.

Ahmadzadeh, F., Carretero, M.A., James Harris, D., Perera, A. and Böhme, W., 2012. A molecular phylogeny of the eastern group of ocellated lizard genus *Timon* (Sauria: Lacertidae) based on mitochondrial and nuclear DNA sequences. Amphibia-Reptilia 33, 1–10.

Ahmadzadeh, F., Flecks, M., Carretero, M.A., Böhme, W., Ihlow, F., Kapli, P., Miraldo, A. and Rödder, D., 2016. Separate histories in both sides of the Mediterranean: phylogeny and niche evolution of ocellated lizards. J. Biogeogr. 43, 1242–1253.

Anderson, S.C., 1999. The Lizards of Iran. Society for the Study of Amphibians and Reptiles. Oxford, Ohio, Vol. 6, pp. 1–442.

Arbour, V.M. and Currie, P.J., 2012. Analyzing taphonomic deformation of ankylosaur skulls using retrodeformation and finite element analysis. PLoS One 7, e39323.

Archie, J.W., 1985. Methods for coding variable morphological features for numerical taxonomic analysis. Syst. Biol. 34, 326–345.

Arnold, E.N., 1973. Relationships of the Palaearctic lizards assigned to the genera *Lacerta*, *Algyroides* and *Psammodromus* (Reptilia: Lacertidae). Bull. Br. Mus. Nat. Hist. Zool. 25, 289–366.

Arnold, E.N., 1998. Cranial kinesis in lizards-variations, uses, and origins. Evol. Biol. 30, 323–357.

Arnold, E.N., Arribas, O. and Carranza, S., 2007. Systematics of the Palaearctic and Oriental lizard tribe Lacertini (Squamata: Lacertidae: Lacertinae), with descriptions of eight new genera. Zootaxa 1430, 1–86.

Augé, M., 1993. Une nouvelle espèce de Lacertidé (Reptila, Lacertilia) des faluns miocènes de l'Anjou-Touraine [A new lacertid species (Reptilia, Lacertilia) from the Miocene faluns of Anjou-Touraine]. Bull. Soc. Sci. Nat. Ouest Fr. 15, 69–74.

Augé, M.L., 2005. Evolution des lézards du Paléogène en Europe [Evolution of the lizards from the Paleogene of Europe]. Mém. Mus. Natl. Hist. Nat. Sér. A Zool. 192, 3–369.

Augé, M., Bailon, S. and Malfay, J.-P., 2003. Un nouveau genre de Lacertidae (Reptilia, Lacertilia) dans les faluns miocenes de l'Anjou-Touraine (Maine-et-Loire, France) [A new genus of Lacertidae (Reptilia, Lacertilia) from the Miocene faluns of Anjou-Touraine]. Geodiversitas 25, 289–295.

Augé, M.L. and Guével, B., 2018. New varanid remains from the Miocene (MN4–MN5) of France: inferring fossil lizard phylogeny from subsets of large morphological data sets. J. Vertebr. Paleontol. 38, e1410483.

Augé, M.L. and Hervet, S., 2009. Fossil lizards from the locality of Gannat (late Oligocene–early Miocene, France) and a revision of the genus *Pseudeumeces* (Squamata, Lacertidae). Paleobiodivers. Paleoenviron. 89, 191.

Augé, M.L. and Smith, R., 2009. An assemblage of early Oligocene lizards (Squamata) from the locality of Boutersem (Belgium), with comments on the Eocene-Oligocene transition. Zool. J. Linn. Soc. 155, 148–170.

Bailon, S., Boistel, R., Bover, P. and Alcover, J.A., 2014. *Maioricalacerta rafelinensis*, gen. et sp. nov. (Squamata, Lacertidae), from the early Pliocene of Mallorca (Balearic Islands, western Mediterranean Sea). J. Vertebr. Paleontol. 34, 318–326.

Barahona, F. and Barbadillo, L.J., 1997. Identification of some Iberian lacertids using skull characters. Rev. Esp. Herpetol., 11, 47–62.

Barahona, F. and Barbadillo, L.J., 1998. Inter- and intraspecifc variation in the post-natal skull of some lacertid lizards. J. Zool. 245, 393–405.

Barahona, F., Evans, S.E., Mateo, J.A., García-Márquez, M. and López-Jurado, L.F., 2000. Endemism, gigantism and extinction in island lizards: the genus *Gallotia* on the Canary Islands. J. Zool. 250, 373–388.

Barahona Quintana, F.F., 1996. Osteologia craneal de lacértidos de la Peninsula Iberica e Islas Canarias: analisis sistematico filogenético [Cranial osteology of lacertids from the Iberian Peninsula and the Canary Islands: a systematic phylogenetic analysis]. Ph.D. dissertation. Universidad Autonoma de Madrid.

Barrett, P.M. and Upchurch, P., 2005. Sauropodomorph diversity through time: Paleoecological and Macroevolutionary Implications. In: Curry-Rogers, K.A. & Wilson, J. (Eds.) The Sauropods: Evolution and Paleobiology. University of California Press, Berkeley, CA, pp. 125–156.

Böhme, W. and Zammit-Maempel, G., 1982. *Lacerta siculimelitensis* sp. n. (Sauria: Lacertidae), a giant lizard from the Late Pleistocene of Malta. Amphibia-Reptilia 3, 257–268.

de Bonis, L., 1974. Premières données sur les carnivores fissipèdes provenant des fouilles récentes dans le Quercy [First data on the fissiped carnivores from recent excavations in Quercy]. Palaeovertebrata 6, 27–32.

de Bonis, L. (2011) Una nueva especie de *Adelpharctos* (Mammalia, Carnivora, Ursidae) del Oligoceno Superior de las "Fosforitas de Quercy" (Francia) [A new species of *Adelpharctos* (Mammalia, Carnivora, Ursidae) from the upper Oligocene of the Phosphorites du Quercy (France)]. Estudios 67, 179–186.

de Bonis, L., Peigne, S. and Hugueney, M., 1999. Carnivores feloides de l'Oligocene superieur de Coderet-Bransat (Allier, France) [Feloid carnivores from the upper Oligocene of Coderet-Brasant (Aliier, France]. Bull. Soc. Géol. Fr. 170, 939–949.

Borczyk, B., Kusznierz, J., Paśko, Ł. and Turniak, E., 2014. Scaling of the sexual size and shape skull dimorphism in the sand lizard (*Lacerta agilis* L.). Vertebr. Zool. 64, 221–227.

Borsuk-Bialynicka, M., Lubka, M. and Böhme, W., 1999. A lizard from Baltic amber (Eocene) and the ancestry of the crown group lacertids. Acta Palaeontol. Polonica 44, 349–382.

Brazeau, M.D., 2011. Problematic character coding methods in morphology and their effects. Biol. J. Linn. Soc. Lond. 104, 489–498.

Brizuela, S., 2010. Los lagartos continentales fósiles de la Argentina (excepto Iguania) [The fossil continental lizards of Argentina (except Iguania)]. Ph.D. dissertation. Facultad de Ciencias Naturales y Museo.

Brusatte, S.L., 2010. Representing supraspecific taxa in higher-level phylogenetic analyses: guidelines for palaeontologists. Palaeontology 53, 1–9.

Caputo, V., 2004. The cranial osteology and dentition in the scincid lizards of the genus *Chalcides* (Reptilia, Scincidae). Ital. J. Zool. 71, 35–45.

Castillo, C., Rando, J.C. and Zamora, J.F., 1994. Discovery of mummified extinct giant lizards (*Gallotia goliath*, Lacertidae) in Tenerife, Canary Islands. Bonn. Zool. Beitr. 45, 129–136.

Catalano, S.A., Goloboff, P.A. and Giannini, N.P., 2010. Phylogenetic morphometrics (I): the use of landmark data in a phylogenetic framework. Cladistics 26, 539–549.

Čerňanský, A. and Augé, M.L., 2013. New species of the genus *Plesiolacerta* (Squamata: Lacertidae) from the upper Oligocene (MP28) of southern Germany and a revision of the type species *Plesiolacerta lydekkeri*. Palaeontology 56, 79–94.

Čerňanský, A., Augé, M.L. and Phelizon, A., 2020. Dawn of lacertids (Squamata, Lacertidae): new finds from the upper Paleocene and the lower Eocene. J. Vertebr. Paleontol. 40(1), e1768539.

Čerňanský, A., Bolet, A., Müller, J., Rage, J.-C., Augé, M. and Herrel, A., 2017. A new exceptionally preserved specimen of *Dracaenosaurus* (Squamata, Lacertidae) from the Oligocene of France as revealed by micro-computed tomography. J. Vertebr. Paleontol. 37, e1384738.

Čerňanský, A., Klembara, J. and Smith, K.T., 2016. Fossil lizard from central Europe resolves the origin of large body size and herbivory in giant Canary Island lacertids. Zool. J. Linn. Soc. 176, 861–877.

Čerňanský, A. and Smith, K.T., 2018. Eolacertidae: a new extinct clade of lizards from the Palaeogene; with comments on the origin of the dominant European reptile group–Lacertidae. Hist. Biol. 30, 994–1014.

Čerňanský, A. and Syromyatnikova, E.V., 2019. The first Miocene fossils of *Lacerta cf. trilineata* (Squamata, Lacertidae) with a comparative study of the main cranial osteological differences in green lizards and their relatives. PLoS One 14, e0216191.

Conrad, J.L., 2008. Phylogeny and systematics of Squamata (Reptilia) based on morphology. Bull. Am. Mus. Nat. Hist. 310, 1–182.

Darevsky, I.S., 1967. Rock Lizards of the Caucasus (Systematics, Ecology, and Phylogeny of the Polymorphic Lizards of the Caucasus of the subgenus *Archaeolacerta*). Nauka, Saint Petersburg Leningrad (in Russian): Published in English for Smithsonian Institution and the National Science Foundation, Washington D. C., translated by the Indian National Scientific Documentation Centre. New Delhi, pp. 1–216.

De Queiroz, K., 1987. Phylogenetic systematics of iguanine lizards: a comparative osteological study. Univ. Calif. Publ. Zool. 118, 1–203.

Denton, R.K. and O'Neill, R.C., 1995. *Prototeius stageri*, gen. et sp. nov., a new teiid lizard from the Upper Cretaceous Marshalltown Formation of New Jersey, with a preliminary phylogenetic revision of the Teiidae. J. Vertebr. Paleontol. 15, 235–253.

Eiselt, J., 1968. Ergebnisse zoologischer Sammelreisen in der Türkei: Ein Beitrag zur Taxonomie der Zagros-Eidechse, *Lacerta princeps* Blanford [Results of zoological collection trips to Turkey: a contribution to the taxonomy of the Zagros-lizard *Lacerta princeps* Blanford]. Ann. Nat. Hist. Mus. Wien. 72, 409–434.

Estes, R., 1983a. The fossil record and early distribution of lizards. In: Rhodin, A. & Miyata, K. (Eds.) Advances in Herpetology and Evolution: Essays in Honor of Ernest E. Williams. Museum of Comparative Zoology, Cambridge, MA, pp. 365–398.

Estes, R., 1983b. Sauria terrestria. Handbuch der Paläoherpetologie. Gustav Fischer, Stuttgart, 249 pp.

Estes, R., De Queiroz, K. and Gauthier, J., 1988. Phylogenetic relationships within Squamata. In: Estes, R. & Pregill, G. (Eds.) Phylogenetic Relationships of the Lizard Families. Stanford University Press, Palo Alto, CA, pp. 119–281.

Evans, S.E., 2008. The skull of lizards and tuatara. In: Gans, C., Gaunt, A.S. & Adler, K. (Eds.) Biology of the Reptilia. Society for the Study of Amphibians and Reptiles, Ithaca, NY. Contrib. Herpetol., pp. 1–347.

Farris, J.S., 1990. Phenetics in camouflage. Cladistics 6, 91–100.

Fu, J., 1998. Toward the phylogeny of the family Lacertidae: implications from mitochondrial DNA 12S and 16S gene sequences (Reptilia: Squamata). Mol. Phylogenet. Evol. 9, 118–130.

Garcia-Porta, J., Irisarri, I., Kirchner, M., Rodríguez, A., Kirchhof, S., Brown, J.L., MacLeod, A., Turner, A.P., Ahmadzadeh, F., Albaladejo, G. *et al*., 2019. Environmental temperatures shape thermal physiology as well as diversification and genome-wide substitution rates in lizards. Nat. Commun. 10, 1–12.

Gauthier, J.A., 1986. Saurischian monophyly and the origin of birds. Mem. Calif. Acad. Sci. 8, 1–55.

Gauthier, J.A., Kearney, M., Maisano, J.A., Rieppel, O. and Behlke, A.D.B., 2012. Assembling the Squamate tree of life: Perspectives from the phenotype and the fossil record. Bull. Peabody Mus. Nat. Hist. 53, 3–308.

Georgalis, G.L., 2017. *Necrosaurus* or *Palaeovaranus*? Appropriate nomenclature and taxonomic content of an enigmatic fossil lizard clade (Squamata). Ann. de Paléontol. 103, 293–303.

Georgalis, G.L., Villa, A. and Delfino, M., 2017. The last European varanid: demise and extinction of monitor lizards (Squamata, Varanidae) from Europe. J. Vertebr. Paleontol. 37, e1301946.

Georgalis, G.L., Villa, A., Ivanov, M., Vasilyan, D. and Delfino, M., 2019. Fossil amphibians and reptiles from the Neogene locality of Maramena (Greece), the most diverse European herpetofauna at the Miocene/Pliocene transition boundary. Palaeontol. Electron. 22, 1–99.

Goloboff, P.A., 2014. Extended implied weighting. Cladistics 30, 260–272.

Goloboff, P.A. & Catalano, S.A., 2016. TNT version 1.5, including a full implementation of phylogenetic morphometrics. Cladistics 32, 221–238.

Goloboff, P.A., Mattoni, C.I. and Quinteros, A.S., 2006. Continuous characters analyzed as such. Cladistics 22, 589–601.

Goloboff, P.A., Torres, A. and Arias, J.S., 2018. Weighted parsimony outperforms other methods of phylogenetic inference under models appropriate for morphology. Cladistics 34, 407–437.

Hipsley, C.A., Himmelmann, L., Metzler, D. and Müller, J., 2009. Integration of Bayesian molecular clock methods and fossil-based soft bounds reveals early Cenozoic origin of African lacertid lizards. BMC Evol. Biol. 9, 1–13.

Hoffstetter, R., 1944. Sur les Scincidae fossiles. I. Formes européennes et nord-américaines [On the fossil Scincidae. I. European and North-American forms]. Bull. Mus. Natl. Hist. Nat. 16, 547–553.

Huelsenbeck, J.P., 1991. When are fossils better than extant taxa in phylogenetic analysis? Syst. Biol. 40, 458–469.

Hugueney, M., 1969. Les rongeurs (Mammalia) de l'oligocène supérieur de Coderet-Bransat (Allier) [The rodents (Mammalia) of the Upper Oligocene of Coderet-Bransat (Allier)]. Docum. Lab. Géol. Lyon. 34, 1–227.

Ilgaz, Ç. and Kumlutaş, Y., 2008. The morphology and distribution of *Timon princeps* (Blanford 1874) (Sauria: Lacertidae) in southeastern Anatolia, Turkey. North West. J. Zool. 4, 247–262.

Khosravani, A., Rastegar-Pouyani, N. and Oraie, H., 2011. Comparative skull osteology of the lacertid lizards *Eremias persica* and *Mesalina watsonana* (Sauria: Lacertidae). IJAB. 7, 99–117.

Klembara, J., Böhme, M. and Rummel, M., 2010. Revision of the anguine lizard *Pseudopus laurillardi* (Squamata, Anguidae) from the Miocene of Europe, with comments on paleoecology. J. Paleontol. 84, 159–196.

Klemmer, K., 1957. Untersuchungen zur Osteologie und Taxionomie der europäischen Mauereidechsen [Analyses of the osteology and taxonomy of the European wall lizards]. Abh. Senckenb. Naturforsch. Ges. 496, 1–56.

Kosma, R., 2004. The dentitions of recent and fossil scincomorphan lizards (Lacertilia, Squamata) – Systematics, Functional Morphology, Palecology. Ph.D. dissertation, Universität Hannover.

Lee, M.S.Y., 1998. Convergent evolution and character correlation in burrowing reptiles: towards a resolution of squamate relationships. Biol. J. Linn. Soc. Lond. 65, 369–453.

Ljubisavljević, K., Urosević, A., Aleksić, I. & Ivanović, A., 2010. Sexual dimorphism of skull shape in a lacertid lizard species (*Podarcis* spp., *Dalmatolacerta* sp., *Dinarolacerta* sp.) revealed by geometric morphometrics. Zoology 113, 168–174.

Losos, J.B., Hillis, D.M. and Greene, H.W., 2012. Evolution. Who speaks with a forked tongue? Science 338, 1428–1429.

Maca-Meyer, N., Carranza, S., Rando, J.C., Arnold, E.N. and Cabrera, V.M., 2003. Status and relationships of the extinct giant Canary Island lizard *Gallotia goliath* (Reptilia: Lacertidae), assessed using ancient mtDNA from its mummified remains. Biol. J. Linn. Soc. Lond. 80, 659–670.

Maddison, W.P. & Maddison, D.R. (2018) Mesquite: a modular system for evolutionary analysis. Version 3.51. http://www.mesquiteproject.org

Mateo Miras, J.A., 1988. Estudio sistemático y zoogeográfico de los lagartos ocelados, *Lacerta lepida* Daudin, 1802, y *Lacerta pater* (Lataste, 1880), (Sauria: Lacertidae) [Systematic and zoogeographic studies of the ocellated lizards *Lacerta lepida* Daudin, 1802 and *Lacerta pater* (Lataste, 1880), (Sauria, Lacertidae)]. Ph.D. dissertation, Universidad de Sevilla, 485 pp.

Miraldo, A., Faria, C., Hewitt, G.M., Paulo, O.S. and Emerson, B.C., 2012. Genetic analysis of a contact zone between two lineages of the ocellated lizard (*Lacerta lepida* Daudin, 1802) in southeastern Iberia reveal a steep and narrow hybrid zone. J. Zool. Syst. Evol. Res. 51, 45–54.

Müller, J., 1996. Eine neue Art der Echten Eidechsen (Reptilia: Lacertilia: Lacertidae) aus dem Unteren Miozan von Poncenat, Frankreich [A new species of true lizards (Reptilia: Lacertilia: Lacertidae) from the lower Miocene of Poncenat, France]. Mainz. Geowiss. Mitt. 25, 79–88.

Müller, J., Hipsley, C.A., Head, J.J., Kardjilov, N., Hilger, A., Wuttke, M. and Reisz, R.R., 2011. Eocene lizard from Germany reveals amphisbaenian origins. Nature 473, 364–367.

Nydam, R.L. and Cifelli, R.L., 2002. A new teiid lizard from the Cedar Mountain Formation (Albian–Cenomanian boundary) of Utah. J. Vertebr. Paleontol. 22, 276–285.

Nydam, R.L., Eaton, J.G. and Sankey, J., 2007. New taxa of transversely-toothed lizards (Squamata: Scincomorpha) and new information on the evolutionary history of "teiids". J. Paleontol. 81, 538–549.

Paulo, O.S., Pinheiro, J., Miraldo, A., Bruford, M.W., Jordan, W.C. and Nichols, R.A., 2008. The role of vicariance vs. dispersal in shaping genetic patterns in ocellated lizard species in the western Mediterranean. Mol. Ecol. 17, 1535–1551.

Pei, R., Pittman, M., Goloboff, P.A., Dececchi, T.A., Habib, M.B., Kaye, T.G., Larsson, H.C., Norell, M.A., Brusatte, S.L. and Xu, X., 2020. Potential for powered flight neared by most close avialan relatives, but few crossed its thresholds. Curr. Biol. 30, 4033–4046.

Pereira, B.C., 2015. Echinoid diversity through time. In: Zamora, S. & Rábano, I. (Eds.) Progress in Echinoderm Palaeobiology, Cuadernos Del Museo Geominero. Instituto Geológico y Minero de España, Madrid, pp. 133–136.

Perera, A. & Harris, J.D. (2010) Genetic variability in the ocellated lizard *Timon tangitanus* in Morocco. Afr. Zool., 45, 321–329.

Poe, S. and Wiens, J.J., 2000. Character selection and the methodology of morphological phylogenetics. In: Wiens, J.J. (Ed.) Phylogenetic Analysis of Morphological Data. Smithsonian Institution Press, Washington, DC, pp. 20–36.

Pol, D. and Escapa, I.H., 2009. Unstable taxa in cladistic analysis: identification and the assessment of relevant characters. Cladistics 25, 515–527.

Prothero, D.R., 1994. The Eocene-Oligocene Transition: Paradise Lost. Columbia University Press, New York, 291 pp.

Pyron, R.A., Burbrink, F.T. and Wiens, J.J., 2013. A phylogeny and revised classification of Squamata, including 4161 species of lizards and snakes. BMC Evol. Biol. 13, 1–54.

Quadros, A.B., Chafrat, P. and Zaher, H., 2018. A new teiid lizard of the genus *Callopistes* Gravenhorst, 1838 (Squamata, Teiidae), from the lower Miocene of Argentina. J. Vertebr. Paleontol. 38, 1–18.

Rae, T.C., 1998. The logical basis for the use of continuous characters in phylogenetic systematics. Cladistics 14, 221–228.

Rage, J.-C., 1987. Extinctions chez les Squamates (Reptiles) à la fin de l'Oligocène en France. Adaptations et modifications de l'environnement [Extinctions in Squamates (Reptiles) at the end of the Oligocene, France. Adaptations and modifications of the environment]. Mém. Soc. géol. Fr. 150, 145–149.

Rage, J.-C., 2013. Mesozoic and Cenozoic squamates of Europe. Paleobiodivers. Paleoenviron. 93, 517–534.

Rauscher, K.L., 1992. Die Echsen (Lacertilia, Reptilia) aus dem Plio-Pleistozän von Bad Deutsch-Altenburg, Niederösterreich [The lizards (Reptilia) from the Plio-Pleistocene of Bad Deutsch-Altenburg, Lower Austria]. Beitr. Paläont. Österr. 17, 81–177.

Reeder, T.W., Townsend, T.M., Mulcahy, D.G., Noonan, B.P., Wood, P.L. Jr, Sites, J.W. Jr and Wiens, J.J. (2015) Integrated analyses resolve conflicts over squamate reptile phylogeny and reveal unexpected placements for fossil taxa. PLoS One 10, e0118199.

Roček, Z., 1980. Intraspecific and ontogenetic variation of the dentition in the green lizard *Lacerta viridis* (Reptilia, Squamata). Vest. Cs. Spolec. Zool. 44, 272–278.

Roček, Z., 1984. Lizards (Reptilia: Sauria) from the Lower Miocene locality Dolnice (Bohemia, Czechoslovakia). Rozpr. Československ. Akad. Věd, Řada Mat. Přír. Věd., 93, 1–69.

Scanlon, J.D., 1996. Studies in the paleontology and systematics of Australian Snakes. Ph.D. dissertation, University of New South Wales, Sydney, Australia.

Scarpetta, S.G., 2020. Effects of phylogenetic uncertainty on fossil identification illustrated by a new and enigmatic Eocene iguanian. Sci. Rep. 10, 1–10.

Schmidt-Kittler, N., Brunet, M., Godinot, M., Franzen, J.L., Hooker, J.J., Legendre, S. and Vianey-Liaud, M., 1987. European reference levels and correlation tables. Münch. Geowiss. Abh. A.. 10, 13–31.

Sereno, P.C., 2007. Logical basis for morphological characters in phylogenetics. Cladistics 23, 565–587.

Sillero, N., Campos, J., Bonardi, A., Corti, C., Creemers, R., Crochet, P.A., Crnobrnja-Isailovic, J., Denoël, M., Ficetola, G.F., Gonçalves, J. *et al.*, 2014. Updated distribution and biogeography of amphibians and reptiles of Europe. Amphibia-Reptilia 35, 1–31.

Simões, T.R., Caldwell, M.W., Talanda, M., Bernardi, M., Palci, A., Vernygora, O., Bernardini, F., Mancini, L., and Nydam, R.L., 2018. The origin of squamates revealed by a Middle Triassic lizard from the Italian Alps. Nature 557, 706–709.

Speybroeck, J., Beukema, W., Bok, B. and Van Der Voort, J., 2016 Field Guide to the Amphibians and Reptiles of Britain and Europe. Bloomsbury, London.

Speybroeck, J., Beukema, W., Dufresnes, C., Fritz, U., Jablonski, D., Lymberakis, P., Martínez-Solano, I., Razzetti, E., Vamberger, M., Vences, M. *et al.*, 2020. Species list of the European herpetofauna – 2020 update by the Taxonomic Committee of the Societas Europaea Herpetologica. Amphibia-Reptilia 1, 1–51.

Stehlin, H.G., 1909. Remarques sur les faunules de mammifères des couches éocènes et oligocènes du Bassin de Paris [Remarks on mammalian faunules of the Eocene and Oligocene layers of the Paris Basin]. Bull. Soc. Géol. France 19, 488–520.

Tennant, J.P., Mannion, P.D. and Upchurch, P., 2016. Sea level regulated tetrapod diversity dynamics through the Jurassic/Cretaceous interval. Nat. Commun. 7, 12737.

Thaler, L., 1966. Les rongeurs fossiles du Bas-Languedoc dans leurs rapports avec l'histoire des faunes et la stratigraphie du Tertiaire d'Europe [The fossil rodents of Bas-Languedoc in their relationship with the history of fauns and the stratigraphy of the Tertiary of Europe]. Mém. Mus. Natl. Hist. Nat. Sér. C. 17, 1–295.

Townsend, T., Larson, A., Louis, E. and Macey, J.R., 2004. Molecular phylogenetics of Squamata: the position of snakes, amphisbaenians, and dibamids, and the root of the squamate tree. Syst. Biol. 53, 735–757.

Tschopp, E., Napoli, J.G.N., Wencker, L.C.M., Delfino, M. & Upchurch, P. (in review). How to render species comparable taxonomic units through deep time: a case study on intraspecific osteological variability in extant and extinct lacertid lizards. Syst. Biol.

Tschopp, E., Russo, J. and Dzemski, G., 2013. Retrodeformation as a test for the validity of phylogenetic characters: an example from diplodocid sauropod vertebrae. Palaeontol. Electron. 16, 1–23.

Tschopp, E., Tschopp, F.A. and Mateus, O., 2018a. Overlap Indices: Tools to quantify the amount of anatomical overlap among groups of incomplete terminal taxa in phylogenetic analyses. Acta Zool. 99, 169–176.

Tschopp, E., Villa, A., Camaiti, M., Ferro, L., Tuveri, C., Rook, L., Arca, M., Delfino, M., 2018b. The first fossils of *Timon* (Squamata: Lacertinae) from Sardinia (Italy) and potential causes for its local extinction in the Pleistocene. Zool. J. Linn. Soc. 184, 825–856.

Tschopp, E. and Upchurch, P., 2019. The challenges and potential utility of phenotypic specimen-level phylogeny based on maximum parsimony. Earth. Environ. Sci. Trans. R. Soc. Edinb. 109, 301–323.

Uetz, P., Freed, P. and Hošek, J., 2018. Species statistics. The Reptile Database. Available at: http://www.reptile-database.org (accessed 23 June 2018).

Vianey-Liaud, M., 1974. L'anatomie crânienne des genres *Eucricetodon* et *Pseudocricetodon* (Cricetidae, Rodentia, Mammalia); essai de systématique des Cricétidés oligocènes d'Europe occidentale [Cranial anatomy of the genuses *Eucricetodon* and *Pseudocricetodon* (Cricetidae, Rodentia, Mammalia); systematic test of the Oligocene cricetids of Western Europe]. Géol. Méditerr. 1, 111–131.

Vianey-Liaud, M., Marivaux, L., 2016. Autopsie d'une radiation adaptative: Phylogénie des Theridomorpha, rongeurs endémiques du Paléogène d'Europe-histoire, dynamique évolutive et intérêt biochronologique [Autopsy of an adaptive radiation: Phylogeny of Theridomorpha, endemic rodents of the Paleogene of historic Europe, evolutionary dynamics and biochronological interest]. Palaeovertebrata 40, 1–68.

Vianey-Liaud, M. and Wood, A.E., 1976. Les Issiodoromyinae (Rodentia, Theridomyidae) de l'Éocène supérieur à l'Oligocène

supérieur en Europe occidentale: [The Issiodoromyinae (Rodentia, Theriodomyidae) from the Upper Eocene to the Upper Oligocene of Western Europe]. Paleovertebrata 7, 1–115.
Vidal, N. and Hedges, S.B., 2005. The phylogeny of squamate reptiles (lizards, snakes, and amphisbaenians) inferred from nine nuclear protein-coding genes. C. R. Biol. 328, 1000–1008.
Villa, A., Abella, J., Alba, D.M., Almécija, S., Bolet, A., Koufos, G.D., Knoll, F., Luján, À.H., Morales, J., Robles, J.M. *et al.*, 2018. Revision of *Varanus marathonensis* (Squamata, Varanidae) based on historical and new material: morphology, systematics, and paleobiogeography of the European monitor lizards. PLoS One 13, e0207719.
Villa, A. and Delfino, M., 2019a. Fossil lizards and worm lizards (Reptilia, Squamata) from the Neogene and Quaternary of Europe: an overview. Swiss J. Palaeontol. 138, 177–211.
Villa, A. and Delfino, M., 2019b. A comparative atlas of the skull osteology of European lizards (Reptilia: Squamata). Zool. J. Linn. Soc. 187, 829–928.
Villa, A., Tschopp, E., Georgalis, G.L. and Delfino, M., 2017. Osteology, fossil record and palaeodiversity of the European lizards. Amphibia-Reptilia 38, 79–88.
Vincent, S.E. and Herrel, A., 2007. Functional and ecological correlates of ecologically-based dimorphisms in squamate reptiles. Integr. Comp. Biol. 47, 172–188.
Wiens, J.J., 1995. Polymorphic characters in phylogenetic systematics. Syst. Biol. 44, 482–500.
Wiens, J.J., 2003. Missing data, incomplete taxa, and phylogenetic accuracy. Syst. Biol. 52, 528–538.
Wiens, J.J., 2015. Explaining large-scale patterns of vertebrate diversity. Biol. Lett. 11, 20150506.
Wiens, J.J., Brandley, M.C., and Reeder, T.W., 2006. Why does a trait evolve multiple times within a clade? Repeated evolution of snakeline body form in squamate reptiles. Evolution 60, 123–141.
Wiens, J.J., Hutter, C.R., Mulcahy, D.G., Noonan, B.P., Townsend, T.M., Sites, J.W. Jr and Reeder, T.W., 2012. Resolving the phylogeny of lizards and snakes (Squamata) with extensive sampling of genes and species. Biol. Lett. 8, 1043–1046.
Wiens, J.J., Kuczynski, C.A., Townsend, T., Reeder, T.W., Mulcahy, D.G. and Sites, J.W. Jr, 2010. Combining phylogenomics and fossils in higher-level squamate reptile phylogeny: molecular data change the placement of fossil taxa. Syst. Biol. 59, 674–688.
Wilkinson, M. and Benton, M.J., 1995. Missing data and rhynchosaur phylogeny. Hist. Biol. 10, 137–150.
Zachos, J., Pagani, M., Sloan, L., Thomas, E. and Billups, K., 2001. Trends, rhythms, and aberrations in global climate 65 Ma to present. Science 292, 686–693.
Zheng, Y. and Wiens, J.J., 2015. Do missing data influence the accuracy of divergence-time estimation with BEAST? Mol. Phylogenet. Evol. 85, 41–49.
Zheng, Y. and Wiens, J.J., 2016. Combining phylogenomic and supermatrix approaches, and a time-calibrated phylogeny for squamate reptiles (lizards and snakes) based on 52 genes and 4162 species. Mol. Phylogenet. Evol. 94, 537–547.

Supporting Information

Additional supporting information may be found online in the Supporting Information section at the end of the article.

A .zip file including the following supplementary material can be downloaded here: https://doi.org/10.6084/m9.figshare.13277564

File S1. Nexus file of the premaxilla taxon-character matrix (.nex format).

File S2. Nexus file of the maxilla taxon-character matrix (.nex format).

File S3. Nexus file of the dentary taxon-character matrix (.nex format).

File S4. List of characters including their character classifications (.xlsx format).

File S5. List of studied specimens (.xlsx format).

File S6. List of references for File S4 and File S5 (.pdf format).

File S7. List of figured mOTUs including their preliminary collection numbers (.xlsx format).

File S8. TNT input files and tree files (.tre format) of analyses of complete premaxilla, maxilla and dentary datasets (k = 5, 12, 20) (.zip format).

File S9. TNT input files and tree files (.tre and .nex format) of analyses of reduced premaxilla, maxilla and dentary datasets (k = 5, 12, 20) (.zip format).

File S10. TNT tree files (.tre and .nex format) of stability analyses of premaxilla, maxilla and dentary datasets (k = 5, 12, 20), including the script for taxa pruning (.zip format).

File S11. TNT input files and tree files (.tre format) of analyses of cross-regional premaxilla, maxilla, and dentary datasets (k = 5, 12, 20) (.zip format).

File S12. Single MPTs or strict consensus trees of the phylogenetic analyses testing the positions of the cross-regional mOTUs individually (.pdf format).

File S13. Strict consensus trees of analyses of complete premaxilla, maxilla and dentary datasets (k = 5, 12) (.pdf format).

File S14. Individual figures of morphotypes (.zip format).

File S15. Table of completeness of the eight fossil wild card taxa (.pdf format).

Appendix 1

List of newly inserted characters, including their states and sources.

No.	New character	Source (and original character numbers)
12	Premaxilla, tooth-bearing portion: curvature, anteroposterior length to transverse width: <0.2 (wide) (0); 0.2–0.4 (intermediate) (1); >0.4 (narrow) (2).	LCMW, pers. obs., 2018
36	Premaxilla, tooth row, shape: U-shaped (0); V-shaped (1).	LCMW, pers. obs., 2018
40	Premaxilla, second pair of ethmoidal foramina: absent (0); present (1).	LCMW, pers. obs., 2019
41	Premaxilla, ascending nasal process, posterodorsal end, shape in anterior view: pointed (0); widely rounded (1).	Barahona & Barbadillo (1997; C3.1), modified (split in two) by Villa et al. (2017; C23)
47	Premaxilla, ascending nasal process, length of articulation with the nasals: less than half nasal length (0); more than halfway to frontal between nasals (1).	modified after Gauthier et al. (2012; C10; exclusion of character state (2): nearly to, or articulates with frontals); Quadros et al. (2018; C3)
48	Premaxilla, ascending nasal process, constriction at the base: absent (0); present (1).	wording modified from Quadros et al. (2018; C4); Brizuela (2010; C3)
62	Maxilla, anteromedial premaxillary process lying between vomers and premaxilla: absent, vomers contact premaxilla (0); present, vomers do not contact premaxilla (1).	Estes et al. (1988; C12); Denton and O'Neill (1995; C4); Nydam and Cifelli (2002; C4); Nydam et al. (2007; C4); Conrad (2008; C25); Quadros et al. (2018; C13)
73	Nasals, anterior width: exceeds nasofrontal joint width (0); is subequal to nasofrontal joint width (1); less than anterior frontal width (2).	Gauthier et al. (2012; C18); Quadro et al. (2018; C6)
74	Nasal, anterior border: nasolateral process present, forming the posterior border and part of the labial border of the external nares (0); nasolateral process absent (1).	Quadros et al. (2018; C7); modified from Conrad (2008; C22); Gauthier et al. (2012; C22)
77	Dermal skull bone ornamentation, frontal/parietal: absent, dermal skull roof smooth (0); present over dorsum (1); present on jugal postorbital bar (2).	Modified after Quadros et al. (2018; C17; wording modified and exclusion of state (1): lightly rugose about frontoparietal suture); modified from Estes et al. (1988; C129); Conrad (2008; C10); Gauthier et al. (2012; C572)
93	Postorbital, overlapping of squamosal: dorsomedially as slender tapering rod attached superficially (0); dorsally (1); postorbital in long V-shaped trough dorsally and then rotating dorsolaterally posteriorly (2); squamosal lies in trough beneath postorbital (3).	Modified from Gauthier et al. (2012; C78; exclusion of state (0): laterally into V-shaped recess in squamosal); Arnold (1998); Quadros et al. (2018; C35)
107	Quadrate, tympanic crest shape: straight or vertically developed (0); curved, forming "C" on outer line (1).	Wording modified after Quadros et al. (2018; C78); modified from Brizuela (2010; C63)
109	Squamosal, base of temporal ramus: diverges from parietal (0); base lies against parietal (1).	Quadros et al. (2018; C46); Gauthier et al. (2012; C162)
110	Supratemporal position on parietal: partly ventral (0); partly ventrolateral (1); all lateral (2); dorsolateral (3).	De Queiroz (1987); Gauthier et al. (2012; C170)
127	Parietal, parasagittal crest strongly developed on the dorsolateral surface for the insertion of the adductor mandible musculature: absent (0); present (1).	Quadros et al. (2018; C22); modified from Denton and O'Neill (1995; C10); Nydam and Cifelli (2002; C10); Nydam et al. (2007; C10); Conrad (2008; C75); Gauthier et al. (2012; C9)
128	Epipterygoid-parietal contact: absent (0); overlaps parietal temporal muscle origin parietal downgrowths (1).	Gauthier et al. (2012; C294); Quadros et al. (2018; C84)
155	Dentary, subdental ridge, shape: straight (0); concave (1).	Bailon et al. (2014)
159	Dentary, Meckelian canal, shape: triangular (0), tubular (1).	ET, pers. obs., 2018
160	Dentary, orientation of teeth at the anterior tip: upright (0); tilted anteriorly or procumbent (1).	LCMW, pers. obs., 2019
175	Coronoid-surangular articulation: coronoid restricted to medial aspect of mandible (0); coronoid extends onto dorsal surface of surangular (1); coronoid arches over dorsal margin of mandible to reach lateral surface of surangular (2).	Gauthier et al. (2012; C390); Quadros et al. (2018; C113)
184	Teeth, premaxillary, crown morphology (if monocuspid): fang-like/pointed (0); rounded (1).	LCMW, pers. obs., 2018
185	Teeth, premaxilla, median tooth: absent (0); present (1).	Wording modified from Scanlon (1996; C4); Lee (1998; C154); Gauthier et al. (2012; C413)
186	Teeth, premaxilla, median tooth: same size as neighbouring premaxillary teeth (0); enlarged (1).	Lee (1998; C155); modified after Gauthier et al. (2012; C414; wording modified and exclusion of state (2) greatly enlarged median premaxillary tooth)
190	Teeth, maxilla and dentary, differences in tooth robustness: (0) absent to minimal; present not more than 50% different in robustness (1); (present, 50% or more difference in robustness (2).	LCMW, pers. obs., 2019

Appendix 2

Positions of premaxilla, maxilla and dentary mOTUs in the trees with the complete and reduced datasets, and the analyses with the stable mOTUs only for each of the three k-values. Completeness scores for the individual mOTUs are given in brackets behind the taxon name. FV, Fouilles Viret; CC1sup, Coderet Couche 1 sup; CE1-0, Coderet E1-0; CH1-100, Coderet H1-100; CH1-75, Coderet H1-75; CCVsup, Coderet Couche Verte sup 1-25; LaC, La Colombière; Roq2, Roqueprune 2; MdGB, Mas de Got B; PdF, Pech-du-Fraysse; Cod, Coderet; *T+L*, *Timon* + *Lacerta*.

	Analysis with a *k*-value of 5			Analysis with a *k*-value of 12			Analysis with a *k*-value of 20		
mOTU	Complete	Reduced	Stable	Complete	Reduced	Stable	Complete	Reduced	Stable
P1 FV (66%)	Lacertoidea (clade with Amphisbaenia)	Lacertoidea (clade with Amphisbaenia)	Lacertoidea (clade with Amphisbaenia)	Polytomy with *D. croizeti*	Anguimorpha	Anguimorpha	Polytomy with *D. croizeti*	Anguimorpha	Anguimorpha
P1 CC1sup (72%)	Lacertoidea (clade with Amphisbaenia)	Lacertoidea (clade with Amphisbaenia)	Excluded	Polytomy with *D. croizeti*	Anguimorpha	Excluded	Polytomy with *D. croizeti*	Anguimorpha	Excluded
P1 CE1-0 (75%)	Lacertoidea (clade with Amphisbaenia)	Lacertoidea (clade with Amphisbaenia)	Lacertoidea (clade with Amphisbaenia)	Polytomy with *D. croizeti*	Anguimorpha	Anguimorpha	Polytomy with *D. croizeti*	Anguimorpha	Anguimorpha
P1 CCVsup (59%)	Lacertoidea	Anguimorpha; Lacertoidea	Lacertoidea	–	Anguimorpha	Excluded	–	Anguimorpha	Excluded
P2 CC1sup (72%)	Lacertoidea (sister/ polytomy to/with *S. merianae* + Lacertidae)	Lacertoidea (sister/ polytomy to/with *S. merianae* + Lacertidae)	Lacertoidea (sister/ polytomy to/with *S. merianae* + Lacertidae)	Clade with *B. major*	Scincoidea	Scincoidea	Clade with *B. major*	Scincoidea	Scincoidea
P2 CE1-0 (75%)	Lacertoidea (sister/ polytomy to/with *S. merianae* + Lacertidae)	Lacertoidea (sister/ polytomy to/with *S. merianae* + Lacertidae)	Lacertoidea (sister/ polytomy to/with *S. merianae* + Lacertidae)	Clade with *B. major*	Scincoidea	Scincoidea	Clade with *B. major*	Scincoidea	Scincoidea
P3 CE1-0 (69%)	Lacertoidea (sister to/ polytomy with *S. merianae* + Lacertidae)	Lacertoidea (sister to/ polytomy with *S. merianae* + Lacertidae)	Lacertoidea (sister to/ polytomy with *S. merianae* + Lacertidae)	Clade with *B. major*	Scincoidea	Scincoidea	Clade with *B. major*	Scincoidea	Scincoidea
P3 Roq2 (59%)	Scincoidea (sister to *B. major*)	Scincoidea (sister to *B. major*)	Scincoidea (sister to *B. major*)	Sister to *B. major*	Scincoidea (sister to *B. major*)	Scincoidea (sister to *B. major*)	Sister to *B. major*	Scincoidea (sister to *B. major*)	Scincoidea (sister to *B. major*)
P4 CE1-0 (59%)	Anguimorpha (sister to *A. veronensis*)	Anguimorpha (sister to *A. veronensis*)	Anguimorpha (sister to *A. veronensis*)	Sister to *A. veronensis*	Anguimorpha (sister to *A. veronensis*)	Anguimorpha (sister to *A. veronensis*)	Sister to *A. veronensis*	Anguimorpha (sister to *A. veronensis*)	Anguimorpha (sister to *A. veronensis*)
P5 FV (66%)	Lacertoidea (clade with Amphisbaenia)	Anguimorpha; Lacertoidea (clade with Amphisbaenia)	Excluded	Clade with *D. croizeti*	Anguimorpha	Anguimorpha	Clade with *D. croizeti*	Anguimorpha	Anguimorpha
P5 CH1-75 (75%)	Lacertoidea (clade with Amphisbaenia)	Anguimorpha; Lacertoidea (clade with Amphisbaenia)	Lacertoidea (clade with Amphisbaenia)	Clade with *D. croizeti*	Anguimorpha	Anguimorpha	Clade with *D. croizeti*	Anguimorpha	Anguimorpha
M1 FV (29%)	–	Lacertidae	Excluded	–	Gallotiinae	Excluded	–	Gallotiinae	Excluded
M1 CC1sup (36%)	–	Gallotiinae	Gallotiinae	–	Gallotiinae	Gallotiinae	–	Gallotiinae	Gallotiinae
M1 CE1-0 (61%)	–	Lacertidae	sister to Gallotiinae	–	Lacertidae	Lacertidae	–	Lacertidae	Lacertidae
M1 CH1-100 (25%)	–	*Podarcis*	Excluded	–	*Podarcis*	Excluded	–	*Podarcis*	Excluded
M1 CCVsup (39%)	–	*Podarcis*	sister to Gallotiinae	–	Lacertidae	Excluded	–	Lacertidae	Excluded
M2 CC1sup (36%)	sister to *L. pouiti*	Gallotiinae	Gallotiinae	–	Gallotiinae	Excluded	–	Gallotiinae	Excluded
M3 CC1sup (50%)	polytomy with "*L." filholi* (PdF)	Gallotiinae	Sister to Gallotiinae	–	Lacertidae	Lacertidae	–	Lacertidae	Lacertidae
M3 CH1-100 (32%)	polytomy with "*L." filholi* (PdF)	Lacertoidea (sister "*L." filholi* (PdF))	Sister to Gallotiinae	–	Lacertoidea (sister "*L." filholi* (PdF))	Lacertidae	–	Gallotiinae	Lacertidae
M4 CC1sup (32%)	polytomy with "*L." filholi* (PdF)	Gallotiinae	Sister to Gallotiinae	–	Lacertidae	Excluded	–	Lacertidae	xcluded
M4 CE1-0 (36%)	polytomy with "*L." filholi* (PdF)	Lacertidae	Sister to Gallotiinae	–	Lacertidae	Lacertidae	–	Lacertidae	Lacertidae
M4 CH1-100 (32%)	polytomy with "*L." filholi* (PdF)	Lacertidae	sister to Gallotiinae	–	Lacertidae	Excluded	–	Lacertidae	Excluded
M4 CCVsup (25%)	–	Lacertoidea	Excluded	–	Lacertoidea	Excluded	–	Lacertoidea	Excluded
M5 CE1-0 (50%)	–	–	Lacertoidea (sister to *S. merianae* + Lacertidae)	–	–	Lacertoidea (sister to *S. merianae* + Lacertidae)	–	–	Lacertoidea (sister to *S. merianae* + Lacertidae)
M6 CE1-0 (25%)	–	–	Excluded	–	–	Excluded	–	–	Excluded

Appendix 2 (Continued)

	Analysis with a *k*-value of 5			Analysis with a *k*-value of 12			Analysis with a *k*-value of 20		
mOTU	Complete	Reduced	Stable	Complete	Reduced	Stable	Complete	Reduced	Stable
D1 FV (75%)	–	*Lacerta*	*Podarcis*	–	*Lacerta*	*Podarcis*	–	*Lacerta*	*Podarcis*
D1 CC1sup (75%)	–	*Lacerta*	*Podarcis*	–	Gallotiinae; *Lacerta*	*Podarcis*	–	Gallotiinae; *Lacerta*	*Podarcis*
D1 CE1-0 (63%)	–	Gallotiinae; *Lacerta*	*Podarcis*	–	Gallotiinae	*Podarcis*	–	Gallotiinae	*Podarcis*
D2 FV (71%)	–	*Lacerta*	*Podarcis*	–	*Lacerta*	*Podarcis*	–	*Lacerta*	*Podarcis*
D2 CC1sup (79%)	–	*Lacerta*	*Podarcis*	–	*Lacerta*	*Podarcis*	–	*Lacerta*	*Podarcis*
D2 CE1-0 (75%)	–	Gallotiinae; *Podarcis*	*Podarcis*	–	Gallotiinae; sister to *T*+*L*	*Podarcis*	–	Gallotiinae; sister to *T*+*L*	*Podarcis*
D2 CH1-100 (75%)	–	Lacertidae	*Podarcis*	–	Lacertidae	*Podarcis*	–	Gallotiinae	*Podarcis*
D2 CH1-75 (46%)	–	Lacertoidea	Excluded	–	Lacertoidea	Excluded	–	Lacertoidea	Excluded
D2 CCVsup (63%)	–	*Lacerta*	*Podarcis*	–	*Lacerta*	*Podarcis*	–	*Lacerta*	*Podarcis*
D3 CC1sup (75%)	–	*Lacerta*	*Podarcis*	–	*Lacerta*	*Podarcis*	–	Gallotiinae; *Lacerta*	*Podarcis*
D3 CH1-100 (75%)	–	Lacertoidea	*Podarcis*	–	Lacertoidea	*Podarcis*	–	Lacertoidea	*Podarcis*
D3 CH1-75 (42%)	–	Lacertoidea	Excluded	–	Lacertoidea	Excluded	–	Lacertoidea	Excluded
D4 CE1-0 (79%)	–	Gallotiinae; *Podarcis*	*Podarcis*	–	Gallotiinae; sister to *T*+*L*	*Podarcis*	–	Gallotiinae; sister to *T*+*L*	*Podarcis*
D4 CH1-75 (50%)	–	Lacertoidea	Excluded	–	Lacertoidea	Excluded	–	Lacertoidea	Excluded
D4 CCVsup (54%)	–	Lacertoidea; Scincoidea	Excluded	–	Lacertoidea; Scincoidea	Excluded	–	Lacertoidea; Scincoidea	Excluded
D4 MdGB (75%)	–	*Podarcis*	*Podarcis*	–	Lacertoidea	Podarcis	–	Sister to *T*+*L*	Podarcis
D5 CE1-0 (42%)	*Iberolacerta* (sister to *I. cyreni*)	*Iberolacerta* (sister to *I. cyreni*)	*Iberolacerta* (sister to *I. cyreni*)	*Iberolacerta* (sister to *I. cyreni*)	*Iberolacerta* (sister to *I. cyreni*)	*Iberolacerta* (sister to *I. cyreni*)	*Iberolacerta* (sister to *I. cyreni*)	*Iberolacerta* (sister to *I. cyreni*)	*Iberolacerta* (sister to *I. cyreni*)
D6 CE1-0 (63%)	*Algyroides* (sister to *A. nigropunctatus*)	*Algyroides* (sister to *A. nigropunctatus*)	*Algyroides* (sister to *A. nigropunctatus*)	*Algyroides* (sister to *A. nigropunctatus*)	*Algyroides* (sister to *A. nigropunctatus*)	*Algyroides* (sister to *A. nigropunctatus*)	*Algyroides* (sister to *A. nigropunctatus*)	*Algyroides* (sister to *A. nigropunctatus*)	*Algyroides* (sister to *A. nigropunctatus*)
D7 CE1-0 (75%)	–	*Lacerta*	*Podarcis*	–	*Lacerta*	*Podarcis*	–	*Lacerta*	*Podarcis*
D7 CCVsup (71%)	–	Lacertoidea	*Podarcis*	–	Lacertoidea	*Podarcis*	–	Lacertoidea	*Podarcis*
D8 CH1-100 (75%)	–	clade with Gallotiinae	Gallotiinae	–	clade with Gallotiinae	Gallotiinae	–	clade with Gallotiinae	Sister to *Timon*
D8 CCVsup (38%)	–	Lacertoidea	Excluded	–	Lacertoidea	Excluded	–	Lacertoidea	Excluded
D8 Roq2 (38%)	–	–	Excluded	–	–	Excluded	–	–	Excluded
D9 LaC (67%)	–	*Podarcis*	*Podarcis*	Sister to *P. tiliguerta*	*Podarcis*; sister to *T*+*L*	*Podarcis*	sister to *P. tiliguerta*	Gallotiinae; sister to *T*+*L; Podarcis*;	Podarcis
D9 Roq2 (58%)	–	*Podarcis*	Excluded	–	Sister to *T*+*L*	Excluded	–	Gallotiinae; sister to *T*+*L*	Excluded
D10 Roq2 (54%)	Clade with Amphisbaenia	Clade with Amphisbaenia	Clade with Amphisbaenia	Clade with Amphisbaenia	Clade with Amphisbaenia	Clade with Amphisbaenia	Clade with Amphisbaenia	Clade with Amphisbaenia	Clade with Amphisbaenia

CC1sup, Coderet Couche 1 sup; CCVsup, Coderet Couche Verte sup 1-25; CE1-0, Coderet E1-0; CH1-100, Coderet H1-100; CH1-75, Coderet H1-75; Cod, Coderet; FV, Fouilles Viret; LaC, La Colombière; MdGB, Mas de Got B; PdF, Pech-du-Fraysse; Roq2, Roqueprune 2; T + L: *Timon* + *Lacerta*.